UNIVERSITY OF NAIROBI

FACULTY OF SCIENCE AND TECHNOLOGY

DEPARTMENT OF CHEMISTRY

USE OF MICROBIAL FUEL CELLS IN GENERATING ELECTRICITY THROUGH VALORIZATION OF FRUIT WASTES FROM SELECTED MARKETS IN NAIROBI COUNTY, KENYA

BY

IMWENE KENNEDY OMUKADA

I56/35963/2019

A Thesis Submitted in Partial Fulfillment of the Requirements for the Award of the Degree of Master of Science in Analytical Chemistry of the University of Nairobi

June 2023

DECLARATION

I declare that this thesis is my original work and has not been submitted elsewhere for examination, award of a degree, or publication. Where other people's work, or my own work has been used, this has properly been acknowledged and referenced in accordance with the University of Nairobi's requirements.

Signature:_____ **Date:** **27th . June. 2023**

IMWENE KENNEDY OMUKADA

I56/35963/2019

Department of Chemistry, Faculty of Science and Technology, University of Nairobi.

This thesis is submitted with our approval as research supervisors.

	Signature:	Date:
Dr. Damaris N. Mbui	_____	28th June 2023

Department of Chemistry
University of Nairobi
PO Box 30197- 00100
Nairobi Kenya
dmbui@uonbi.ac.ke

Dr. John Onam Onyatta	_____	27/06/2023

Department of Chemistry
University of Nairobi
PO Box 30197-00100
Nairobi Kenya.
john.onyatta@uonbi.ac.ke

DEDICATION

This thesis is dedicated to my beloved parents, the late Mr. Pascal, my Mum Anjeline, my brothers Evans, Hannington, Kelvin, Ian, sister Brigit, my dear wife Esnas, and to my children Cynthia, Gloria, Clarence, and Agatha. Your support towards the realization of this dream is priceless.

ACKNOWLEDGEMENT

I am sincerely grateful to almighty God for giving me good health and stability of heart throughout the rigorous process of writing this thesis. His grace is indeed sufficient.

My special and most sincere gratitude goes to my academic supervisors, Dr. Damaris Nduta Mbui and Dr. John Onam Onyatta, for professional counsel and guidance every step of the way, and to Dr. James Kamau Mbugua for his stimulating discussions and constant encouragement throughout the planning and execution of this study, I say thank you. I acknowledge the management and staff of KEPHIS, Analytical Chemistry, and Food Safety Laboratory, Directorate of Veterinary Services (DVS) - Analytical Chemistry Laboratory and the University of Nairobi for supporting this project with proximate properties analyses and bacteriological studies; your support goes a long way.

Lastly, I to acknowledge my research colleagues, Dr. Edwin Madivoli, Dr. Sithole Nastassia Thadiwe, Mr. Pius Kinoti Kairigo, Mr. Martin Kinyanjui, Mr. Jared Nyang'au, Mr. Solomon Chogo, Mr. Victor Ochieng, and Mrs. Joyce Nyoike, who contributed in many ways to the realization of this work.

ABSTRACT

In this study, generation of electricity from market fruit-waste was investigated in microbial fuel cells. Standard procedures were used to examine the proximate qualities of various market fruit wastes. An H-shaped double-chamber microbial fuel cell was fabricated to break down the substrates. Fruit waste samples were collected from a few marketplaces, were separately reduced in size using a kitchen knife, blend, and loaded into the anodic chamber with goat rumen fluid as a biocatalyst. As a final electron-acceptor, oxygen molecule was used in the cathode chamber from distilled water. Bacteriological analysis was performed. The obtained results for bacterial counts from both Cow rumen fluid as well as cow dung were $3.15 \pm 0.01 * 10^{10}$ CFU/mL and $1.50 \pm 0.02 * 10^{10}$ CFU/g, respectively. Proximate properties of the waste indicated that tomatoes had highest moisture content, whereas banana fruit waste had the lowest, with a percentage ranging between 74.30 % - 95.16 %. The % protein level was most deficient in tomatoes and highest in bananas in the range of 0.57 % - 3.05 %. Avocado gave the highest % fibre levels while tomato gave lowest percentage levels in the range of 2.61 % - 0.76 %. The potential results obtained from a DT9205A digital multi-meter over twenty-two (22) days showed that voltage from fruit waste increased with time. The average voltage obtained was highest in banana waste and lowest in tomato waste, while the mixture gave an average of 0.159 ± 0.05 V. The average current obtained had highest tomato content and lowest banana content at 0.021 ± 0.008 mA and 0.018 ± 0.007 mA, respectively, while the mixture of fruits gave an average of 0.022 ± 0.006 mA. All of the fruits had power and power densities output in the range of (3.047 to 4.038 μW) and (572.4 to 758.5 $\mu W/m^2$) respectively. Furthermore, the experimental data were subjected to kinetic analysis using kinetic models, and these are the corresponding constants: the Monod model: of ($99.57\ gL^{-1}$ - $99.63\ gL^{-1}$); Andrew Haldane's model: ($50.09\ gL^{-1}$ - $50.18\ gL^{-1}$) and Han-Levenspiel Model: ($91.09\ gL^{-1}$ - $100.75\ gL^{-1}$). The values obtained using the Han-Levenspiel model were found to be in good agreement with the experimental observations. There was no statistically significant difference in power output ($P < 0.05$) in all the fruit wastes. Automation, using the Arduino sensor showed a voltage range of 0.05 -0.34 V, 0.03-0.356 V, and 0.08 – 0.35 V with a current range of 0.005 - 0.078 mA, 0.001-0.084 mA in tomato and avocado respectively. The study found that voltage and current generated in a microbial fuel cell were impacted by substrate-proximal characteristics. Microbial fuel cells (MFCs) could be used to generate clean energy from market trash, providing clean and very inexpensive electricity while also addressing solid waste management, particularly at fruit markets. In addition, goat rumen fluids could serve as a suitable inoculum for electricity generation. Further work needs to be done on Microbial fuel cells using a suitable catalyst.

TABLE OF CONTENTS

LIST OF TABLES

LIST OF FIGURES

LIST OF APPENDICES

LISTS OF ABBREVIATIONS AND ACRONYMS

AOAC	Association of Analytical Chemistry
CBD	Central Business District
FAO	Food and Agricultural Organization
GHG	Green House Gases
LPG	Liquefied Petroleum Gases
MFC	Microbial Fuel Cell
MSW	Municipal solid waste
NBSC	National Bureau of Statistics of China
NEMA	National Environment Management Authority
RCRA	Resource Conservation and Recovery Act
SDG	Sustainable Development Goal
UNCED	United Nations Conference on Environment and Development
USEPA	United States Environment Protection Agency

UNITS OF MEASUREMENTS

g	grams
kΩ	kilo ohms
m^2	meters square
mA	milli-amperes
mL	milliliter
mV	milli-volts
μW	microwatts
V	Volts

CHAPTER ONE

INTRODUCTION

1.1 Background Information

The problem of Solid waste management is worsening globally, especially with the increase in population and industrial activities, necessitating the need to investigate alternative ways of managing solid waste. Heaps of garbage are a health hazard and, they necessitate land for disposal, among other issues. The energy crisis and environmental pollution have in the recent past promoted research on efficient techniques such as environmental-catalysis to generate bio-energy, Land reclamation, climate change mitigation and solid waste management (Osman *et al.*, 2023). During United Nations Conference on the Environment and Development (UNCED) in Rio de Janeiro City in Brazil in the year 1992 the United Nations recommended a waste hierarchy as a general principle of solid waste management (Schneider & Lorenz, 1993; Kaymaz *et al.*, 2022). Waste minimization and maximization of sound solid waste management practices, for example, reducing, recycling, reusing, and disposing of waste (for instance organic waste) in an environmentally friendly manner were highly encouraged (Wang *et al*., 2009).

In most developing countries, most waste is burnt, in an attempt to reduce it, otherwise it is disposed of in heaps (Figure 1.1), making sound solid waste management, a real challenge (Cheng, 2010). When waste is burnt, it releases toxic compounds into the natural environment, the majority of which cause various respiratory disorders, including a rise in greenhouse gas (GHG) emissions into the atmosphere. These catalyze ozone layer depletion and hasten climate change. Kenya's 2019 National Sustainable Waste Management Policy estimated that Kenya generates 22,000 tons of garbage per day (Ogutu *et al.*, 2019). Given the current population of 45 million people, the amount of solid waste generated annually is approximately eight million tons (Kituku *et al.*, 2020; Mungai *et al.*, 2020). Due to a 10% increase in urbanization, the Kenyan urban population is expected to generate nearly 13 million tons of solid waste per year by 2030, roughly two times the waste generated in 2019. Out of the waste generated, approximately 65% is organic, 20% is plastic, 10% is paper, and 1% is medical waste (Kituku *et al.*, 2020). Generation of power is a key element in any society, and nations are continually searching for ways to meet their energy needs.

Currently, the main source of electrical power in Kenya is geothermal works. Kenya is rated eighth in the world in terms of geothermal power production (Merem *et al.*, 2019). Geothermal power is a low-cost, environmentally friendly energy, but it requires expensive advanced technologies to produce (Ondraczek, 2014). It is critical to explore other alternative sources of energy that are less expensive to generate, and, preferably, renewable (Singh *et al.*, 2012). Energy production from organic wastes is one example of such energy. Obtaining energy from organic waste would provide a two-fold answer to global environmental problems: energy would be produced, and the issue of solid waste management would be efficiently addressed.

Figure 1.1: A heap of fruits waste at Muthurwa market, Nairobi County

1.1.1 Resource Recovery Processes from Waste for Bioenergy Generation

Waste is a major problem on a global scale that has negative effects on the environment and society. In order to reduce environmental harm, promote sustainability, and advance circular economy, waste valorization is attracting enormous scientific and industrial interest. Waste can be recycled into energy, fuels, and other high-value goods. In many nations, a number of waste-to-energy technologies have been created and effectively applied at an industrial scale to recover energy and products (Clauser *et al.*, 2021). According to Kwan *et al.* (2015), organic waste is often nutrient-rich and primarily made up of polysaccharides (typically starch 30 to 60%), proteins 5 to

10%, and lipids 10 to 40%. They can act as a necessary and inexpensive feedstock for biorefineries, enabling them to generate items with higher added values while reducing generated amount of organic waste that needs to be treated. Several industrial areas, including the food, cosmetics, pharmaceuticals, and energy sectors, could be tied to the concept of a biorefinery (Zhu, 2015). Utilizing cost-effective, efficient, and environmentally friendly technologies to reduce pollution, provide clean energy, and synthesis valuable molecules has received more attention in recent years. Utilizing resources effectively, including reducing food waste and applying new resources for the production of bioenergy, is one of the cornerstones to sustainable growth. Sustainability, which considerably accelerates human civilization advancement, is a development that satisfies the needs of present generation without compromising capacity of future generations to meet their needs (Osman *et al.,* 2023).

1.1.2 Microbial Fuel Cell

Bioelectrochemical system in this case MFC is a device that generates bioelectricity by utilizing organic matter (Lovley, 2012; Nitisoravut *et al.,* 2017). MFC uses the principle that when microbes digest organic matter, chemical-energy held within an organic compound is transformed to electric energy (Sun *et al.,* 2016). As a result, microbes are thought to be the catalysts in this electricity-generating mechanism (Saratale *et al.,* 2017; Logan *et al.,* 2006). Microorganisms require two critical reagents during the electrical energy conversion process that is organic matter (substrate) and an electron acceptor. These reagents are utilized in the metabolic process of cellular respiration, which is the breakdown of organic materials to produce chemical energy which is stored in chemical bonds. Anode-respiring bacteria (ARB) oxidize organic substrates to produce electrical current. In order to develop an electrical current, ARB must transfer electrons to a solid anode through extracellular electron transfer (Torres *et al.,* 2010). The electron equivalents are transported to an electron transport chain in the cell membrane as hydrogen atoms via nicotinamide adenine dinucleotide (NADH). As electrons travel through the respiratory chain and protons are transferred outside the cell, a proton gradient is formed. The re-entry of protons into the cell relates to synthesis of energy store molecule, Adenosine-Triphosphate (ATP). The difference in potential between the electron donor, NADH, as well as terminal electron-acceptor in the respiratory chain determines amount of energy that bacteria can conserve in the form of ATP (Ramsay, 2019). Since the bacteria that use oxygen for respiration can conserve the most energy, oxygen must be excluded

from the anode compartment for anode respiration to occur. An anode-respiring bacteria (ARB) transport electrons generated to a solid anode devoid of molecular oxygen and other soluble electron terminal acceptors. Electrons leave the electron transport chain at a lower redox potential than oxygen metabolism in this form of metabolism (Song, 2017).

1.1.3 Microbial Fuel Cell Electron Generation

Electrons are generated in designed Fuel Cell chambers by three primary processes, namely, glycolysis process, the Kreb's cycle, and finally Electron Transport Chain (Jaiswal *et al.*, 2020). Glycolysis is a metabolic pathway that converts foods into pyruvate or pyruvic acids (CH_3COCOO^-) and hydrogen ions (H^+). In this pathway, free energy is released, and it is used to make the high-energy molecule (ATP) and other molecules (NADH). The second phase is the Kreb's cycle, which is a series of chemical reaction mechanisms through which microorganisms (aerobic bacteria) generate electrical energy by oxidizing acetate molecules obtained from molecules of carbohydrates, lipids, as well as proteins into carbon dioxide gas. These substances, (e^-) and (H^+), are collected by the carrier molecules like Nicotinamide Adenine Dinucleotide (NAD^+) together with Flavin Adenine Dinucleotide (FAD) and transferred into the last cycle, namely the electron transport chain. The Electron Transport Chain is a protein complex that moves electrons from electron donors to electron acceptors via redox processes and connects this electron transfer with the passage of protons (H^+) across the membrane (Ueki, 2021). The carrier molecules donate the electrons accumulated in the previous steps to a new carrier termed Enzyme Complexes, the last carrier molecule, also known as final-electron-acceptor, in this case, oxygen - cellular respiration under anaerobic conditions. A lack of oxygen inhibits the Kreb's and electron transport chains; however, glycolysis is unaffected. As a result, the difference in energy gain between aerobic cellular respiration and glycolysis is critical for generating electricity from microbial fuel cells; this enhances cellular respiration performance that motivates microorganisms to transfer their electrons via MFC's internal circuit, resulting in generation of energy. This is an example of the new ecologically friendly renewable energy sources projected to contribute significantly in small-scale as well as off-grid applications.

1.1.4 Bacterial Growth Phases

As mentioned in the previous section, when biodegradable waste is placed in the anodic chamber of a microbial fuel cell, along with a supply of bacteria and protozoa (through inocula, such as cow dung or rumen fluid), and a substrate like sucrose is placed in the cathodic section a current of electricity is created, (Zhao *et al*., 2012). According to studies by Kim *et al.* (2013), the voltage generated is directly related to the microbial growth rate. The growth rate of these microbes is well defined by a number of phases, namely the lag, log, stationary, and death phases (Figure 1.2). Microorganisms during the lag phase adapt slowly to their surroundings after which they develop, metabolize the organic matter present and reproduce, thereby increasing their numerical numbers. The log phase is a period characterized by the number of microorganisms increasing exponentially. The stationary phase occurs when the microbial population is constant since the rate of reproduction is approximately equal to the rate of death of the microbes. The death stage occurs when more microorganisms die than the ones that are being generated (Maier *et al.*, 2015).

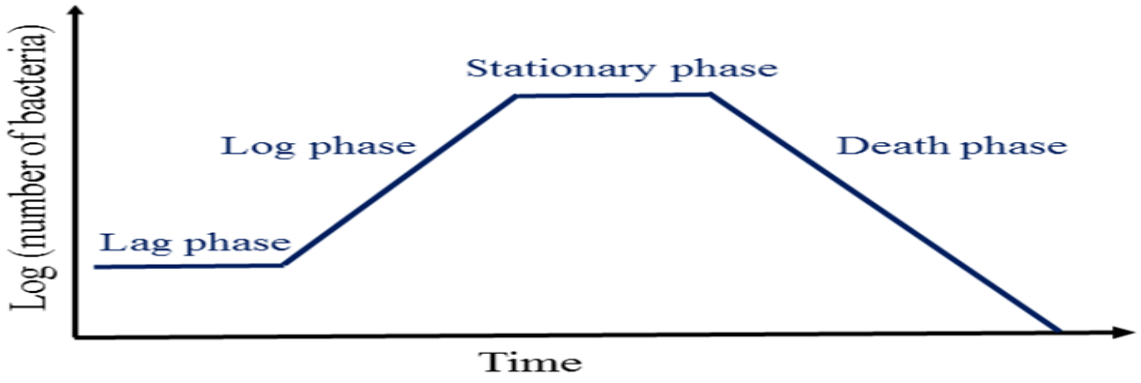

Figure 1.2: A typical bacterial growth curve, (Ram *et al.*, 2019)

1.1.5 Utilization of Ruminal Microorganism

By utilizing organic waste that has been transformed into energy by microorganisms, a shift towards renewable energy generation is slowly but steadily gaining momentum over the ever-dwindling non-renewable energy (Ray, 2019). Rumen fluid is an ecosystem housing a wide range of biological organisms, making it a primary fermentation location in a cow (Zhou *et al.*, 2015). It is anaerobic (meaning it uses little or no oxygen) and operates at a temperature one degree above

body temperature (39 ℃ or 102.5 ℉) and a pH range of 5.7 to 7.3. According to Wang *et al.* (2012) rumen contains between one and ten million bacteria per millilitre (e.g. *Streptococcus Bovis or Clostridium spp*) and approximately one million protozoa per millilitre (e.g. *Epidinium Ecaudatum, Epidinium spp*). The principal volatile fatty acids (VFA) produced by microorganisms in the rumen are acetic - (CH_3COOH), propionic-(C_2H_5COOH) *a*nd butyric -(C_3H_7COOH) acids (Wang *et al.*, 2012).

1.1.6 Anaerobic Digestion Process

One of the most accepted choices for slaughterhouse waste management is the anaerobic digestion process since it produces energy-rich biogas, lowers emissions of Green-House Gas (GHG), and effectively controls pollution in abattoirs (Kabeyi & Olanrewaju, 2022). Similarly, Moukazis *et al.* (2018) observed that anaerobic digestion could remove a lot of chemical oxygen demand (COD) as well as biological oxygen demand (BOD) from slaughterhouse effluent for a lot less money than comparable aerobic systems. Slaughterhouse waste has a more significant biogas potential compared to animal manure and has been estimated to be in between a range of $(120 - 160\ m^3)$ biogas per ton of wastes. However, because slaughterhouse waste has a low C : N ratio (4:1), it must be co-digested with substrates having high C : N ratios, some examples include animal dung, food waste, crop leftovers, and poultry litter (Bazrafshan *et al.*, 2012).

1.1.7 Automation of the Microbial Fuel Cell

Electrochemical measurements require accurate and expensive instrumentation, which limits bio-electrochemical studies (Mahari & Gandhi, 2022). Microbial fuel cell applications in the real world are currently limited as a result of their few thousand power density (mW/m^2). MFCs are being worked on to try increase their performance and lower their construction and operation costs (Jiang *et al.*, 2011). For example, instead of utilizing a multi-meter to monitor the potential delivered by a biocathode MFC, an alternative automatic voltage and current data logging from MFCs employed a low-cost potential-measuring device (Arduino UNO).

In this research, double-chamber H-shaped MFCs were used as biomarkers for Bioelectricity generation activities from various fruit wastes from markets in Nairobi, Kenya.

1.2 Statement of the Problem

Solid Waste Management is a big challenge, especially in developing countries where heaps of garbage are often observed (Figure 1.1). Dumped wastes are hazardous to human health because they attract rodents and pests that jeopardize human life. Additionally, dumpsites encroach on territory that could otherwise be used for more commercially feasible enterprises, rendering the land unusable. Human survival necessitates the use of both renewable and non-renewable energy sources. However, certain energy sources have drawbacks, such as the use of firewood and charcoal, which has led to deforestation and emission of Green House Gases (GHGs) into atmosphere, causing a variety of problems that are often irreversible. Similarly, the usage of petroleum products (kerosene, LPG, and other similar fuel sources) depletes natural resources, putting humanity in a precarious position.

In resource recovery, waste is changed into useful products as new outputs: in this case, waste is converted into renewable energy. Velenturf *et al.* (2019) stated that reuse and recycling are part of the circular economy in resource recovery when natural resource extraction and waste generation are minimized. Materials and products are becoming more sustainably developed for long-term use. Thus, generating electricity from waste using microbial fuel cells will address waste management, supply renewable energy, alleviate climate change, and revitalize the economy. In this perspective, the current generation will be able to take care of their fundamental requirements while not jeopardizing capacity of upcoming generations to do the same.

1.3 Objectives of the Study

1.3.1 General Objective of the Study

The general objective of this study was to evaluate the production of electricity in microbial fuel cells from fruits waste obtained from selected markets in Nairobi, Kenya.

1.3.2 Specific Objectives of the Study

The specific objectives of this study were:

i) To characterize fruit waste from selected markets in Nairobi for their proximate properties.

ii) To determine voltage and current yield arising from the various fruits wastes in microbial fuel cells.

iii) To investigate the effects of concentration of inoculum, external resistance, temperature and pH on electricity production from market wastes.

iv) Design and fabricate a low-cost portable voltage measuring and data logging system using an Arduino Mega Board.

v) To determine economic value addition of the biodegraded fruit waste by the microbes from the microbial fuel cell.

1.4 Justification and Significance of the Study

Global issues including managing solid waste, reducing climate change, and producing green energy have prompted treaties and agreements between states to try and find solutions. A possible solution to the waste management problem is using the waste to generate electrical energy, by making use of microbes, which can transform chemical energy in an organic compounds into electricity. This process would also provide an alternative route of renewable energy generation.

Findings of this research would be used to pave way for the design of suitable technologies for electrical energy generation from solid wastes. As a result, this might be extended across the entire country to help Kenya achieve its Big Four Agenda, as articulated by the Kenyan government. It could also help policymakers in designing appropriate policies that strengthen renewable energy practices for the generation of electricity and hence contribute to implementation of the Kenya Vision 2030 plan for the Sustainable Development Goal number 7, which promotes universal access to affordable, dependable, sustainable, and clean energy and, whenever possible, leaves no one behind on use of renewable bioenergy. Bioelectricity is generally considered to be clean energy, and using waste to make it would help to solve the problem of disposing of solid waste.

CHAPTER TWO

LITERATURE REVIEW

2.1 Solid Waste

Solid wastes are undesirable byproducts of human activities, and their management has a direct effect on human and environmental health (Monyoncho, 2013; Leton & Omotosho, 2004). Globally, increasing amounts of complicated waste are dumped (Vergara and Tchobanoglous, 2012). According to the United States Environment Protection Agency (1976), solid waste is any material that has been abandoned, discarded, dumped, or classified as "waste-like." They can be solids, liquids, or gases which can further be categorized based on the proximate analysis of each class (Hui *et al.*, 2014). Small market towns have a larger problem with residential solid waste management than large cities, owing to a lack of providers of commercial services (Adzawla *et al.,* 2019). As low-income countries increasingly urbanize, authorities face a severe difficulty managing garbage (Adzawla *et al.,* 2019).

2.2 Utilization of Fruit and Vegetable Wastes

A lot of biodegradable materials, such as waste from vegetables and fruits, are left in the open to decay, primarily due to lack of adequate recycling and recovery procedures, creating foul odours and attracting birds, mosquitoes, and other pests, all of which are health hazards (Abdel *et al.,* 2018). However, by adapting to correct disposal systems, such as putting the waste through a fermentation process under optimal conditions, they can be used to produce biofuel because the decomposition of wastes by microorganisms produces end-products with high humus content. According to Kraan (2013) Carbohydrate-rich biomass can be a significant source of renewable energy.

Studies by Maldonado-Celis *et al.* (2019) and Torres-León *et al.* (2016) suggested that fruit wastes comprised nutritional and phytochemical components varied during development and after harvest. Mbugua *et al.* (2020) suggested that composition of various fruit and vegetable wastes from selected markets in Nairobi County significantly impacted power generation.

2.3 Global Solid Waste Generation Statistics

Given the huge rise in world population, it is estimated that about 35% of food supply is wasted (Parfitt *et al.,* 2015). While many industrialized countries seek ready-made sustainable waste management solutions like the use of waste in garment industries (Rasel *et al.,* 2019), countries like India have taken up the formal research challenge by establishing institutes such as "The Council of Scientific and Industrial Research (CSIR)" to pursue research and development in waste management. In 2001, India produced approximately 46 million tons of waste, and it's anticipated by 2048, waste generation will have increased to 125 million tonnes, making India the world's greatest waste generator (Kumar *et al.,* 2017). Furthermore, agricultural waste contributes roughly 50 Mega Tons (MT), or about 30% of total vegetable waste output in India (Kapoor *et al.,* 2020). If this agricultural or organic waste could be used for bioenergy generation, it would be economically beneficial. The National Bureau of China (2012) projected that municipal solid waste increased to 163.95 million tons in 2011, down from 108.25 million tons in 1996. Tai *et al.* (2011), stated that it might become a severe environmental hazard if this waste was not properly disposed of.

2.4 Municipal Solid Waste in African Countries

Management of municipal solid waste is an economical, social, and environmental problem that affects all of Africa. For example, in Nigeria's largest cities, it is not uncommon to witness piles of waste littering the streets and others dumped in drains, abandoned plots, and waterways. Because of this, infectious diseases have spread over the population. The problem appears to worsen due to urbanization, population expansion, improved lifestyles, and lack of funding to effectively manage solid garbage (Babalola *et al.,* 2010). South Africa's urbanization, population, industrialization, and modernization sectors have all increased (Simatele *et al.,* 2017), a factor that has increased waste generation (thus increased pollution) and electrical energy demands (and subsequent energy poverty). According to the National Waste Information Baseline (NWIB), South Africa generated approximately 108 million tonnes of waste in 2011, with 59 million tonnes of general waste being generated at a rate of 0.2 – 1.29 kg/capita/day (Tshivhase *et al.,* 2020). In

Ghana, the amount of solid trash generated in urban areas is increasing, and in some situations, generated waste surpasses collection capacity (Akuyea, 2013; Bowan *et al.*, 2014). For example, trash generation rates in Kumasi and Accra are roughly 0.6 kg/person/day and 0.40 kg/person/day, respectively (Ketibuah *et al.*, 2004), with, between 10 % and 20 % of the waste generated going uncollected (Akuyea, 2013).

2.4.1 Solid Waste in Kenya

Solid garbage is produced in varied volumes in Kenyan market towns. The characteristics of produced wastes vary depending on socioeconomic, meteorological, the cultural factors, and the institutional capacities (Vergara & Tchobanoglous, 2012). In a majority of these market towns, unsustainable solid waste management procedures are applied. For example, in Ongata Rongai, Kenya, open dumping and burning are commonplace (Gitau, 2018). Pollution of the land, water, and air is a result of these non-sustainable practices (Modak *et al.*, 2010). Waste reduction, recycling, recovery, and treatment are examples of sustainable waste management practices (Seadon, 2010). One example is the practice of composting processes in Juja town, Kenya (Mwangi *et al.*, 2017). Market towns with significant population growth rates, such as Embu, generate more household solid waste, with an annual population growth rates vary between 1.4 percent and 3.9 percent (Mochache *et al.*, 2020). According to a similar study, Kisumu, like many other Kenyan market towns, has serious solid waste management shortcomings. Various experts have calculated Kisumu's daily trash generation, which is largely estimated to be ranging between 200 and 450 tons per day Budzianowski *et al.* (2018); organic material accounts for 62.5 to 67 % of the total (Gutberlet *et al.*, 2017).

Nairobi, like many other African cities, lacks appropriate practicing systems on managing municipal waste resulting in a significant short and long-term effects on health of both people and animals, as well as the environment (Njoroge *et al.*, 2014). Nairobi Solid Waste Management Plan states that domestic garbage accounts for 68% of all the waste generated in Nairobi County in Kenya, making it prudent to concentrate on the types of the solid wastes produced as well as the ways utilized by homeowners to dispose of waste (NEMA, 2014).

2.4.2 The State of Energy in Africa

Energy demand in African countries has risen over time, owing to rapid population expansion, the emergence of small-scale industries, and indigenous technological breakthroughs. With over 200 million people, Nigeria is one of the most densely inhabited nations in Africa. For nations like Nigeria, Sustainable Development Goal number 7, intersects with a number of objectives in playing a significant role in socio-economic development, as well as provision of clean and affordable energy is vital (Ramchandra & Boucar, 2011).

According to Kuamoah (2020). the energy crisis experienced in Ghana for three to four years was a result of water levels being low in Akosombo dam. With the low thermal electricity generation and decline of the availability of natural gas, the energy crisis in most African countries is yet to be solved. As a result, African countries must transition to more ecologically friendly, clean, and sustainable renewable energy sources and encourage localized waste-to-electricity generation as an alternative solution. Generally, a country like Ghana produces a lot of vegetable waste, and therefore, there's a lot of potential for energy generation from waste generated by the agricultural sector or from domestic sources (Akuyea, 2013; Abdel *et al.,* 2018). According to studies, an estimated 2,975.6 million tons of biogas produced mostly from municipal solid waste, animal waste, and agricultural residues could meet the monthly electricity demand of 8.7 million urban families and 12 million rural homes (Amo-Asamoah *et al.,* 2020). Furthermore, channeling this energy to the industrial sector may cover more than double electricity usage annually. For the present waste generation to energy profile, a framework is required to incentivize electricity generation from waste (Kuamoah, 2020; Kemausuor *et al*., 2014; Ofori Boateng *et al.,* 2013).

2.4.3 The State of Energy in Kenya

Energy is a critical factor to a nation’s economic development. It is a requirement that has an impact on the production of practically all goods and services in the Country. It also has an impact on all major aspects of development, including the environment, social, and economic aspects. Agriculture, population, livelihood, and a variety of other factors affected by energy (Takase *et al.,* 2021). Kenya is one of the countries in Sub-Saharan Africa (SSA) that is still experiencing an

energy crisis and a severe socio-economic deficit. For a long time, access to modern and sustainable energy has been regarded as a privilege in Kenya. Furthermore, it is among the least developed countries in Sub-Saharan Africa (SSA) in terms of yearly GDP growth and current developmental progress (Mwenzwa & Misati, 2014). Kenya's energy consumption is outpacing the country's population growth and economic expansion. The Kenyan government's Vision 2030 program has laid out ambitious goals for future economic growth, with the goal of putting Kenya's economy middle-income by 2030 (Kiprop *et al.,* 2017). The country's main issue is a lack of renewable capacity as a result of a lack of investment in power generation and its reliance on hydroelectric power. As a result, the concept of energy recovery will be required to address the need for managing municipal solid waste from the market (the primary source) to dump sites, thereby reducing the need for additional land space for open dumping sites, recovering other recyclable materials, reducing greenhouse gas emissions, and even creating more job opportunities in Kenya (Kazimierczuk, 2019).

Nairobi, Kenya's capital city, creates a total of 803,000 tons of solid garbage per year, which is disposed at the Dandora Dump Site. After Nairobi, the largest cities are Mombasa, Nakuru, and Kisumu, which produce 1124 million tonnes. In Kenya's metropolitan regions, a total of 5.26 million tons are anticipated to be produced per year (Njiru & Letema, 2018). This waste could be utilized to produce methane gas, which can be used to generate energy, a strategy that could solve the challenges involving municipal waste management as well as availability of relatively cheap, renewable and reliable energy.

2.5 Waste Management in Kenya

Solid waste management challenges in Kenya are real (Gakungu *et al,*. 2012) and Gakungu, 2011), and its disposal and collection systems are inefficient and harmful to the environment. According to Allison and Blottnitz (2010), approximately (30 – 40 %) of solid garbage generated in urban settlement goes uncollected; only about half of human population is served, and about 80% of collection transportation is grounded. Unless sustainable waste management issue if not properly addressed, garbage will overflow into all of Kenya's municipalities (Aurah, 2013). In Kenya, the Local Government had preserved all legislation and policies on solid waste management under the Local Authorities Act 265, which deals with establishing legislative frameworks, institutional

arrangements, financial plans, and technical systems. The Local Authorities Act 265 was later replaced by National Environment Management Authority (NEMA), with a far greater purpose of enforcing and ensuring compliance with environmental regulations (a clean and healthy environment and the requirement that the environment is protected for present and future generations). NEMA, a government agency, was and continues to be the leading institution in environmental management field, with an aim to protect as well as improve environment through facilitation, coordination, research, and enforcement while encouraging individual, corporate institutions, and collective participation in pursuit of sustainable development.

Nairobi's solid waste management has largely been exhibiting little use of municipal solid waste procedures, disposal of uncontrolled garbage, unregulated government-private sector cooperation, insufficient or non existence of public services plan, as well as lack of critical infrastructural systems on solid waste management specifically on waste segregation (Muniafu & Otiato, 2010). Furthermore, the sector lacks appropriate waste reuse and recovery legislation, regulations, and framework, resulting in poor waste collection estimated at 1,500 tons only per day in Kenya's largest Capital City of Nairobi with a numerical population of around 3 million people, translating to about 25 % of waste generation daily in the Capital alone (Mbaki, 2019).

2.6 Characteristics of Solid Waste Generated in Nairobi, Kenya

Unscientific treatment, inappropriate garbage collection, and ethical issues have plagued solid waste management in many underdeveloped countries, resulting in environmental degradation, water poisoning, and air pollution (Kumar *et al.*, 2017). Kenya is among these underdeveloped countries. According to the Republic of Kenya National Environmental Policy Document (2014), an environmental-friendly solid waste management strategy was developed to help the country's national agenda improve and promote significant waste reduction, collection, and disposal. Increased solid waste generation in Nairobi has resulted from growth in population, rural-urban migration, and increased urbanization, and yet a corresponding trash-handling capacity has not matched this rise. This generation rate is expected to increase by around 4 million tonnes annually

(Njoroge *et al.*, 2014; Ogutu *et al.*, 2021). Figure 2.1 shows the breakdown of types of waste generated in Kenya and the percentages thereof.

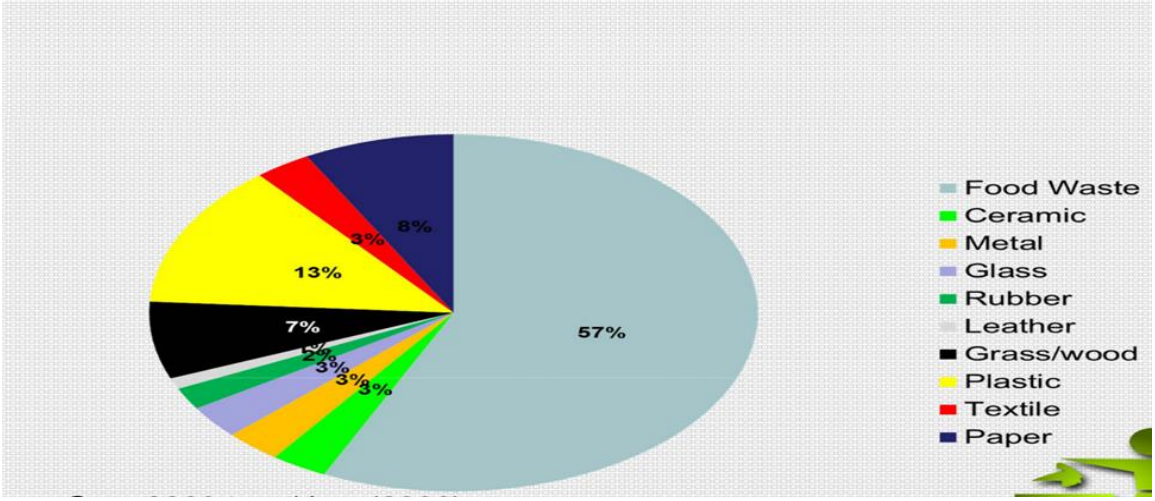

Figure 2.1: Solid Waste in percentage collection in Capital City, Nairobi (Andole, 2016)

In Nairobi and throughout Kenya, SWM continues to be a significant environmental and public health concern. As a result, a suitable model for estimating trash generation should be created, taking into account the changing patterns of waste formation and categorization.

2.7 H – Shaped Microbial Fuel Cells

Designed double chambered Microbial Fuel Cell (MFC) is a device that generates bioelectricity by utilizing organic matter, (Lovley, 2012). Based on how bacteria transport electrons to the anode, MFC is divided into two categories. There are two different MFC types: mediator MFCs and mediator-less MFCs. In mediator MFC, supplementation of synthetic mediators facilitates continuous electron transport to the anode electrode via reduction-oxidation coupling (Pandit *et al.*, 2018). In both direct and indirect mediator type of MFCs, soluble mediators are recycled in a process through simultaneous reduction (receiving generated electrons from cell) and oxidation (donating generated electrons to anode). While the mediator-less microbial fuel cells are categorized subject to the ability of the microbes to transport generated electrons directly or alternatively through self-synthesized electron shuttles from the cells to the surface of electrode.

Direct transfer of generated electrons in mediator-less MFCs is done by microorganisms known as ‘exoelectrogens’ whereas any other microorganism can be used in a mediator double MFC (Pandit *et al.,* 2018). The H-shaped double chamber MFC is built with the aerobic and anaerobic portions (Pushkar & Mungray, 2016). Microbes and a suitable substrate are placed in anaerobic (anode) chamber. The anaerobic degradation of the substrate releases electrons, which are carried to the cathode through an external circuit. At the same time, the protons created are selectively transported through the proton exchange membrane (PEM) to the aerobic side of the fuel cells chambers (Sharma & Li, 2010). Despite holding high potential, the MFC technology bears certain bottlenecks such as reduction of molecular oxygen (O_2) at the cathode, aeration of the anodic chamber via the salt-bridge, higher capital cost involved in fabrication & operation of MFC reactors, requirement of continuous supply of electrons-donoting substrate in anode chamber, expensive cathode catalysts as well as exchange membrane, low power output, and energy recovery in scaled-up reactors just to name a few (Khandelwal, 2021).

2.7.1 Design Parameters in Microbial Fuel Cell

Figure 2.2 represents a schematic diagram of a designed microbial fuel cell double chambered separated by a proton exchange membrane. The microbial fuel cell technology works on two different principles, namely (i) Batch mode type, and (ii) Continuous mode (Du *et al.,* 2007). Due to the efficient working principle of a Proton Exchange Membrane on account of protons transfer

across it, the electro-neutrality between the two sections in an Microbial Fuel Cell device is a vital pre-requisite (Dewan *et al.*, 2010).

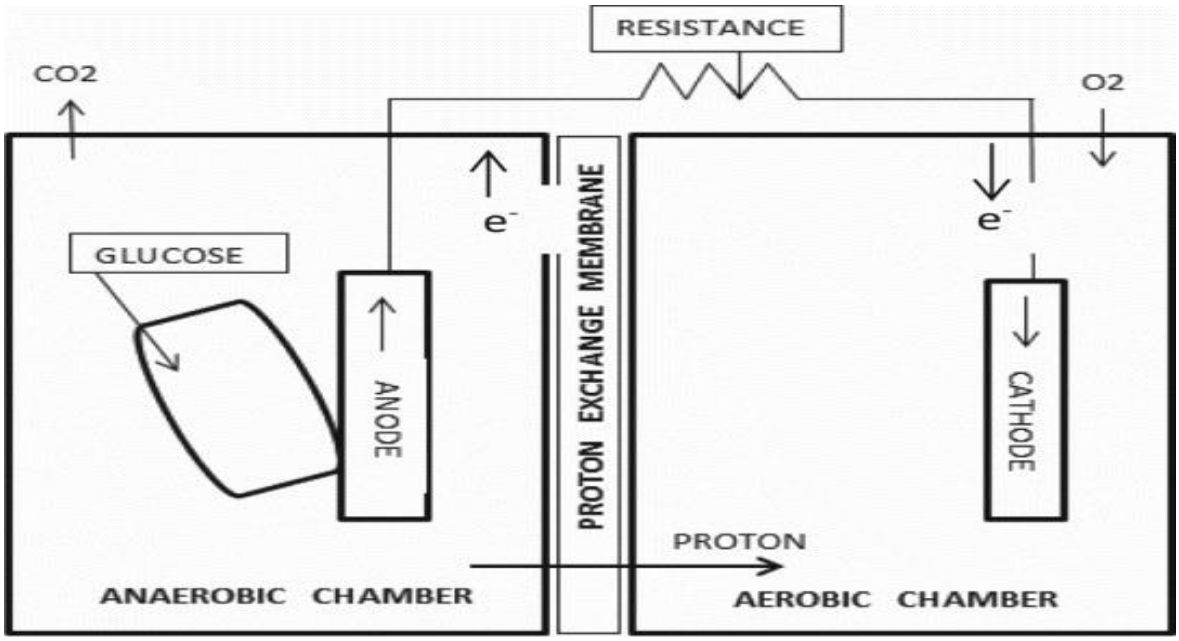

Figure 2.2: A typical dual chamber Microbial Fuel Cell (Akshay *et al.*, 2016)

Equations 2.1 and 2.2 represent reactions that take place in an MFC when using acetate as an electron donor. In the anodic chamber, the substrate is broken down and converted into acetate, (Equation 2.1).

ANODE: $CH_3COO^-_{(aq)} + 2H_2O_{(l)} \longrightarrow 2CO_{2(g)} + 7H^+_{(aq)} + 8e^-$ (2.1)

CATHODE: $2O_{2\,(g)} + 8H^+_{(aq)} + 8e^- \longrightarrow 4H_2O_{(l)}$ (2.2)

Assuming neutral pH and other conditions typical of an MFC environment as described by Logan (2008) and Song (2017), reduction half potentials (E'_H) of - 0.28 volts and + 0.82 volts for reactions at the chambers were observed.

The highest cell potential (E'_{emf}) in an MFC is achieved under an open circuit (maximum resistance conditions). In the case of acetate, the maximum emf is recorded with the balanced oxidation-reduction reaction shown in equation 2.3.

OVERALL: $CH_3COO^-_{(aq)} + 2O_{2(g)} + H^+_{(aq)} \longrightarrow 2CO_{2(g)} + 2H_2O_{(l)}$ (2.3)

The theoretical open-circuit voltage (OCV) which can be achieved under these conditions is a potential of + 1.1 V. (Logan *et al.,* 2006; Logan, & Regan, 2006). Limitations at the cathode, however, prohibit the E'_H, cathode of + 0.82 V from being obtained in practice. As a result, the MFCs fed with acetate has an OCV of less than + 1.1 V. So far, 0.80V has been achieved from an MFC using oxygen as an electron acceptor (Song, 2017; Cheng & Logan, 2007).

2.7.2 Internal Resistance and its Measurements:

In addition to cathode limitation, several other losses prevent the theoretical (E'_{emf}) from being achieved in the MFCs actual cell potential (E_{cell}) when measured with the multi-meter as described by Equation 2.4 below.

$$E_{cell} = OCV - IR_{int} \quad (2.4)$$

Where:

OCV – open circuit voltage, R_{int} – is the internal resistance in the MFCInternal resistance is a major factor affecting an MFC's performance. With a high (R_{int}), the MFC will have low output.

Methods for reducing (R_{int}), include: utilizing an electrolyte with more substantial ionic conductivity, expanding surface-area of carbon rods and decreasing space between the anode and cathode (Logan *et al.,* 2006 & Cheng, 2006).

The electrochemical impedance spectroscopy (EIS), power density peak, polarization slope, and current interruption methods are some of the techniques that can be used to calculate R_{int} (Logan, 2008). Current interrupt technique was used to investigate MFC internal-resistance in this study.

2.7.3 Substrate Concentration

The concentration of substrate in the anodic chamber has a direct impact on the MFC's performance. Low substrate concentrations restrict bacteria's biological activity in the anodic chamber, whereas high substrate concentrations saturate the anode and impede chemical reactions at the cathode (You *et al.,* 2006). Depending on the MFC's operation mode, substrate concentration has a different effect on performance (Batch or Continuous). In Batch mode MFCs, the substrate

concentration drops as the working time increases. In the continuous mode, the retention duration has a similar effect on the effective substrate concentration (Song, 2017).

2.7.4 Basics of Current Production by Bacteria in MFC

Microbial fuel cells (MFCs) use microbes to consume the substrate and produce power simultaneously. Several bacteria, for example, *Geobacter, Fibrobacter carcinogen, Clostridium lochheadii, Selenomonas ruminantium, and Megasphaera elsdenii* have been utilized in MFCs to generate electricity with varied Coulombic-efficiency (Chae *et al.,* 2009 and Parameswaran *et al.,* 2009). Since most of these bacteria can be found in rumen fluid, and therefore rumen fluid can be employed as an inoculum. Slaughterhouse effluent has high chemical oxygen demand (COD), biological oxygen demand (BOD), and moisture content levels, making it a good candidate for anaerobic digestion process. Slaughterhouse effluent also contains very high levels of the suspended organic particles such fat, grease, hair, grit, manure, as well as undigested feed, all of which contributes to organic matter decomposition. One of the most extensively utilized anaerobic treatment procedures for biogas production from abattoir wastes in poor countries is up-flow anaerobic sludge blanket (UASB) approach (Reddy *et al.,* 2014).

Slaughterhouse waste is a protein-rich substrate that can produce sulphide during anaerobic breakdown. Increased sulphide concentrations in the digester chamber can lead to the production of high levels of hydrogen sulphide in the biogas, and this can impede methanogens, (Dykstra & Pavlostathis, 2021). Besides sulphides, ammonia is produced during anaerobic digestion process, and this can raise the digester pH to values greater than 8.0, and inhibit the growth of some VFA-consuming anaerobic organisms (Moukazis *et al.,* 2018).

2.7.5 Power Output of MFCs Catalyzed by Bacteria

A study by Vendruscolo (2015) and Gil *et al.* (2003) showed that the reuse of wastewaters from many sources established that organic sources have an effect on MFC power output, for example starch processing and meatpacking wastewaters as observed by Heilmann and Logan (2006), and potato-producing plants (Nair *et al.,* 2023). Agricultural wastes such as corn stover and carbohydrates were tested as fuel after pretreatment (Cercado *et al.,* 2010). Chaturvedi and Verma (2016) in their findings, affirmed impact of organic sources on power output in microbial fuel cells

and that power density varies from 1 mW/m^2 to $3600 mW/m^2$, with most values ranging between 10 mW/m^2 and 1000 mW/m^2. In MFCs, a diverse range of microorganisms have been employed to generate energy. For example, Lin *et al.* (2017) employed bacteria such as *Escherichia coli* for power generation in MFC for the first time. Literature has shown that pure microbial cultures have numerous limitations for technical application because of the necessity for sterile conditions, which leads to high costs. In contrast, mixed cultures or microbial consortia are robust and more productive than pure strains (Jiang *et al.,* 2017).

2.7.6 Theory of Microorganisms Growth Kinetics

This study used the existing inhibitory growth models and bio-kinetic parameters to model microorganisms' growth kinetics.

2.7.6.1 Kinetics of Anode Respiration

2.7.6.1.1 Models of Substrate Utilization and Current Density at the Anode

The kinetics of anode respiration bacteria (ARB) are closely linked to energy generation and substrate use. Several models have been devised to determine the kinetic parameters of ARB due to the participation of the anode biofilm (Song, 2017). When selecting kinetic parameters, the gradient in substrate concentration and potential difference in between terminal electron acceptor and the anode terminal are two factors to consider (Lee *et al.,* 2009). The Monod model (Equation 2.4), in which bacteria's development is limited by a single substrate, was found to be the most often utilized model (Liu & Bruce, 2004; Liu *et al.,* 2005). However, since this model ignores the effect of self-inhibition, an enhanced Haldane Andrew's kinetics model (equation 2.6) has been presented, which includes the substrate inhibition effect, which may result from a high Osmotic pressure or substrate toxicity (Manchala *et al.,* 2017; Priyadarshini *et al.,* 2021) (Equation 2.5). Han-Levenspiel model (equation 2.7) was used to demonstrate microbial growth that stops completely when a critical inhibitor concentration (S_m) was reached. It accounts for different types of inhibition (competitive, uncompetitive, and non-competitive) (Priyadarshini *et al.,* 2021).
Monod Model:

$$r = r_{max} * \frac{S}{(K_S + S)} \qquad (2.5)$$

Andrew's Kinetic Model:

$$r = r_{max} * \frac{S}{\left(K_S + S + \frac{S^2}{K_{IH}}\right)} \quad (2.6)$$

Han-Levenspiel Model:

$$r = r_{max} * \frac{S\left(1 - \frac{S}{S_m}\right)^n}{S + K_S * \left(1 - \frac{S}{S_m}\right)^m} \quad (2.7)$$

Where:

r- Is the substrate utilization rate ($gL^{-1}.d$), the maximum output current density (mA/m^2) or maximum power density (mW/m^2), or voltage (mV) at each substrate concentration; $\mathbf{r_{max}}$ – Is the substrate utilization rate ($gL^{-1}.d$), the maximum output current density (mA/m^2) or maximum power density (mW/m^2), or Voltage (mV) among all ranges of substrate Concentration; **S** – Is the substrate concentrations (mL). ; $\mathbf{K_S}$– Is the half-saturation coefficient (gL^{-1}). ; $\mathbf{K_{IH}}$– Is the self-inhibition coefficient (gL^{-1}). ; $\mathbf{S_m}$– Is the critical inhibitory concentration above which growth stops (gL^{-1}). ; **n** and **m**– Are the empirical constants used to account for different types of inhibition.

Oliveira *et al.* (2007) observed that the basic model (analytical and semi-empirical model) and the mechanical models are the two types of fuel cell models commonly used. Analytical models are typically one-dimensional (1-D) models, with the primary goal of predicting the cell or current output and the effect of various parameters on them. However, they do have some drawbacks, including, but not limited to, accuracy limitations for operation and design conditions. In another study by Chezeau and Vial (2019), the Monod model is the most widely used kinetic model in describing bacterial growth in general and molecular hydrogen (H_2) producing bacteria in particular. In a similar study Lee *et al.* (2013) employed Monod model to calculate kinetics of *S. putrefaciens* biofilm generation in Leachate fed-batch MFC. The results obtained for the half-saturation coefficient (K_S) of bacteria in an organic matter-fed Microbial Fuel Cell was 214.6 gL^{-1}, and the growth yield coefficient was found to be 0.65.

2.7.7 Automation of the Microbial Fuel Cell

With the increasing need for measurement systems in every aspect of life, it has been essential for a data logger system to save the acquired data values to analyze its trends. Open-source electronic prototyping platforms such as Arduino are extensively used in projects due to the ease of programming and their ability to interface several additional modules as and when required, with more ease. These platforms can be extended for use as monitoring devices and data loggers (Bagyaveereswaran *et al.*, 2017). In this work, a low-cost portable voltage measurement and data logging system was designed using an Arduino Mega board.

2.7.7.1 Hardware Description of Arduino UNO Mega

The Arduino device is a microcontroller board which is based on the ATmega1280 (Blum, 2013). A prototype composed of an Arduino (mega) board with 10 bits analog to digital converter (ADC) resolution, LCD, and voltage sensor device interfaced with current-sensor device which are then connected on a breadboard is shown in Figure 2.3. It has 54 digital input/output pins, 14 of which can be used as Pulse Width Modulation (PWM) outputs, 16 analog inputs, 4 Universal asynchronous receiver/transmitter (UARTs) (hardware serial ports), a 16 MHz crystal oscillator, a Universal Serial Bus connection, an In-Circuit Serial Programming (ICSP) header, and a reset button. It, therefore, contains all the components needed to support a microcontroller by connecting it to a desktop computer or a laptop with a USB cable and/or by powering using an alternating current and direct current adapter or a normal battery (Webb & Møller-Holst, 2018; Nastro *et al.*, 2017).

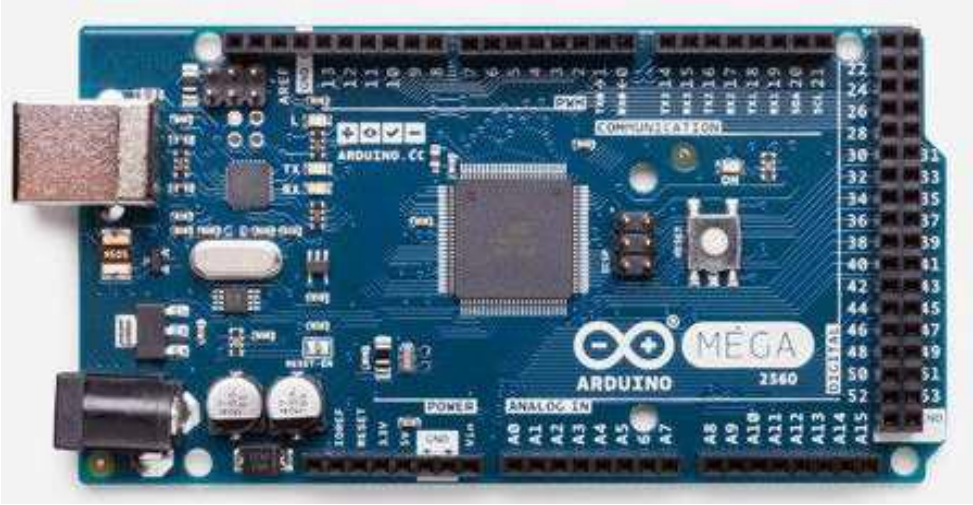

Figure 2.3: Arduino Mega Board (Babu *et al.,* 2019).

2.7.7.2 Voltage (potential) Sensor

An easy-to-use module called a voltage sensor is suitable for use with Arduino or any other micro-controller with a 5 V input tolerance to measure external voltage higher than Arduino's 5 V maximum allowable value (Mulder *et al.,* 2008). Figure 2.4 shows the voltage sensor module's pins.

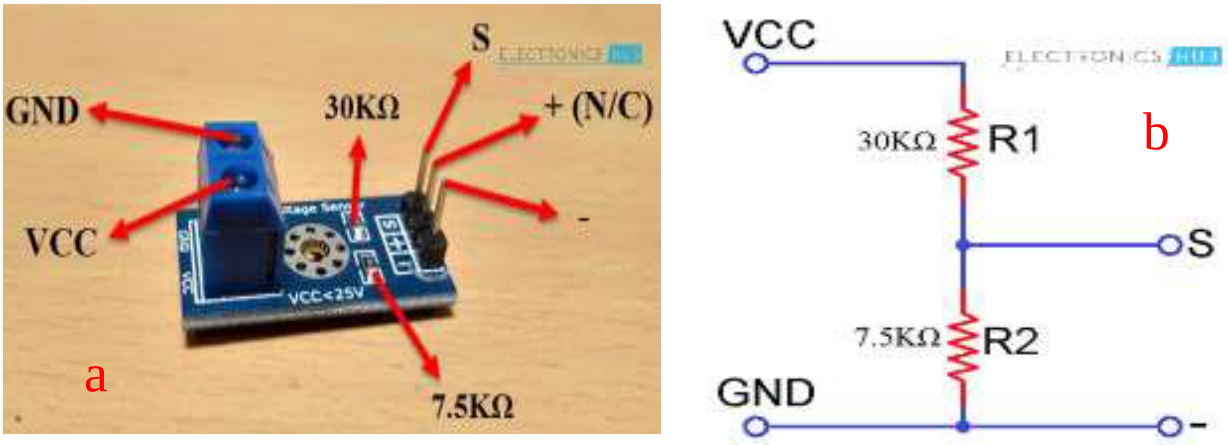

Figure 2.4: A voltage Sensor Module (a) Voltage sensor. (b) Internal Circuit of Voltage sensor Webb and Møller-Holst (2018).

Where:

- VCC: - is (+) terminal of voltage to be measured

- GND: -is (-) terminal of voltage to be measured
- + means Not connected (N/C)
- – is the GND of Arduino
- R1/R2 represent the Resistors
- S is the Switch

2.7.7.3: The Current Sensor Module

The ACS712 Current Sensor is a gadget of Allegro Microsystems that can be used to precisely detect both alternating and direct currents. The sensor uses the Hall Effect, and an integrated circuit (IC) has a built-in Hall Effect device. Analog voltage produced by ACS712 Current Sensor is proportional to both AC as well as DC (Słowik *et al.*, 2017).

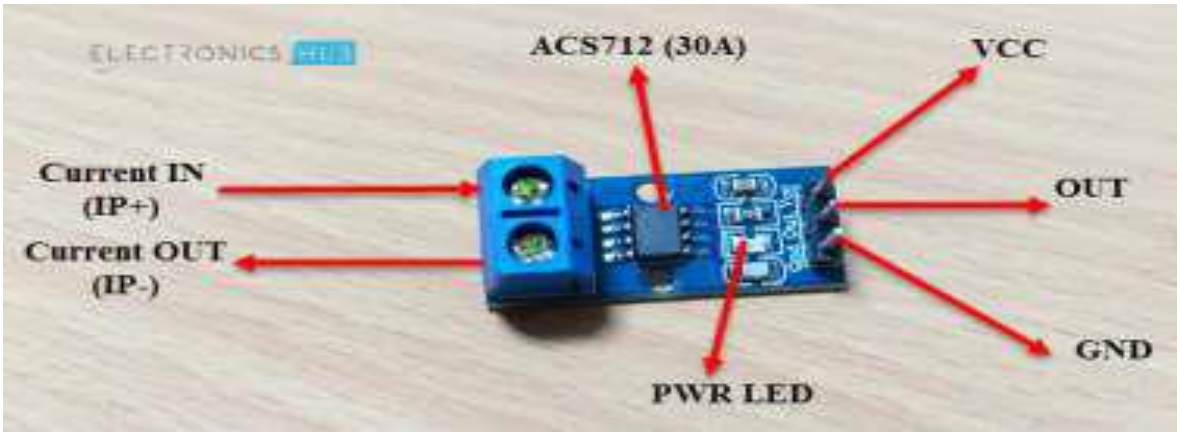

Figure 2.5: An ASC712 Current Sensor Module (Webb and Møller-Holst, 2018)

- VCC: - is (+) terminal of voltage to be measured (0 – 25 V)
- GND: - is (-) terminal of voltage to be measured
- OUT: - is the Analog Input of Arduino
- +: - is Not connected (N/C)
- –: - is the GND of Arduino

In this research, H-shaped double chamber MFCs were set up using a micro-controller board "Arduino UNO" and sensors device for monitoring the voltage (potential) and current output generated from market fruit waste (tomato fruit waste) and cow dung.

CHAPTER THREE

MATERIALS AND METHODS

This chapter describes all reagents, instruments, as well as procedures used to meet the study's goals.

3.1 Materials and Reagents

All chemicals were used in their original form; they were never further refined. The methods indicated that they belonged to the general or analytical grades. The following categories apply to them:

Bacterial studies: Goat Rumen Fluid and Cow-dung. Petri dishes, Autoclave, Analytical grade inorganic reagents KH_2PO_4, K_2HPO_4, $MgSO_4$, NH_4SO_4, $CaCl_2$, $FeSO_4$, Carboxy Methyl Cellulose (CMC) and Agar. All reagents used were sourced from commercial provider; Sigma-Aldrich Co. Ltd and utilized without additional purification).

Proximate analysis: Weighing balance (Kitchen balance – 5 kg), Dosi-fibre unit, Oven, thermometer, muffle furnace, Crucibles, Kjeldahl apparatus, Soxhlet apparatus, Mixed indicator, Volumetric flasks, Distlled water, KOH, Antiforming agent (n-octanol), Petroleum Ether, analytical grade HCl, H_2SO_4, Magnesium Oxide (Catalyst) and 2 % Boric Acid solution.

Double Chamber H-Shaped MFCs: Plastic containers, wicks, Sodium Chloride (NaCl), Agarose, Elctrode - Graphite rods, pH meter, Copper wire, Laboratory thermometers, Polyvinyl Chloride pipes, fruit wastes samples.

Automation of Microbial Fuel Cell: A breadboard, designed Arduino device, a Liquid Crystal Display (LCD), voltage, and current devices

Electricity production: pH meter, thermometer, water bath, thermostatic heater, General grade reagents, NaOH and Vinegar were used for the purposes of adjusting MFCs pH conditions.

Bio-fertilizer: Biosludge, Earthworms, Homemade Vermicomposter Chamber, Fourier Transform Infrared Spectrophotometer (FT-IR), Shimadzu (Model IRAfinity-1S).

Data Analysis: Software used; Microsoft excel 2013 and 2016, Minitab 17, Origin 8 and ANOVA

3.2 Study Area

In this research samples utilized included goat rumen fluid from a slaughterhouse in *Huruma* Estate (1˚15'16. 4" S 36˚52'42.4"E), fruit wastes from *Fig-tree Ngara* market (1°16'27.9" S 36°49'20.6" E), *Muthurwa* market (1˚17'13.3"S 36˚49'56.2"E), *Kangemi* market (1˚15'52.0"S 36˚44'54.4"E), and *City park* market (1˚15'42.1"S 36˚49'33.6"E), all located in the City Nairobi. Figure 3.1 shows the sampling locations.

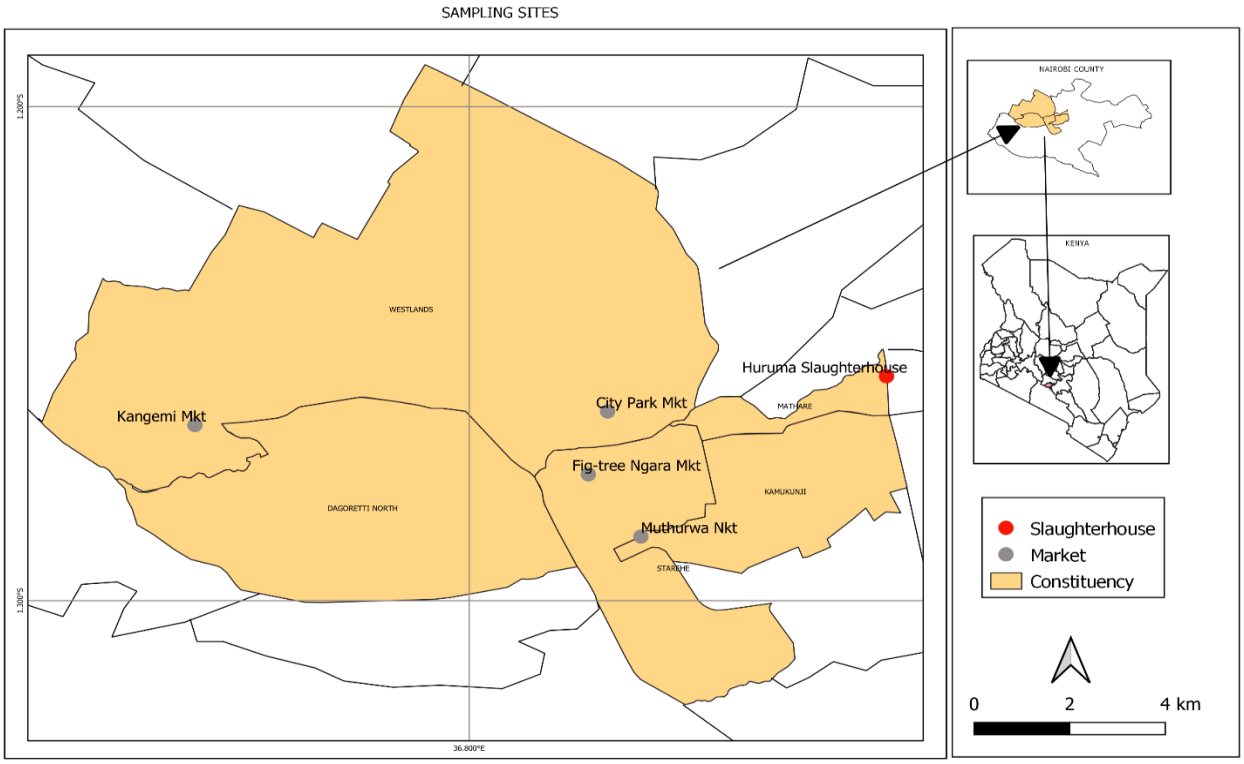

Figure 3.1: The map of Nairobi Sub-Counties and the sampling sites

3.3 Analytical Procedures

This section describes the methods that were employed in the study. All reagents were of analytical grade unless otherwise noted. Laboratory experimental procedure was done in three replicates, and

the mean ± standard deviation values measured for the purpose of guaranteeing the validity and reliability of the data obtained.

3.3.1 Sampling of Wastes

Fruit wastes samples were collected in clean plastic bucket containers from selected markets in Nairobi County in four different sampling sites analysis. For bacteriological studies, samples of cow rumen fluid as well as cow-dung were both sampled from *Huruma* slaughterhouse in five-liter container and in sampling bags. These were sealed and then transported for bacteriological analysis at the University of Nairobi Microbiology Laboratory. (Kamau *et al.,* 2018). This study's selection of landfill and slaughterhouse waste samples was motivated by three factors: first, the amount of waste produced everyday and its management; second, the presence of carbohydrates levels; and third, the desire to advance the circular economy concept (Arias *et al.*, 2023).

3.3.2 Sample Pre -Treatment Procedure

The dirt was removed from waste samples by washing and discarded. Waste was thereafter segregated according to the fruit source, and each sample was kept at ambient temperature in the laboratory for a period of three days to allow it to decompose naturally. Fruit wastes were then size reduced by cutting to small pieces with a knife, then blended using a kitchen mixer to speed up the anaerobic bacteria's digesting process.

3.3.3 Bacteriological Analysis

In this study, a method of standard-plate-count test (SPCT) was utilized to determine total bacterial count in both rumen fluid and cow-dung samples (Mathuriya, 2013). The total viable count (TVC) of microorganisms process was carried out using the Miles and Misra, (1938) method as described by Masoura & Gkatzionis (2022). As shown in Equation 3.1 below.

$$\mathrm{CFU/mL} = \frac{\text{Number of colonies} * \text{Total dilution factor}}{\text{Volume of culture plated in mL}} \tag{3.1}$$

3.3.3.1 Reagents and culture media preparation

Analytically graded inorganic reagents K_2HPO_4 1.25 g, KH_2PO_4 1.5 g, $MgSO_4$ 20 g, NH_4SO_4 6.0 g, $CaCl_2$ 0.12 g, $FeSO_4$ 0.0015 g, Carboxy Methyl Cellulose (CMC) 10.0 g and nutrents agar 20 g were dissolved in 1000 mL double distilled water (ddH_2O) to prepare the culture media. The prepared media was then sterilized by autoclaving at 121 ℃, 15 psi for 35 minutes and subsequently introduced into sterilized petri dishes that were initially oven dried at 180 ℃ for 1 hour.

3.3.3.2 Isolation of bacteria

At first, 1 mL of the rumen fluid was diluted with 9 mL sterile double distilled water (ddH_2O)(v/v) where 10^{-1} to 10^{-5} serial dilutions were prepared. Then 0.3 mL of samples was taken from each dilution and streaked into petri dishes containing CMC medium and incubated at 37 ℃ for 24 hours (Cowan & Steel's, 1974). After 24 hours of incubation, no clear zone was formed around the bacterial culture. Therefore iodine was applied in order to visualize the clear zones produced by cellulolytic bacteria. Subsequently, the well grown colonies were chosen to obtain a pure culture of bacteria using two loops of an inoculating needle to transfer and inoculate onto a petri dish containing CMC medium (Cappucino & Sherman, 1987). The selection of cellulolytic species was conducted based on the ratio of clear zone to colony diameter after 48 hours on carboxy methyl cellulose (CMC) media. The procedure was repeated for 1 gram of Cow dung.

No ethical approval was needed in theses experiments, since rumen fluid was collected from rumen after normal slaughtering of cattle.

3.3.4 Proximate Properties Analysis

The proximate analyses were done on the homogenized waste samples. Analyzed parameters included; fat content, nitrogen-free extract, ash content, moisture content, crude proteins, fibre content, carbohydrates and energy levels using procedures for their respective analyses as outlined in Association of Analytical Chemists techniques (AOAC, 1990; Braga *et al.,* 2003).

3.3.4.1 Analysis of Moisture Content

Content level of moisture in fruit waste was evaluated using oven drying technique (Charbel *et al.,* 2015; Nielsen, 2010; Carneiro *et al.,* 2018). A quantity of 1.00 ± 0.01 grams of fruit-waste sample was put in a clean crucible and weighed. Waste sample in the crucible was then dried at 105 ℃ for 6-12 hr until it attained a steady weight. It then underwent a 30-minute cooling process in a desiccator before being weighed again. Using Equations 3.2 and 3.3, the percentage of moisture content was calculated.

$$M_{wet} = \frac{W_1 - W_2}{W_1} * 100 \quad (3.2)$$

$$M_{dry} = \frac{M_{wet}}{1 - M_{wet}} \quad = \text{Dry Matter (DM)} \quad (3.3)$$

Where:

W_1 = sample weight before heating plus the weight of crucible, W_2 = sample weight after heating plus weight of the crucible, M = moisture content.

All other analyses were carried out using samples free from moisture.

3.3.4.2 Assessment of Ash Content

Amount of ash content in the sample were tested by heating a sample on a designed muffle furnace at a temperature of 600 ℃ for 2 hours. This was cooled and then the sample weighed again. An empty clean crucible was weighed and its readings recorded. A mass of 1.00 ± 0.01 grams of sample was placed in a dry, clean crucible and weighed. It was thereafter, ignited at 600 ℃ for 2-4 hours and thenweighed again. Equations 3.4 and 3.5 were used to determine the ash levels.

$$\text{Ash(wet)} = \frac{W_5 - W_3}{W_4} * 100 \quad (3.4)$$

$$\text{Ash(dry)} = \frac{\text{Ash(wet)}}{100 - \text{Moisture content}} * 100 \quad (3.5)$$

Where: W_5 = weight of crucible + ash (after ignition), W_3 = weight of the empty crucible and W_4= sample weights prior to ignition + crucible weight.

3.3.4.3 Analysis of the Crude Protein

According to Chang and Zhang (2017) and Di Marzo *et al.* (2021), the Kjeldahl method was used to determine protein levels in samples. 1.00 ± 0.05 grams of dried fruit sample was put in a digestion tube and about 10.0 ± 0.2 mL in volume of Sulphuric acid (H_2SO_4) was added. The sample was then heated gradually until it attained a temperature of 200 ℃ in a heating digestion block. Thereafter, NaOH was added to make mixture alkaline. This formed a solution of ammonium sulphate and was allowed to cool. The digest was later transferred to a clean 250 mL volumetric flask (VF) and topped-up to the mark using prepared distilled water. About 5.0 ± 0.1 mL of the sample in the volumetric flask was pipetted into a distillation flask, and about 200 mL distilled water and magnesium oxide catalyst (Heavy) added in to the flask. 10 mL of 2 % boric acid solution was put into the receiver Erlenmeyer conical flask, a few drops of mixed indicator added and a receiver conical flask placed under the condenser of the steam distillation apparatus so that the end of the tip of a condenser was just inside the boric acid-indicator solution. After about 100 ± 10 mL of distillate was collected, the distillation was stopped, and subsequently, the distillate was titrated against a standard 0.01 N hydrochloric acid (HCl) solution. Equations 3.6 and 3.7 were then applied to determine the total amount of crude protein.

$$\text{Crude protein} = 6.25 * \%\,\text{N} \tag{3.6}$$

$$\%\text{N} = \frac{(\text{S} - \text{B}) * \text{N} * 0.14 * \text{D}}{\text{W}_\text{s} * \text{V}} * 100 \tag{3.7}$$

In the equation, (S) stands for titration reading of sample, (B) for reading titration of blank, (N) for the HCl normality, (D) for sample dilution following digestion, and (V) for the volume utilized for distillation, (W_s) = initial weight of sample and 0.14 = milli-equivalent weight of Nitrogen (N).

3.3.4.4 Calculation of Crude Fat (Lipids)

Using the Soxhlet equipment and the ether extract procedure, the total amount of crude fat in the samples was determined (Ramluckan *et al.,* 2014). A plate was dried at 105 ℃ for 2 hrs and then cooled in a desiccator (López-Bascón *et al.,* 2020). A mass of 2.5 ± 0.1 grams of dried waste sample was wrapped in a filter paper and then loaded into a fat-free thimble and then placed into

a thimble holder. The receiving round bottommed flask was filled with 75 mL petroleum ether and then fitted into the Soxhlet device, after which the extraction process was started. The solvent vapour passed through side-tube into the reflux-condenser unit, where it condensed before dripping back into the thimble chamber. Once the thimble chamber was full, the analyte of interest in the sample drained back into round bottomed flask through a siphoning device. Since extracted analytes have higher boiling points than extraction solvent, they accumulate in the round bottom flask while solvent recirculate. After extraction for about 4-6 hours, achieved extract analyte was transferred into a glass dish and placed in a water bath (35 ℃). Ether was then concentrated by evaporation before extract clean-up and analysis. Equation 3.8 was employed to calculate the total crude fat.

$$\text{Crude lipids} = \frac{\text{Weight of ether extract}}{W_s} * 100 \qquad (3.8)$$

Where: W_S - is the initial weight of the sample.

3.3.4.5 Determination of Crude Fibre

In determining crude fibre, 1.0 ± 0.05 g of fruit-waste sample was obtained and transferred into a clean porous crucible (Möller, 2014). The crucible containing waste sample was thereafter loaded into a Dosi-fibre equipment. Into each of the column in the fibre unit, a volume of 150 mL 1.25 % sulfuric acid (H_2SO_4) solution was added. A foam-suppresser (n-octanol was used as an antifoam) was added dropwise to prevent entrained air from forming and increasing the viscosity, which may lead to defects in the product. The mixture was allowed to boil for 30 minutes and then connected to a vacuum to drain the sulfuric acid. It was then washed three times with 30 mL of hot deionized water. After draining the last wash, about 150 mL of 1.25 % preheated laboratory grade potassium hydroxide (KOH) and 3-5 drops of foam-suppresser were added. The mixture was then boiled for 30 minutes and then washed with distilled water. The sample was dried at temperature of 150 ℃ for one hour, cooled, and weighed (W_6) using analytical balance. Additional drying of the sample took place using a muffle furnace at a temperature of 55 ℃ for a period of 3 hrs, cooled, and re-weighed (W_7). The amount of crude fiber on the sample was then calculated using Equation 3.9.

$$\text{crude fiber} = \frac{W_6 - W_7}{W_s} * 100 \quad (3.9)$$

Where: W_S - initial sample weight, W_6 - crucible plus weight of digested sample and first drying, and W_7 – crucible plus sample-weight after the second drying (muffle furnace).

3.3.4.6 Determination of Nitrogen Free Extract

Amount of soluble carbohydrates is represented by nitrogen-free extract. It was calculated from the difference between the dry matter and all the other proximate properties (Equation 3.10 and 3.11).

$$\%\ \text{NFE} = \%\ \text{DM} - (\%\ \text{C.L} + \%\ \text{C.P} + \%\ \text{Ash} + \%\ \text{C.F}) \quad (3.10)$$

$$\%\text{DM} = M_{\text{dry}} = \frac{M_{\text{wet}}}{1 - M_{\text{wet}}} * 100 \quad (3.11)$$

Where: NFE stands for a nitrogen-free sample, DM for dry matter, CL for crude lipids, CP for crude protein, and CF for crude fiber Nielsen (2010).

3.3.4.7 Carbohydrates Content

Carbohydrate level in the market fruit sample was analyzed by the different methods described by Shakappa & Talari (2016) and Devindra *et al.* (2016). The levels of carbohydrate content was calculated using Equation 3.12 below. The sum of the other attributes was subtracted from 100.

$$\text{Carb} = 100 - \%\ \text{M.C} + \%\ \text{A.C} + \%\ \text{C.P} + \%\ \text{C.L} + \%\ \text{C.F} \quad (3.12)$$

Where: Carb is carbohydrate content, MC is the moisture content, CL is crude lipids, CP is crude protein, AC is the ash content, and CF is crude fiber.

3.3.4.8 Determination of Energy Levels

Fruit waste samples' energy content was determined by summing up the crude protein (equation 3.6) and carbohydrates content (equation 3.12) multiplying the summation by four and adding the

number of oil lipids (equation 3.8) multiplied by 9. Finally, the findings were presented as calories per 100 grams of fruit waste sample (Nielsen, 2010).

$$\text{Energy (kcal/100 g)} = (\text{C.P} + \text{Carb}) * 4 + \text{C.L} * 9 \quad (3.13)$$

Where: Carb is carbohydrate content, CL is crude lipids, CP is crude protein.

3.4 Microbial Fuel Cells Construction

The microbial fuel cells were constructed as discussed in section 3.4.1.

3.4.1 Fabrication of the Double Chamber MFCs

A double chamber H-shaped MFC was fabricated using plastic bowl containers, wicks, Polyvinyl chloride (PVC) pipes, driller, pipe joiners, and masking tape. Two 2 L plastic containers were used as the anodic and cathodic chambers. The lids of the 2 L plastic containers were perforated with two small holes. to allow an entry point for the external conductor which consisted of a copper wire. The wire was attached to Carbon rods (electrodes) whose dimensions were recorded as 0.7 cm in diameter and 5.7 cm long. Wicks were boiled in a solution of 1 M NaCl solution and 3 % agarose for 15 minutes period before being frozen at - 4 ℃ to solidify and form a salt bridge. After the prepared salt-bridge had hardened, it was made leak-proof by passing it through polyvinylchloride pipes and attaching it to cathodic and anodic chambers with an adhesive glue as shown in Figure 3.2 (Kamau *et al.*, 2017; Mbugua *et al.*, 2020).

Figure 3.2: (a) Boiling Wicks and (b) Double chamber microbial fuel cell setup

3.4.2 Circuit Assembly

Figure 3.3 below comprises a photo showing the design of an open circuit double chamber Microbial electric cell, with an electronic digital multi-meter data acquisition system model DT9205A connected to copper wires emanating from both cathode and the anode electrodes used in monitoring the daily current and voltage output.

Figure 3.3: Microbial fuel cells open circuit voltage

3.5 Experimental Procedure for a Microbial Fuel Cell Using Market Fruit Waste

This study used fruit wastes coupled with rumen fluid in microbial fuel cells anode chamber. Goat rumen fluid provided microorganisms, which aided in breaking down of the substrate. These microorganisms required no safety measures during their use.

3.5.1 Control procedure from fruit wastes and Goat rumen fluid

In the control experiments, about 200 mL of blended tomato, Banana, avocado, watermelon, as well as mango samples of fruit wastes were loaded into a 2 L plastic bowl fabricated Microbial fuel cells and voltage produced recorded daily using a data acquisition system (multimeter model-DT9205A) for five days. Anaerobic digestion (anode reaction) process setup was not inoculated with goat rumen fluid and therefore, this was then considered a control experiment. The same was done for rumen fluid as a blank with no substrate provided to the microbes and current and voltage readings were obtained from the setups for 22 days using a digital multimeter. Procedure 3.5.1; was repeated three times for purposes of computing the means and standard deviations of the outputs as well as to guarantee the validity and reliability of the data obtained.

3.5.2 Electricity Generation from fruit wastes samples inoculated with Goat Rumen Fluid

The fruit samples were individually and separately reduced in size by chopping thereafter homogenized using a blender, after which 100 mL of each piece was loaded into the anodic chambers of the respective Microbial Fuel Cells. The same procedure was repeated with a mixture of all fruit samples. An aliquot of 250 mL goat rumen fluid was added into anode chamber to intentionally introduce bacteria, whereas distilled water (500 mL) was added into cathode chamber to supply oxygen (O_2) molecule as terminal-electron-acceptor. The voltage and current produced was measured and recorded daily for 22 days. Procedure 3.5.2 was repeated three times.

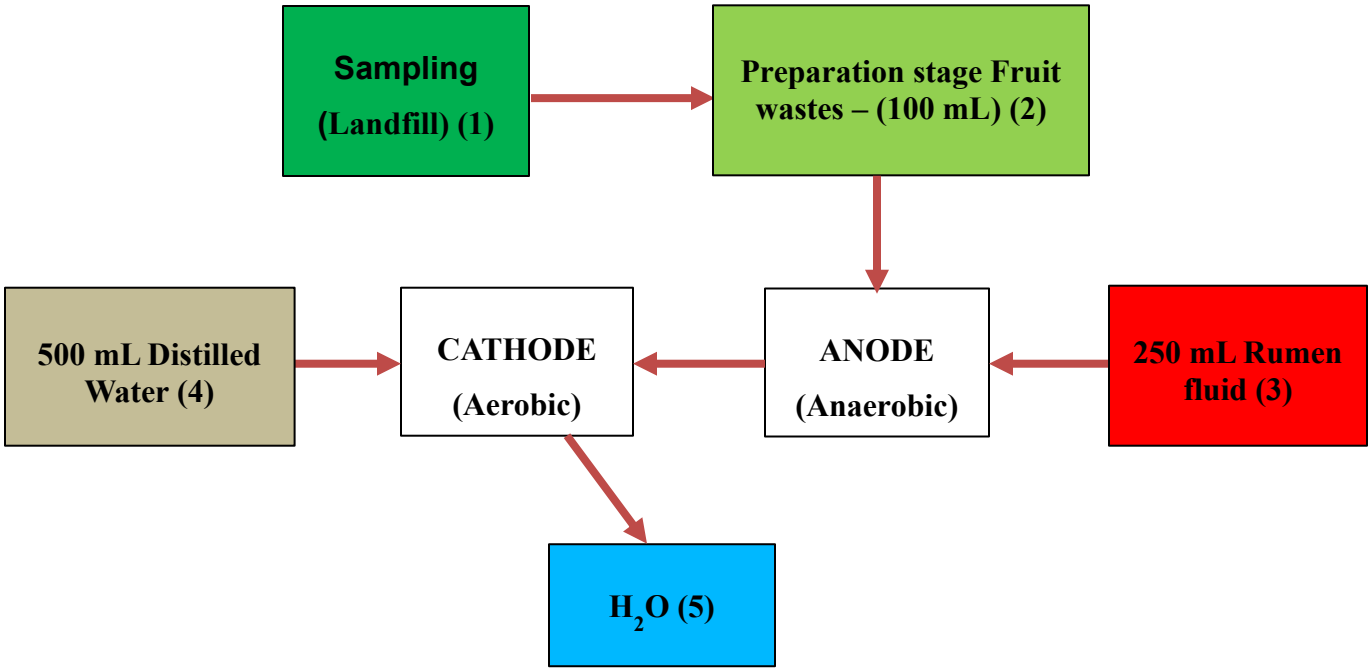

ANODE: $CH_3COO^-_{(aq)} + 2H_2O_{(l)} \longrightarrow 2CO_{2(g)} + 7H^+_{(aq)}$ (3.14)

CATHODE: $2O_{2\,(g)} + 8H^+_{(aq)} + 8e^- \longrightarrow 4H_2O$ (3.15)

Figure 3.4: Graphical representation of experimental procedure in a double-chamber MFC

3.5.3 Output in terms of voltage and current

The results of voltage (potential) and current from a double chamber MFC were recorded at 24-hour intervals for 22 days. The equivalent power of each of the 22 days' maximum generated voltage and the current output was recorded, and power density was estimated using equations (3.16) and (3.17).

$$P = VI \tag{3.16}$$

$$\text{Power Density} = \frac{\text{Power}}{\text{TSA}} \tag{3.17}$$

Where: P denotes power, V denotes voltage, I denotes current and TSA - is the total surface area.

3.5.4 Optimization of Microbial Fuel Cell Parameters

Procedures were administered to optimize MFC operation conditions. The optimized parameters included external resistance, Microbe concentrations, temperature, and pH.

3.5.4.1 Optimization of Microbe Concentration

The influence of microbe concentration on electricity generation was investigated. 100 mL of homogenized fruit wastes was introduced into MFC's anodic chamber, 250 mL of rumen fluid too was added, and the current and voltage monitored daily for 22 days. The procedure was repeated using 300 mL and 500 mL volumes of rumen fluid. The current and voltage readings were obtained, and analysis was done.

3.5.4.2 Optimization of External Resistance

The constructed double chamber MFC was used to determine impact of external load on generated voltage. The anodic chamber was fed with 100 mL of different fruit wastes and 250 mL rumen fluid. Four resistors of various capacities, i.e., R_1= 1 kΩ, R_2= 5 kΩ, R_3= 10 kΩ, and R_4= 15 kΩ were connected to copper wires from MFC chambers and the generated current and voltage recorded. The internal resistance was investigated using the current interrupt technique (Wei *et al.,* 2021). Figure 3.5 shows a 5 kΩ ± 5 % resistor.

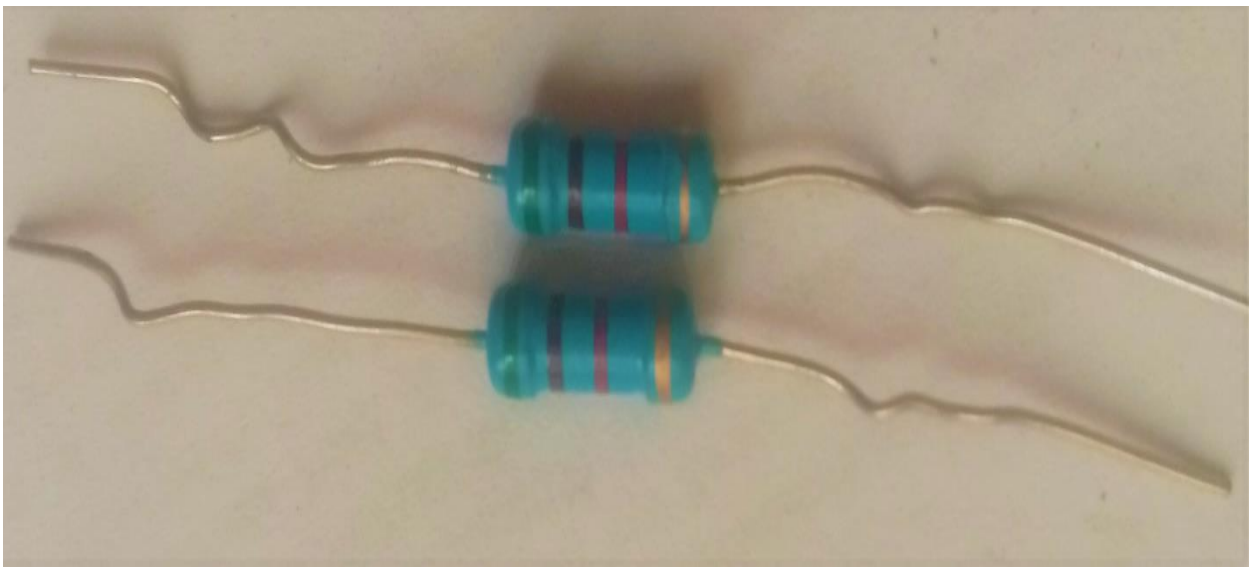

Figure 3.5: Picture of 5 kΩ resistor

3.5.4.3 pH Variation

In investigating the effect of pH on generation of voltage and current outputs from MFCs, the anaerobic section (anode) was fed with 100 mL of blended fruit waste samples and inoculated with 250 mL goat rumen fluid. In this set, the pH of individual waste, waste mix and goat rumen fluid were taken before loading to the anodic chamber. pH influence was observed by loading blended fruit sample to rumen in a ratio of 1:2 in MFC and pH conditions adjusted by NaOH, vinegar solution and a calibrated pH meter. The working pH values that were investigated were 2, 7 and 11.

A cumulative daily electricity generated was recorded by digital multimeter model DT9205A for 22 days, and the voltage and current data were collected, evaluated, and analyzed.

3.5.4.4 Optimization of Temperature

In the experiments on the influence of temperature on potential and current generation from the MFCs, anodic chambers were fed with 100 mL of different market fruit wastes (substrate) and further inoculated with 250 mL of goat rumen fluid. The setup was maintained at different temperatures, namely 25 ℃, 37 ℃, and 55 ℃ in a water bath (Figure 3.6), and for each temperature, the voltage and current readings monitored, recorded, and analyzed.

Figure 3.6: Temperature variation in a water-bath

3.5.5 Kinetic Modelling Studies

Batch microbial fuel cell containing specific fruit waste with different ratios of carbohydrates, moisture content, protein, Ash, Nitrogen Free Extract and crude fat content were all set-up and power generation was carried out at varied pH values, varied temperature, microbe concentrations and various additional operating parameters. Kinetics which describe and evaluate power output was achieved when fitting acquired experimental measurements to documented kinetic models in trying to predict bacterial growth and substrate degradation rates, Substrate self-inhibitory effects as well as Critical inhibition coefficients with respect to power generation per given type of fruit wastes (Song, 2017).

Resource recovery rates from selected market fruit waste samples in MFC were modeled using Monod kinetic model, Haldane Andrew's kinetic model and Han-Levenspiel kinetic model (Chezeau and Vial, 2019).

3.5.6 Automation of the Microbial Fuel Cell

A breadboard was used to interface and connect a designed Arduino device, as well as voltage, and current devices to form a prototype. Designed MFC injected with cow manure was used to test the Arduino UNO's ability to monitor cell potential. Volume each chamber was 1500 cm^3 and contained five-carbon graphite rods giving a total surface area of 0.00666 m^2. A 1000-ohm external resistor was employed in the experiment. NaCl salt bridge was used to separate the compartments. Cow dung and tomato waste were used to inoculate the anode chamber, while the cathodic part was filled with distilled water. Initial pH of the anolyte and catholyte in the process was 7.23.
The voltage of the cells was measured every minute using Arduino device as well as digital multimeter (model-DT9205A). Arduino UNO had 10 bits analog to digital converter (ADC) resolution, meaning that when using the default voltage reference of 5 V, every digital unit represented 4.88 mV, which is a low resolution. To overcome this anomaly, a voltage reference of 0.83 V was set to improve the ADC resolution. The AA battery of 1.2 V was used as a constant source of DC power. It was then implemented as a voltage divider using a resistor of 33 kΩ as well as 32 kΩ of internal resistance of the Arduino board. The convectional principle of the voltage divider equation in this study was Vf = Vi * 32/(32+33), it was expected that final voltage would

be about 0.73 mV. After the multi-meter recordings, the output was 0.83 mV; this voltage (0.83 mV) was taken as the actual voltage and incorporated into the code. Thereafter current readings were recorded across LED. The diagram shown in Figure 3.7 demonstrates the flow process. Dip Trace v3.3.4 was used to connect the components to the device (sensor), as shown in the schematic design (Figure 3.8). In Figure 3.7, the block diagram shows the link of the components to the Arduino board. The current and voltage sensors are connected to analog pin A0 and pin to A3, as shown in Figure 3.8.

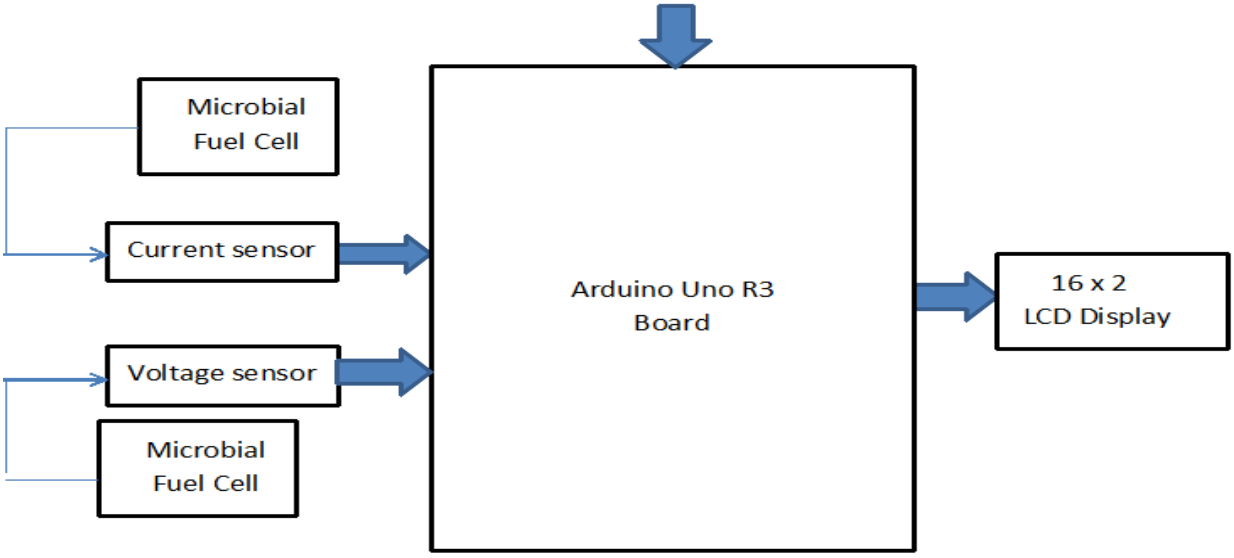

Figure 3.7: Flowchart for Arduino board

The resultant output signal in the forms of voltage and current was then displayed on an LCD screen attached to analog pins SDA and SCL (Figure 3.7) in the Arduino board powered via a 5V pin and then grounded (GND). Since the Arduino board has one 5V pin and three GND pins, a solderless breadboard connected all the components into one device, as displayed below.

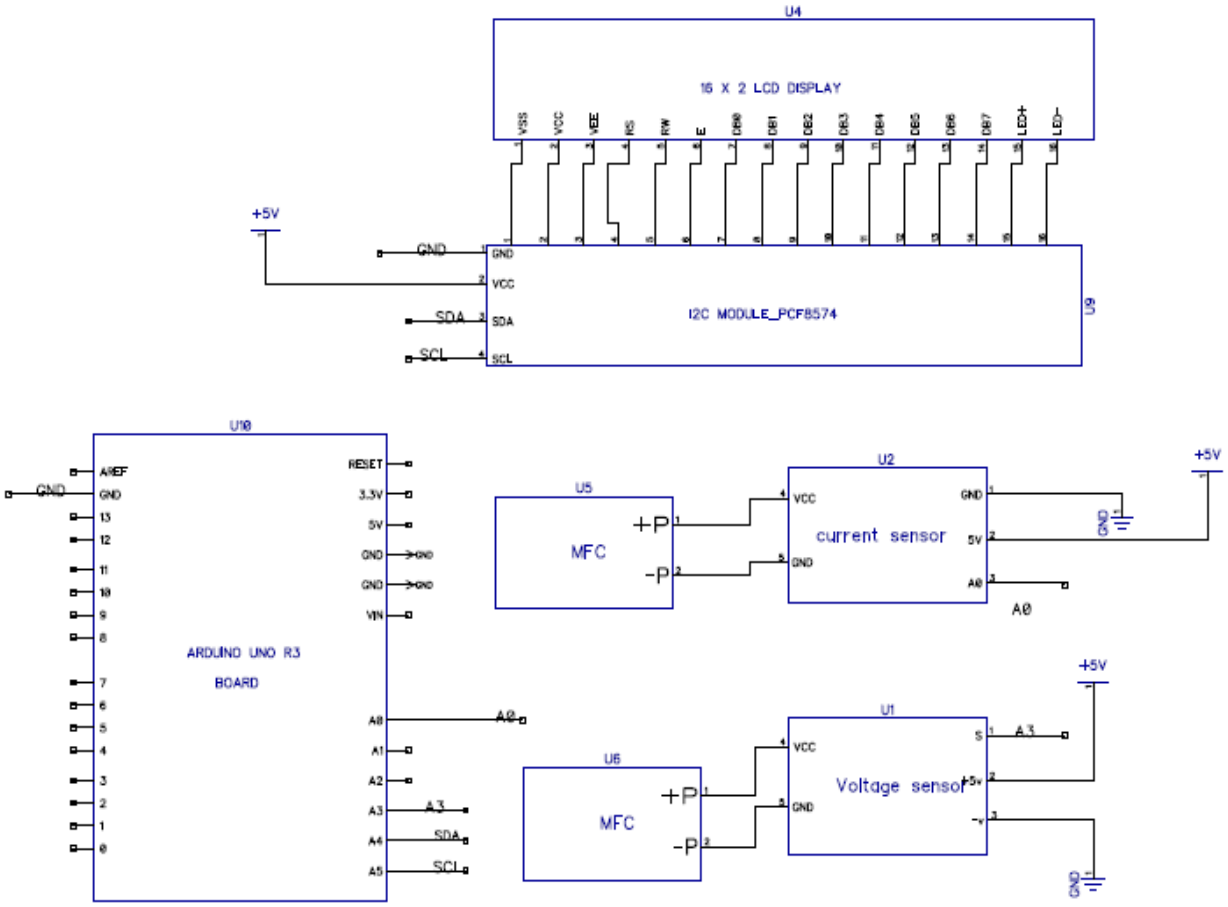

Figure 3.8: A Schematic diagram of the Arduino, Sensors, and LCD connection

Microbial fuel cell (MFC), digital multi-meter, Arduino-based sensor connections, for potentia and current recording is demonstrated in Figure 3.9 below.

Figure 3.9: Voltage and Current output monitoring device

Monitoring device's codes were designed with instructions to record data from MFC after every 60 seconds. After that, the overall voltage was averaged and examined. Then, based on a better match at low level voltages, an adjustment factor was created, based on prior testing and findings by El Hammoumi *et al.* (2018). A printing command in a monitoring device code was thereafter changed to work in tandem with an interface in this case PLX-DAQ in Microsoft Excel. Various statistical factors were used to analyze voltage data collected during operation of microbial fuel cell. Equations 3.18 and 3.19 were used to calculate the absolute and relative errors:

$$\mathrm{Abs}_{\mathrm{error}} = \left|\mathrm{E}_{\mathrm{Arduino}} - \mathrm{E}_{\mathrm{Multimeter}}\right| \tag{3.18}$$

$$\mathrm{Relative}_{\mathrm{error}}(\%) = \frac{\left|\mathrm{E}_{\mathrm{Arduino}} - \mathrm{E}_{\mathrm{Multimeter}}\right|}{\mathrm{E}_{\mathrm{Multimeter}}} * 100 \tag{3.19}$$

Where: $E_{\text{Multi-meter}}$ is the voltage reading of the multi-meter at any specific time, and E_{Arduino} is the potential reading with the Arduino UNO at the time of the readings.

3.5.7 The Data Collection

The potential and current generated were recorded on the digital multi-meter data acquisition system (model-DT9205A) in 24 hours for 22 days. We determined corresponding powers, current densities, and power densities values from the generated current and voltage values from microbial fuel cells.

3.5.8 The Data Analysis

The various mean and standard deviation values were computed. The results were obtained using Microsoft Excel 2013, Minitab 17, and multivariate analysis method by JMP (version 11) from SAS statistical applications.

3.5.9 Economic Value Addition on the Biodegraded Fruit Waste

The biosludge that remained in the anodic chamber of Microbial Fuel Cell after the 22 days that current and voltage were monitored, was put in a locally made vermicompost chamber for further 45 days, a process that was regarded as vermicomposting, after which it was investigated for bio-fertilizer. Shimadzu's IRAfinity-1S Fourier-Transform-Infrared Spectrophotometer utilized to analyze functional-groups in composite as well as in vermicompost sample. FT-IR technique works by creating an evanescent wave by utilizing the total internal reflection feature. Spectral resolution was set at a wavenumber 4 cm^{-1} while scanning range was from 400 cm^{-1} to 4000 cm^{-1} (Wang *et al.*, 2006).

Figure 3.10: (a) Shows Homemade vermicomposter chamber and (b) Powder Vermicast.

The vermicast (organic fertilizer) was then applied on a maize plantation and the growth process of the plants monitored. This was compared with the application of synthetic fertilizer on the plants as animal manure was used as the control. The results were obtained and are discussed in the next session.

CHAPTER FOUR

RESULTS AND DISCUSSION

4.1 Fruit Wastes

According to Muiruri *et al.* (2020), Nairobi City County has human population estimated at 4.0 million people. The County produces about 3,200 tons of waste daily, with fruit waste giving the highest percentage of the total waste produced. Thus, the main type of waste generated in Kenyan markets is biodegradable waste (organic waste). In this study, fruit waste samples were obtained from four different Nairobi City markets, and fed into microbial fuel cells' anodic chamber, together with goat rumen fluid from *Huruma* slaughterhouse. Current and voltage outputs were monitored. The results were obtained and are discussed in this section.

4.1.1 Proximate Values of the Wet Fruit Wastes

The fruit wastes from *Muthurwa, Kangemi, Fig tree Ngara,* and *City park* markets were found to comprise Mango (*Mangifera indica*), Banana (*Musa spp*), Tomato (*Lycopersicon Lycopersicum*), Watermelon (*Citrullus lanatus*), and avocado *(Persea Americana).* Proximate features of several fruit-waste samples from selected markets in Nairobi County.

Table 4.1 below shows the analysis on the wet fruit wastes samples. The crude protein, fiber, fat, carbohydrates, moisture, ash, nitrogen-free extract, and energy levels were all within the ranges compared to previous research as reported in this study (Mbugua *et al.,* 2020). In tomato fruits, moisture content was highest (95.16 ± 4.00 %) and lowest in banana fruit which had a range of 74.30 % - 95.16 %. The percent Protein level was most deficient in tomatoes (0.57 ± 0.01 %) and highest in bananas in the range of 0.57 % - 3 .05 %. At the same time, avocado had the highest percent fiber level (2.61 ± 0.98 %) while the fiber level was lowest in tomato in the range of 2.61 % - 0.76 %. This could be attributed to the naturally high fibre and fats content in avocado fruit than tomato. The ash level in mango, tomato, watermelon and avocado were in the range of 0.44 % - 0.84 % while it was highest in banana (1.67 ± 0.05 %).

Table 4.1: Proximate values of the wet fruit waste

Sample	**% Moisture**	**% Protein**	**% Fat**	**% Ash**	**% Fiber**	**% Carb.**	**% NFE**	**Energy (Kcal/100g**
Tomato	95.16±4.00	0.57±0.01	0.12±0.01	0.46±0.01	0.76±0.01	2.93±0.09	15.08±1.11	2.93±0.05
Banana	74.3±2.10	3.05±0.12	0.5±0.07	1.67±0.05	1.24±0.14	19.24±1.0	93.66±19.34	19.24±2.00
Avocado	82.83±3.00	1.32±0.14	9.03±1.36	0.84±0.02	2.61±0.98	3.37±0.55	100.03±12.9	3.37±1.11
Mango	86.82±3.89	0.87±0.07	0.68±0.08	0.44±0.02	1.28±0.21	9.91±1.00	49.24±2.88	9.91±1.00
Water Melon	92.85±4.55	0.90±0.09	0.33±0.04	0.74±0.04	0.76±0.09	4.42±0.88	24.18±2.45	4.42±0.78

Nitrogen free extract (NFE) values were computed from obtained readings on crude-protein, carbohydrates content, and crude lipids by factors 4 and 9 kcal/100 g for calculation, (Mbugua *et al.,* 2020; Pereira *et al.,* 2008). As observed in above Table 4.1, the highest NFE of all collected samples was reported in avocado at 100.03 % and lowest in tomato at 15.08%, while banana, mango, and watermelon wastes at 93.66, 49.24, 24.18 %, respectively. The energy obtained from wet fruit wastes was lowest in tomato (2.93 ± 0.05 Kcal/100 g) and highest in banana (19.24 ± 2.00 Kcal/100 g). This could be attributed to the low moisture content and high carbohydrates levels in these fruits. The level of proteins and fats in the wet fruits were in the range of 0.57 - 3.05 % and 0.33 – 9.03 % respectively. All fruit waste was found to have low outputs of crude proteins and lipids, ranging from 0.57 to 3.05% and 0.33 to 9.03%, respectively.

In a wet sample of tomato fruit-waste the level of moisture content output was 95.16 ± 4.00 %, which was similar to an earlier research by Mohammed *et al.* (2017) who reported a value of 90.75 %. For all the wet fruit wastes studied, the levels of moisture content were within the levels reported by various researchers. Hossain *et al.,* 2010 reported moisture range of 88.19 - 90.67 % while our study reported moisture levels of 74.3 ± 2.10 - 95.16 ± 4.00 % (Table 4.1). NFE was reported be highest in avocado waste at 100.03 ± 12.9 % and lowest in tomato at 15.08 ± 1.11 %, while banana, mango, and watermelon wastes were at 93.66, 49.24, 24.18 %, respectively.

Mathuriya (2013) had also reported high levels of moisture content in organic waste ranging from 73.69 % - 98.66 %. Sarma *et al.,* (2022) indicated that high moisture are critical factor for creating more electron-mobile solutions as well as transmission of electrons generated to microbial fuel cells cathode chamber. Adebule *et al.* (2018) and Mbugua *et al.* (2020) reported that moisture of more than 10 % was found to enhance voltage output by more than three times.

4.1.2 Proximate Properties on Dried Fruit Wastes

The proximate analysis of dried fruit wastes performed on analysed crude proteins, fiber, fat (Lipids), carbohydrates, moisture content, ash content, nitrogen-free extract, as well as energy levels showed that moisture content was low in tomato fruits at 4.84 % and highest in banana waste at 25.7 %. The % Protein level was lowest in Mango and highest in Watermelon in the range of 6.61 % - 12.72 %. At the same time, Tomato was highest in % Fiber levels but lowest in Banana having a range of 15.75 % - 4.85 % in all the market fruit waste.

Table 4.2: Proximate features on dry-weight fruitwaste

Sample	**% Moisture**	**% Protein**	**% Fat**	**% Ash**	**% Fiber**	**% Carb.**	**% NFE**	**Energy (Kcal/100g)**
Tomato	4.84±1.76	11.89±2.90	2.57±0.23	9.53±1.11	15.75±2.00	55.42±4.03	55.36±4.23	292.37±13.23
Banana	25.7±3.66	11.89±1.11	1.97±0.01	6.53±0.21	4.85±0.22	50.06±4.34	49.06±3.44	261.53±9.84
Avocado	17.17±3.00	7.69±0.43	52.64±5.68	4.92±0.07	15.22±0.95	3.35±0.06	2.36±0.01	513.94±24.89
Mango	13.18±3.44	6.61±0.44	5.23±0.67	3.33±0.10	9.74±0.78	61.91±1.50	61.91±2.78	321.15±23.00
Watermelon	7.14±0.88	12.72±2.67	4.63±0.01	10.49±0.76	15.68±1.11	49.34±3.77	47.34±2.89	289.91±56.78

In proximate properties analysis, sugars and starch are represented by nitrogen-free extract (NFE), which is produced via differences rather than measurement. Insoluble carbohydrates are represented by crude fiber, whereas soluble carbohydrates are represented by NFE (Dhont & Berghe, 2003). As shown in Table 4.2 Nitrogen-free extract reported in this current study ranged from 3.36 - 61.91 %. The moisture content was higher in all wet fruit waste; for instance, the

banana had the lowest level at 74.3 ± 2.1 % and tomato highest at 95.16 ± 4.00 % as compared to dried waste, for banana it was 25.7 ± 3.66 %, and tomato was 4.84 ± 1.76 % respectively. On a dry basis, all other calculated parameters were greater than the wet weights. The findings indicate a correspondence of the dried fruit waste with the analysis of the wet fruit waste.

In both Table 4.1 and Table 4.2, proximate properties results of carbohydrates content levels was highest as compared to crude proteins, ash content, fiber, and fats except for avocado fruit waste in dry samples. The overall pattern for all of the samples of fruit waste indicated proximate analysis on dry samples were higher than in wet samples. This could be explained by dilution effect due to moisture content in wet samples.

4.2 Analysis of the Inoculum

Table 4.3 shows the findings of the bacteria count from cow dung and rumen fluid. Total bacterial counts (TBCs) in cow-dung was $1.50 \pm 0.02 * 10^{10}$ cfu/g, and $3.15 \pm 0.01 * 10^{10}$ cfu/mL in rumen fluid. Compared to cow dung, rumen fluid had double the number of microorganisms which is attributed to rumen being actively involved in the digestion process which naturally involves microbes. These results were comparable to those obtained by Ozbayram *et al.* (2018) and Han *et al.* (2016), who observed two times more bacteria in cow rumen waste.

Table 4.3: Total bacterial count from Rumen fluid and Cow dung samples

Sample	Count	Unit
Rumen fluid	$3.15 \pm 0.01 * 10^{10}$	cfu/mL
Cow dung	$1.50 \pm 0.02 * 10^{10}$	cfu/g

From the results presented in Table 4.3, rumen fluid was used as inoculum in the MFCs. Rumen fluid is an ecosystem that is home to a very wide range of biological organisms, including bacteria protozoa, fungi (Castillo-González *et al.*, 2014; Kamra, 2005). Due to rumen's anaerobic media, temperature of 39 °C and pH of between 6.0 and 6.9 would encourage the establishment of microbial communities, which are in charge of breaking down and digesting food as well as producing sugars and acids. Ruminal microorganisms are susceptible to ruminant feeding habits,

age, and health (Kamra, 2005). According to Ezekoye & Ezekoye (2009), a crucial factor in assessing the quality of manure is the total viable count. In three samples of cow dung taken from various farms, a total 1.78 x 10^5 – 2.84 x 10^5 cfu/g of bacteria were found (Kiyasudeen *et al.*, 2015). Ambar *et al.* (2017) reported a total viable count (TVC) of 9.55 x 10^8 cfu/g and 1.32 x 10^8 cfu/mL from cow-manure as well as cow-rumen fluid respectively. The microbes count in the present study, therefore, compared well with those from previous studies which indicated that due to variations in microbial variety and population size, inoculum sources significantly affect the rate of substrate degradation.

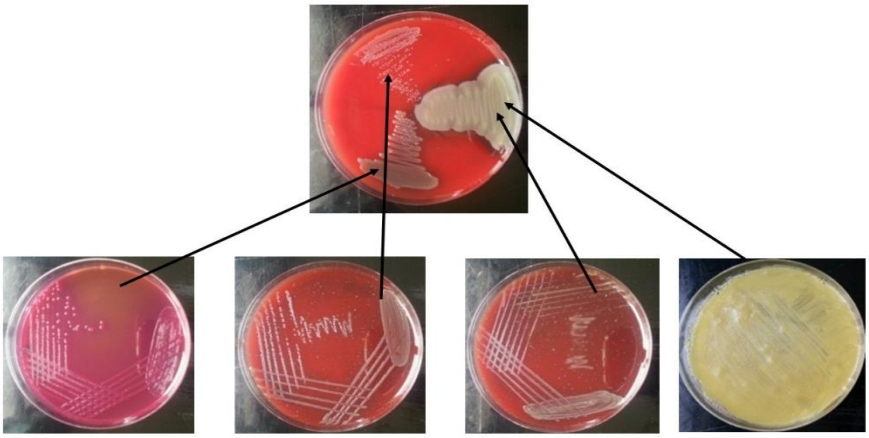

Figure 4.1: The cultured and isolated bacteria from Rumen fluid

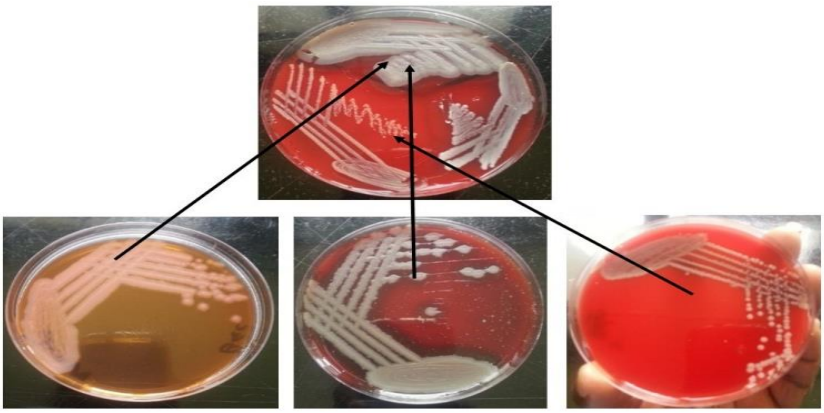

Figure 4.2: The cultured and isolated bacteria from Cow dung

In Figure 4.1, the top dish was stained by rumen sample and four distinct cultures isolated as shown. The same procedure was repeated for the cow dung sample and three distinct cultures were

isolated as shown in Figure 4.2. The isolates were then subjected to microbial count and expressed in colony-forming-units cfu/mL and cfu/g for rumen and cow-dung sample respectively as shown in Table 4.3.

4.3 Control Experiment

Fruit wastes provide a perfect environment for bacteria and other microbes of all kinds to survive and thrive. In this study, two control procedures were conducted to validate the fabricated MFC method. In the first control, different blank substrates (i.e. No inoculation) were loaded into the anodic chambers, and the voltage output was monitored, while in the second control, rumen fluid was loaded into the anodic compartments without the substrate. This was done to see what effect the presence or absence of bacteria had and extent to which they degrade the respective substrates. The results from the generated voltage in the Control experiments from days 1-5 are outlined in Figure 4.3.

The average voltage results for the rumen fluid blank were in the range of, 108.1 ± 26.2 mV, while for the other blanks of the fruit waste without rumen fluid, the voltage readings were observed to be as follows: Avocado 88.7 ± 21.7 mV, Tomato 82.9 ± 19.3 mV, watermelon 86.8 ± 20.3 mV, mango $95.7.3 \pm 19.7$ mV while for banana, was 101.3 ± 22.2 mV.

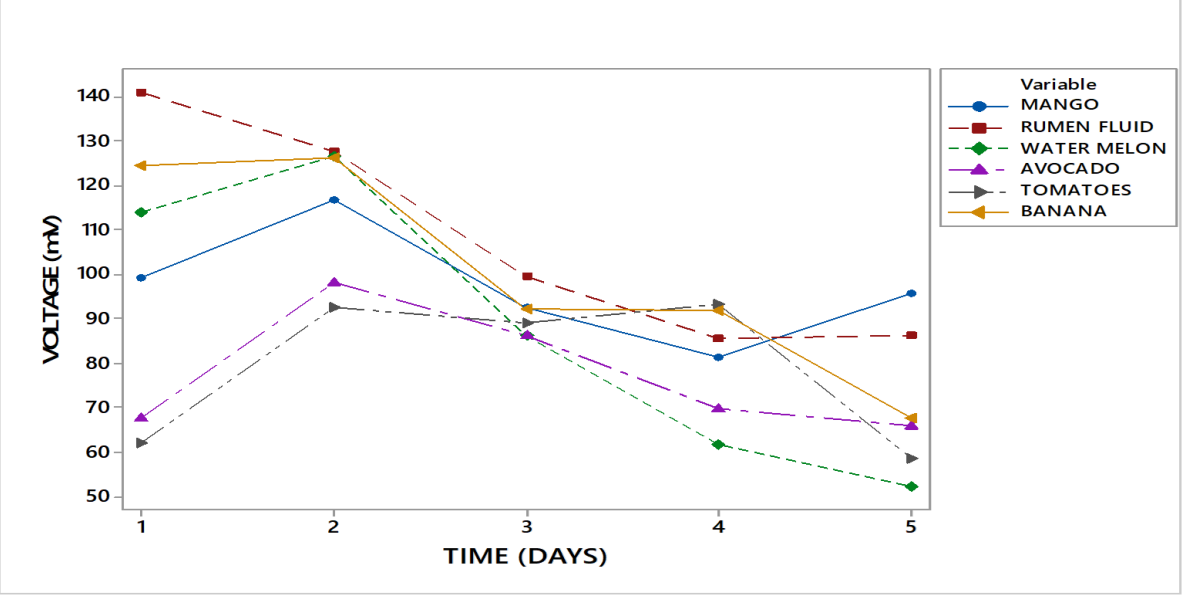

Figure 4.3: Generated Voltage in Control experiment from day 1-5

The results in Figure 4.3 showed that the banana waste blank had the highest voltage ($67.8 - 126.3$ mV) compared to the rest that ranged from $52.3 - 126.5$ mV. This could indicate that the mango fruit degrades more easily and faster compared to the rest of the fruit waste. In the blank with rumen fluid only, the trend of voltage generation was observed to decrease from 140.9 to 85.5 mV. This could be explained by a significant amount of bacteria in the presence of little substrate, therefore the microbes reached the death phase very quickly, as the food is exhausted. In this case, the food to microorganism ratio (F/M value) is very low, and therefore the microbes do not survive. In other words, in this blank, the substrate is the limiting factor. Among the fruit waste, the avocado and tomato generated the lowest voltage in the range of 58.4 – 116.7 mV. Generally, the voltage of the fruit wastes increased gradually before declining. A study by Qadri *et al.* (2015) indicated that many microorganisms, mainly bacteria, thrive in the optimal habitat provided by fruits. Potential infections were discovered on both healthy and unhealthy fruits and vegetables, as demonstrated by the mango (Diskin *et al.*, 2017), and onion bulbs (Yurgel *et al.*, 2018). The microbial composition of mangoes varied depending on storage circumstances over time (Maldonado-Celis *et al.*, 2019; Torres-León *et al.*, 2016; Galsurker *et al.*, 2018).

In Figure 4.4, a plot of daily current outputs for five days was obtained when goat rumen fluid and various fruit wastes (substrate) were used as blanks. The average current outputs were in the range of: 0.077 ± 0.037 mA for rumen fluid; 0.046 ± 0.015 mA for Avocado; 0.061 ± 0.01 mA for tomato; 0.084 ± 0.01 mA for watermelon; 0.071 ± 0.011 mA for mango and highest in banana fruit having a value of 0.082 ± 0.02 mA (Figure 4.4).

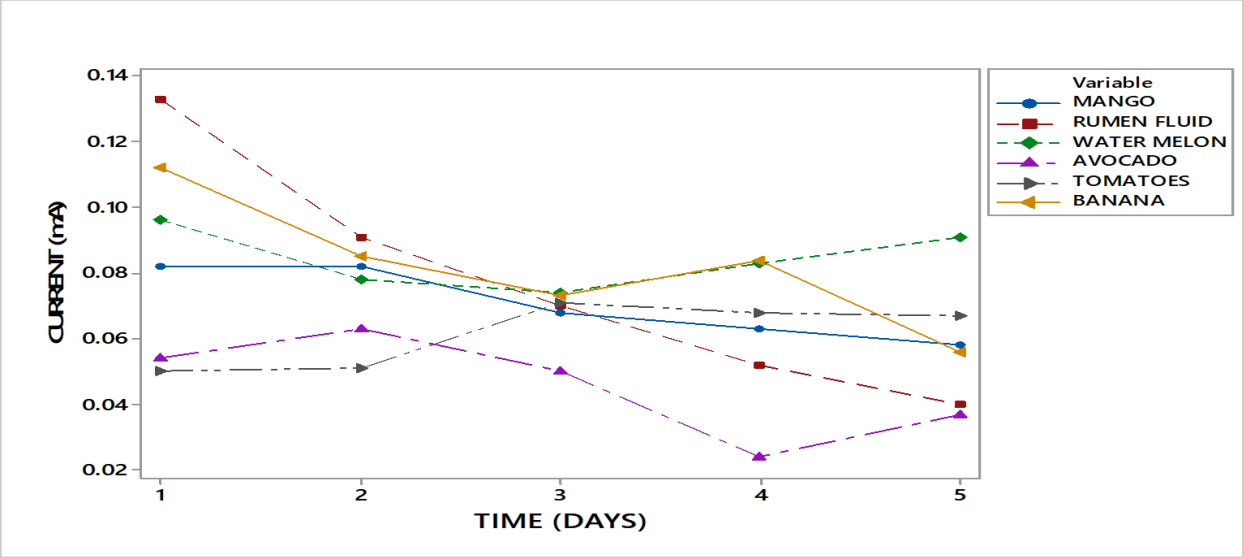

Figure 4.4: Generated Current in Control experiment from day 1-5.

In Figure 4.4, it is observed that microbes in the respective fruit wates influenced the generation of current. The current outputs were in the range of: rumen fluid $0.04 - 0.133$ mA, Avocado $0.024 - 0.063$ mA, Tomato $0.05 - 0.071$ mA, watermelon $0.074 - 0.096$ mA, mango $0.058 - 0.082$ mA while in banana wastes, the current ranged between 0.056 - 0.112 mA showing that, there are bacteria present in fruits, which degrade organic matter therein and produce voltage. Current generated without rumen can be attributed to the rate of microbial degradation. The substrate in the fruit is not the limiting factor like in rumen, but the number of microbes and their rate of degradation may have influenced the current/voltage generated.

The bacteria in the fruit environment can influence spoilage, a term used to describe any change in the state of food that makes it unfit for human consumption (Akinmusire, 2011). Bhale (2011) observed that internal fruit tissues have sufficient carbohydrates, minerals, vitamins, and acids. Bacterial deterioration promotes tissue weakening due to pectin degradation, and the whole fruit may eventually degenerate. Following the metabolization of starch and sugars, noxious smells and tastes, and lactic acid and ethanol occur (Rawat, 2015). Some spoilage microbes can colonize plant tissue that is otherwise healthy and create lesions (Kaczmarek *et al.*, 2019). Fruit contamination by microorganisms can happen before, during, or after the growing season as well as during handling, shipping, post-harvest storage, and marketing. Fruits become less appetizing and sometimes harmful to consumers as a result of spoilage (Hasan and Zulkahar, 2018).

4.4 Investigation on Power Production from Fruit Waste

The generation of voltage (potential), current output, power and power densities outputs by various market fruit wastes (substrates) with the goat rumen fluid being used as biocatalyst is discussed in this sections.

4.4.1 Voltage Generated by Fruit Waste

The voltages obtained when 250 mL ($7.9\ X\ 10^{14}$ cfu) goat rumen fluid was used for the various fruit wastes (substrate) over a period of 22 days was high as compared to the voltage output when the volume of goat rumen fluid was increased to 300 mL ($9.5\ X\ 10^{14}$ cfu). The Table labelled *Appendix* 1 shows the average voltage outputs recorded using the digital multi-meter data acquisition system (model-DT9205A). The trend obtained is shown in Figures 4.5. The average output was: 176.78 ± 95.17 mV in avocado, 215.97 ± 88.28 mV in banana, 187.57 ± 98.54 mV in mango, 186.39 ± 72.99 mV in watermelon, 145.76 ± 68.73 mV in tomato, and 158.77 ± 50.95 mV in mixture sample.

The study showed that over the 22 days period, the voltage kept increasing, which is attributed to the activation loss or over-voltage. Because no external resistance was applied, the voltage data collected from the MFC was regarded as the open-circuit voltage. Moreover, high carbohydrate content levels resulted in high voltages, as evidenced in voltage output recorded on the 17th day. The mixture of the various fruitwastes produced significantly less voltage than individual fruit waste. This could be due to antagonism in competing for reactive activities inside an assortment of the waste, which hampered voltage production (Agbossou *et al.*, 2004). Rismani-Yazdi *et al.* (2008) observed an activation loss to be a portion of the available energy lost while driving transfer of generated electrons to and from electrodes. For example, anode's hydrogen oxidation reaction may be swifted, while the cathode's oxygen reduction reaction is slow (Ferreira *et al.*, 2005), and therefore, the voltage drop would be dominated by the cathode reactions. Equation 4.1 of the Tafel formula describes relationship between activation over-potential and current density (Agbossou *et al.*, 2004).

$$V_{act} = a \ln\left(\frac{i}{i_o}\right) \qquad (4.1)$$

Where; a - (Tafel slope) and $i_o(\mathrm{A/m^2})$, (exchange current density) are coefficient constants that can be estimated empirically. The current density, i $(\mathrm{A/m^2})$, is the ratio of fuel cell current, if C(A), over active cell area expressed in cm^2. However, Tafel equation 4.1 is only valid for $i > i_o$. The typical value of i_o is about 0.1 $\mathrm{mA/cm^2}$ (Agbossou *et al.*, 2004). This would explain why as the generated voltage increases, current decreases in microbial fuel cells.

We found that market fruit waste was degraded with an efficiency range of (21.11 % - 35.95 %) for the first ten days and a range of (44.40 % - 88.75 %) for the following seven days, notably by anaerobic process. The bacterial degradation rate raised from initial percentage average of 31.58 % in between 1^{st} to 10^{th} day to an average percentage of 60.70 %, an upward increase of 52.03 % degradation rate. These findings justify the influence of specific bacterial growth curve phases and their degradation rate. Detailed data of average voltage output is shown in (*appendix* 1).

A plot of voltage (mV) output recorded daily for 22 days is presented in Figure 4.5. On the 17^{th} day, banana gave the highest average voltage output of 0.336 V while lowest voltage output was obtained in a mixture of fruit waste at 0.216 V. The voltages for the other samples were: 0.240 V, 0.311 V, 0.282 V, and 0.325 V for tomato avocado, watermelon, and mango fruit waste, respectively.

The results for the generated voltage from the different fruitwastes during the experimental period (1-22 days) are presented in Figure 4.5. The results indicated a general rise in voltage generated from day one, however generation declined after day 17 when the maximum voltage was attained.

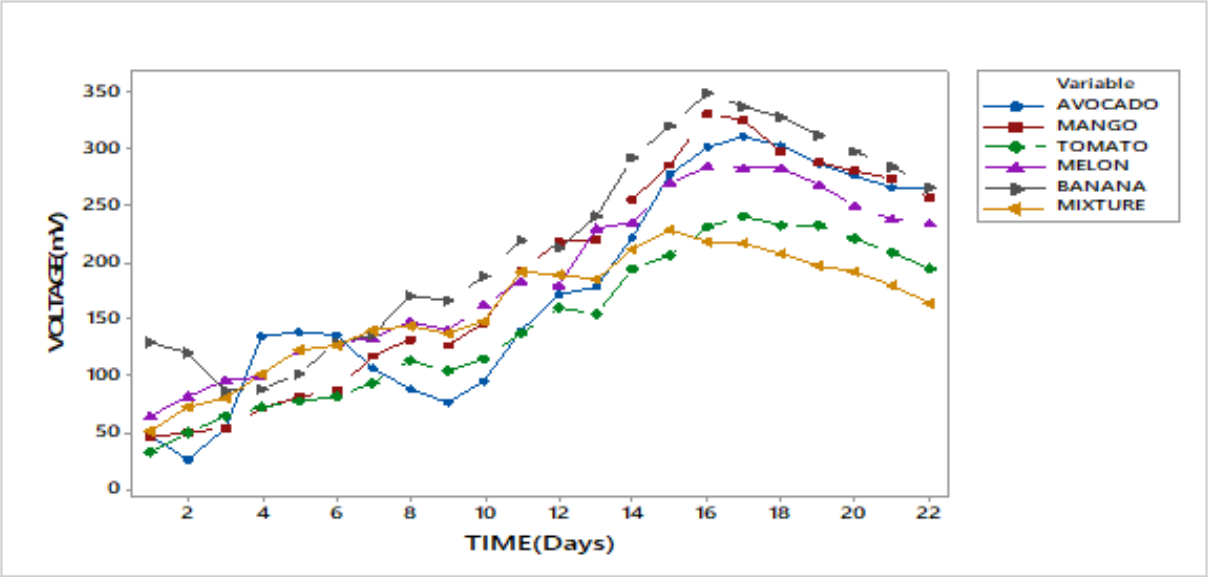

Figure 4.5: Voltage generated from the different fruit wastes during the experimental period

The amount of energy required to break down avocados' high fat content explains a low voltage output observed in Figure 4.5 despite the relatively high carbohydrate content. Kumar *et al.* (2012) observed that, in an open-circuit, organic waste generated voltage of 179.7 mV after 40 minutes. The voltage kept rising proportional to time for all fruit waste examined. A similar survey by Kamau *et al.* (2017) indicated that when using 500 g of organic waste as substrate in an open-circuit MFC, a potential of 0.27 V was generated which kept increasing for 5 days after which it started declining; suggesting that there were enough nutrients in the substrate to generate the voltage observed.

4.4.2 Current generated by Different Market Fruit Wastes

Current generated in an open circuit by goat rumen fluid using a double chamber MFC was recorded each day for 22 days (Figure 4.6). The current generated increased from day one to day nine, then decreased after day nine, according to the findings. The maximum average current was generated on day 9 which was 0.033 mA in tomatoes, while the minimum average of current was 0.027 mA in banana fruit.

A plot of daily voltage output for 22 days from various market fruit wastes is presented in Figure 4.6.

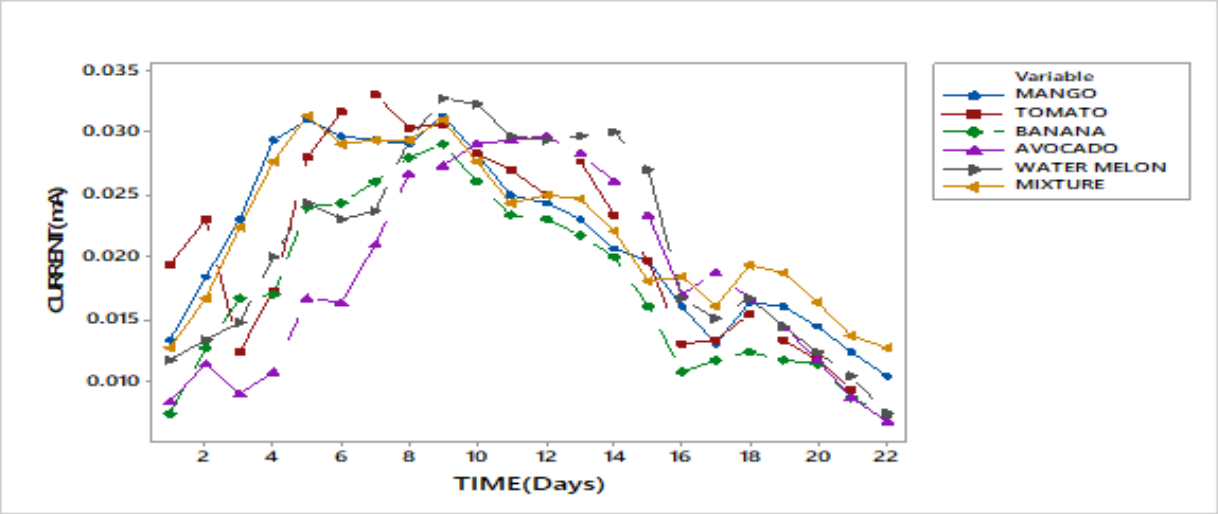

Figure 4.6: Generated Current from different fruit waste from day 1-22

From Table 4.1 on proximate values of the wet fruit wastes, the tomato sample recorded a high moisture content (95.3 ± 4.0 %) followed by watermelon (92.85 ± 4.55 %) and lowest in the banana sample (74.3 ± 2.1 %). The flow of current is triggered by the flow of electrons across conductors. The rate constant of reactions in the liquid phase is inversely proportional to the viscosity of the solvent (Forner *et al.*, 2019). When the viscosity is low (the moisture content is high) we expect that the electrons would move faster across the system, thus a higher current is generated (Xu *et al.*, 2018). In contrast, when viscosity is low, we expect electrons would move slower across the system, and the current generation is therefore low. Tomato fruitwaste peak was at 0.033 mA; banana peaked at 0.029 mA and avocado at 0.027 mA,. Adebule *et al.* (2018) and Mbugua *et al.* (2020) observed that, in Microbial Fuel Cells, high moisture content facilitated the creation of increased electron mobility in the solution which enhanced the flow of electrons in the cathodes.

4.4.3 Generated power from the market fruitwaste

Power generated by goat rumen fluid using double chamber MFC was recorded daily for 22 days for various fruit wastes (Figure 4.7). Maximum generated average power was 4.4 µW on day nine in the banana fruit, while the lowest generated average power was 2.51 µW in mixture of fruit waste on the 9th day. The power data recorded was from an open-circuit source, having no load applied in it.

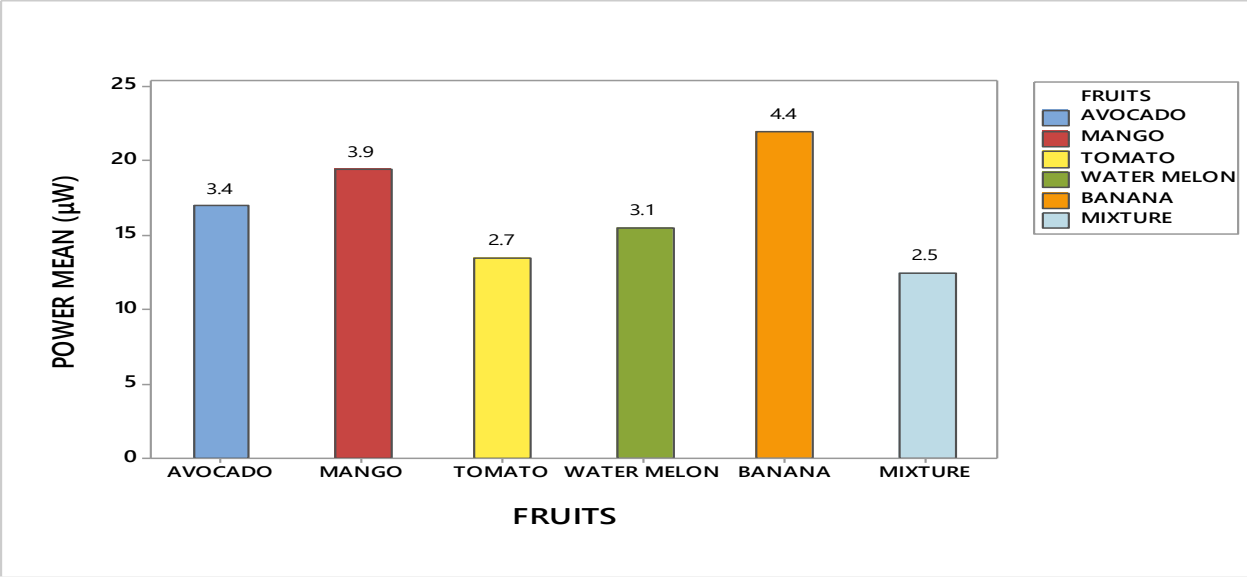

Figure 4.7: Average Generated power values from the different fruit waste

It is observed in Figure 4.7 that the highest power output was recorded for banana 4.4 µW and the lowest power output in mixture of waste at 2.5 µW while avocado recorded an output of 3.4 µW, 3.1 µW for watermelon, 3.9 µW for mango, and 2.7 µW for tomato fruit wastes respectively. Bruce *et al.* (2006) reported that the efficiency of MFCs is measured in relation to generated power and coulombic efficiency. Kamau *et al.* (2018) observed that power generated from market fruit wastes ranged between a power output of 0.081 µW to 12.06 µW for watermelon and 0.08 µW to 10.24 µW for fruit's mixture, which was comparable to the power output in the present study. Equations 4.2 to 4.4 were utilized to determine equivalent power, current density, and power density.

$$P = VI \text{ (Similar to earlier equation 3.16)} \quad (4.2)$$

$$\text{Current Density} = \frac{\text{Current}}{\text{TSA}} \quad (4.3)$$

$$\text{Power Density} = \frac{\text{Power}}{\text{TSA}} \text{ (Similar to earlier equation 3.17)} \quad (4.4)$$

Where: (V) denotes voltage, (I) denotes current, and (TSA) denotes Total Surface Area.

$$S.A = 2\pi r^2 + 2\pi rh = 2\pi r\,(h + r).$$

$$\text{Diameter} = 0.7 \text{ cm}, \text{Height} = 5.7 \text{ cm}, \text{Radius} = 0.35 \text{ cm}$$

$$\text{TSA} = [2 * 3.143 * 0.35\ \text{cm}\ (5.7\ \text{cm} + 0.35\ \text{cm})]$$

$$\text{TSA} = 13.3106\ \text{cm}^2 \qquad \text{But: } 1\text{cm}^2 = 0.0001\ \text{m}^2$$

$$\text{TSA} = 0.001331\text{m}^2 \qquad \text{But since we used four (4) pieces of electrodes}$$

$$\text{TSA} = (0.001331\ \text{m}^2 * 4) = 0.005324\ \text{m}^2$$

4.4.4 Generated power density from the market fruitwaste

The Power density(mW/m^2) generated from the various fruit wastes according to Equation 4.4 is presented in Table 4.4. The mean power generated by the fruit wastes was highest in banana fruits waste at $0.826 \pm 0.380\ \text{mW/m}^2$, $0.582 \pm 0.196\ \text{mW/m}^2$ in watermelon, $0.507 \pm 0.190\ \text{mW/m}^2$ in tomato, $0.733 \pm 0.290\ \text{mW/m}^2$ in mango, $0.639 \pm 0.250\ \text{mW/m}^2$in avocado and a mixture recorded output of $0.469 \pm 0.164\ \text{mW/m}^2$.

Table 4.4: Generated power density of different fruit waste

FRUITS	POWER DENSITY (mW/m^2).
AVOCADO	0.639 ± 0.250
MANGO	0.733 ± 0.290
TOMATO	0.507 ± 0.190
WATER MELON	0.582 ± 0.196
BANANA	0.826 ± 0.380
MIXTURE	0.469 ± 0.164

According to the results in Table 4.4, the generated power density increased from day 1 through day 17, then decreased on day 18. Because no external resistance was applied, the power density measured was open-circuit voltage. As a result, internal impedance was responsible for the power density generated. The generated power density trend for the 22 days from different fruit wastes is shown below (Figure 4.8).

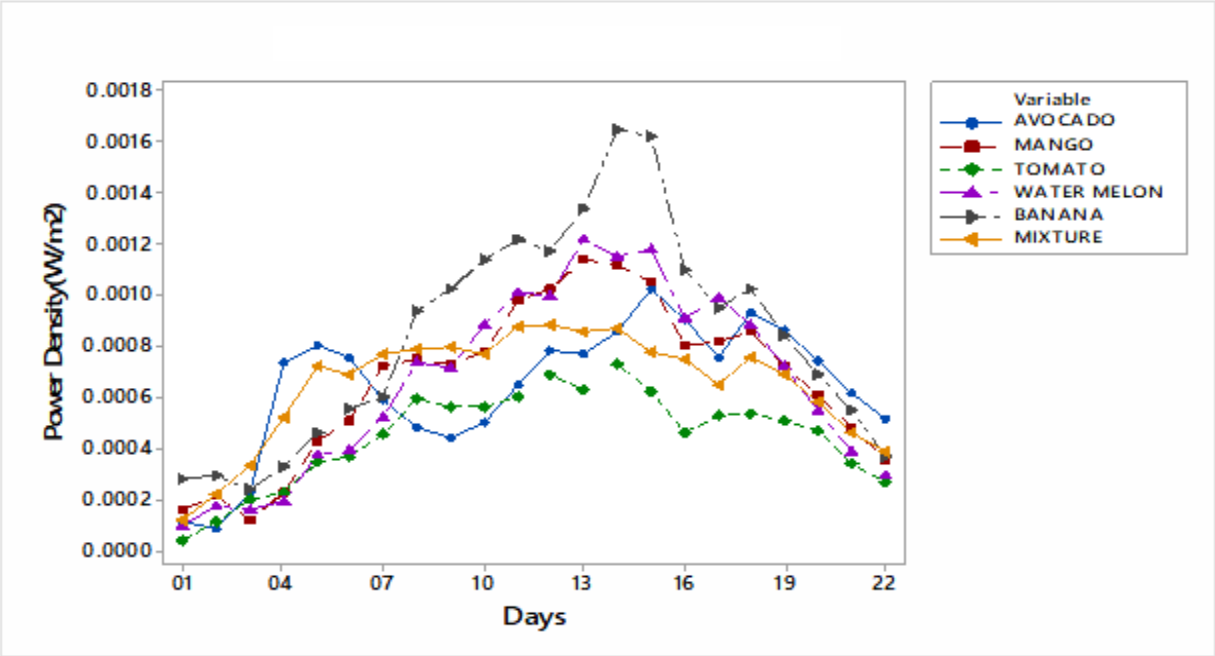

Figure 4.8: Average generated power density from different fruit waste

The average power density outputs for 22 days from various market fruitwastes are presented in Figure 4.9. The results indicated that the mango sample gave the highest output. Each fruit's acidity level was measured, with mango fruit having the highest values, followed by tomato and watermelon, and banana recording the lowest amounts. Acidic fruits contain citric acid that could break up into charged anions and cations. These ions can conduct electricity as the charged particles can flow within the acid, (Deziel, 2018).

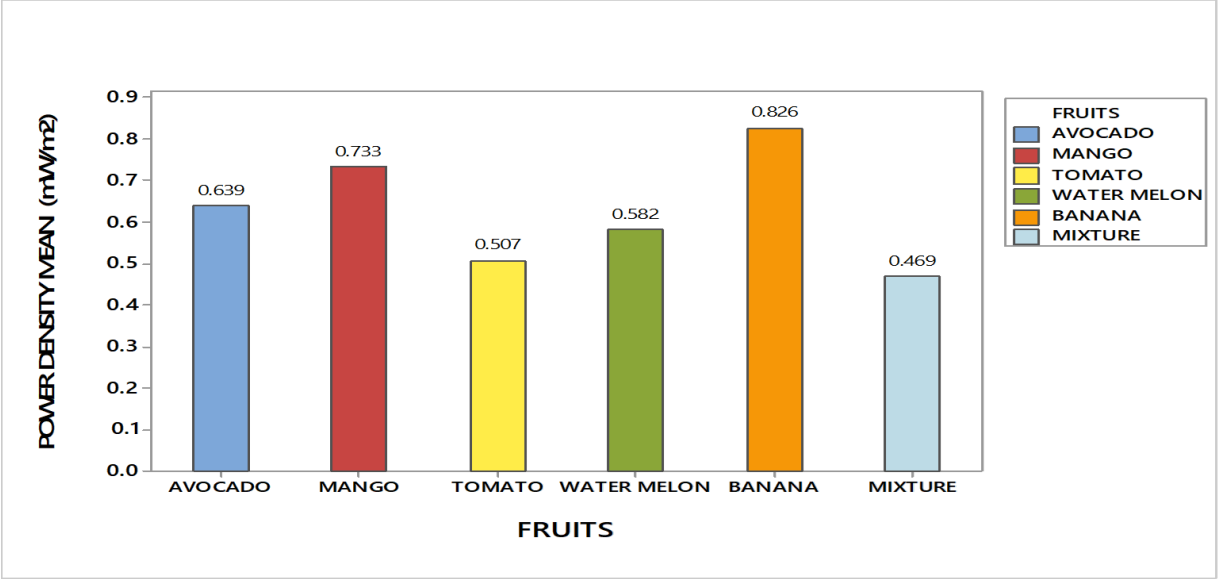

Figure 4.9: Generated average power density from different fruit waste

The power densities (mW/m^2) mean values of the various fruit wastes are presented in Figure 4.9. Savvidou *et al.* (2022), observed power-density output of 340 $\mu W/m^2$ recorded when using cow dung (substrate), while Zhang *et al.* (2011) recorded a power density output of 8.15 W/m^2. Parkash *et al.* (2015), using cow dung as substrate (fed on anodic portion), produced a maximum power density of 0.947 $\mu W/m^2$ on day five, while on day 1, a minimum power density generated was 0.269 $\mu W/m^2$. This study showed that from day 1 to 6, the maximum generated potential, current, power, as well as the power densities results showed comparable characteristics. A considerable population of microorganisms existed before and after the period of electric energy generation, according to measurements of the microbial load; their presence implies and establishes their role in aiding the release of protons and electrons, which results in the generation of electricity as a whole. As a result of the MFC chambers' microbial activities, power density output was continually produced during the experiment with a subsequent decline in production that was attributed to the exterminated organisms. The upward and downward trend followed a similar pattern as is reported by Adegunloye and Olotu, (2018). On day 5, all of the fruit waste output measurements were found to be at their highest levels as compared to the first experiment day, which could be attributed to high substrate impedance caused by incorrect substrate and water mixing, as well as the microbes were still in the lag phase (Leicester *et al.*, 2023).

4.5 Optimization of various Parameters

The optimum condiditions required to maximize the electricity output in a microbial fuel cell are discussed in the following sections in which it is shown that various organic wastes (100 mL) were catalyzed by microorganisms during the oxidation process in an anodic chamber to release voltage and currents.

4.5.1 Optimization of inoculum concentration

The study showed that various inoculum concentrations improved the efficiency of electricity output when the operational parameters for instance pH conditions, temperature, and external resistance, were kept constant. Voltage variation was observed in 250 mL ($7.9\ X\ 10^{14}$ cfu), 300 mL ($9.5\ X\ 10^{14}$ cfu), and 500 mL ($1.6\ X\ 10^{15}$cfu) volumes in all the fruit wastes which indicated that inoculum volume significantly impacted on the MFC performance during electricity production.

4.5.1.1 Voltage generated by fruitwaste degradation

A plot of average voltage outputs from different inoculum concentrations against various market fruitwastes is shown in Figure 4.10

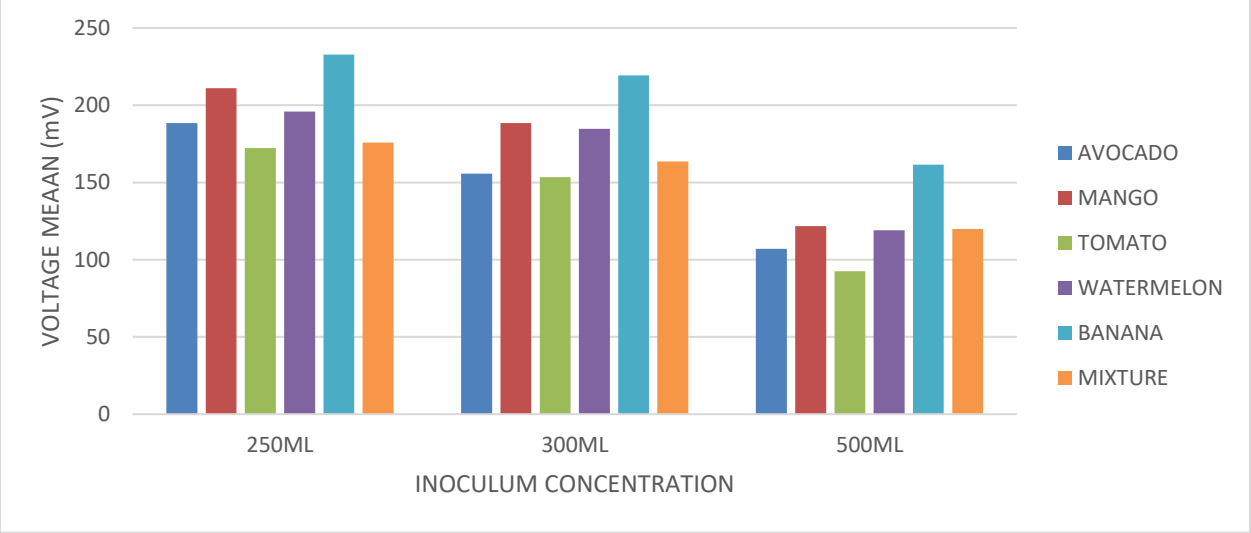

Figure 4.10: Generated voltage of different inoculum volumes from various fruitwastes

In Figure 4.10, it is shown that the average voltage output in all the fruit waste was low in 500 mL ($1.6\,X\,10^{15}$ cfu) and high in 250 mL ($7.9\,X\,10^{14}$ cfu), inoculum volumes which could be attributed to the fact that at low inoculum concentration, the bacteria had access to sufficient resources, resulting in a high rate of electron generation with low competition for food.

Voltage output for various inoculum concentrations are indicated in Figures 4.11 to 4.13. In Figure 4.11, a trend showing daily voltage when goat rumen fluid volume of 250 mL ($7.9\,X\,10^{14}$ cfu), were used for the various fruit wastes (substrate), the average voltage, average current density and average power density outputs were in between the range of: 172.34 ± 59.91 mV - 232.82 ± 87.2 mV; 3.306 - 4.151 $\mathrm{mA/m^2}$ and 0.068 - 0.828 $\mathrm{mW/m^2}$ respectively for rumen volume of 250 mL ($7.9\,X\,10^{14}$ cfu), which could be interpreted by the fact that at low inoculum concentrations, the food to microorganism ratio was kept favorable for the entire study period resulting in a high rate of electron generation with little competition for food. For the higher inoculum concentrations, there were many microbes but the substrate was constant, which meant the food to microorganism ratio was low and not optimized, and thus the lower potential.

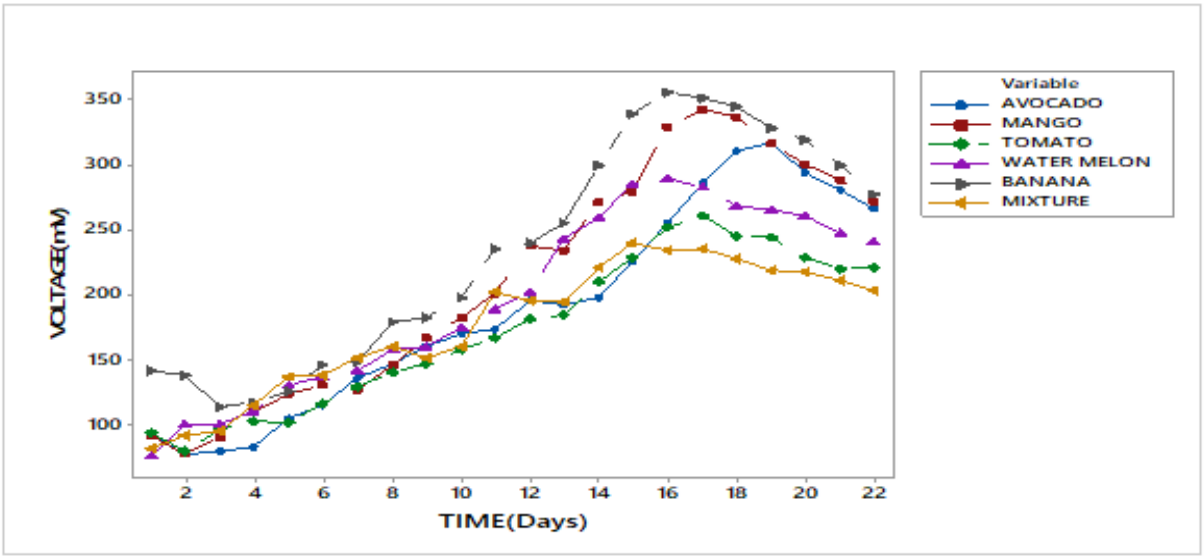

Figure 4.11: Generated voltage of 250 mL inoculum from various fruit waste

The voltage initially increased and then decreased towards day 22 (Figure 4.11). Banana waste gave the highest average voltage output of 355.00 ± 0.40 mV and the lowest average voltage output of 233.30 ± 0.42 mV was recorded in the fruit mixture, which could be attributed to the

microbial competition inside the assorted wastes, which hampered voltage production (Agbossou *et al.*, 2004). The other average voltage outputs were 251.30 ± 0.40 mV; 254.00 ± 0.46 mV; $289.80 \pm 0.2\ 0$ mV; and 328.70 ± 0.47 mV for tomato, avocado, watermelon, and mango respectively. A rate of voltage generation in a volume of 250 mL goat rumen fluid remained constant throughout experimental period. as compared to the other inoculum concentrations; suggesting that the microbes had an almost adequate substrate and little competition for the available food. Kamau *et al.* (2018) used 250 mL of cow rumen fluid as inoculum, the results did not show a significant difference with the present study where goat rumen fluid was used as inoculum, as evidenced by the similarity in the highest voltage (current) results observed.

In Figure 4.12, a graph of daily trend of voltage output when goat rumen fluid of 300 mL volume ($9.5\ X\ 10^{14}$ cfu), were used for the various fruit wastes (substrate), the average voltage, current and power densities outputs were in the range of: 153.48 ± 64.30 mV - 219.27 ± 88.90 mV; 2.648 - 3.437 mA/m^2; 0.476 - 0.609 mW/m^2. This is attributed to presence of slightly fewer nutrients for the microbes to feed on giving low electron production rate in comparison to 250 mL inoculum concentration.

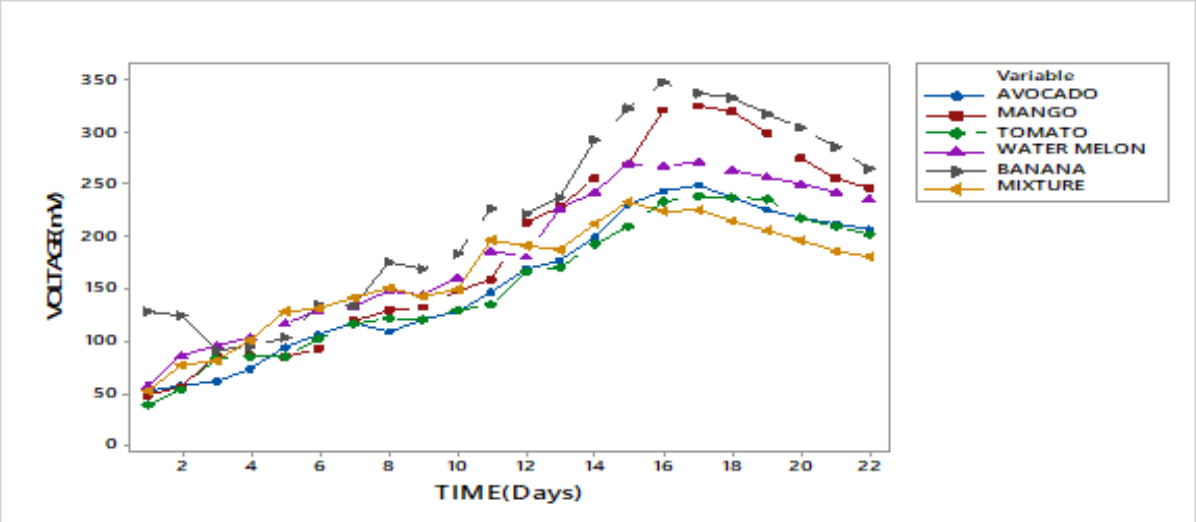

Figure 4.12: Generated Voltage of 300 mL inoculum from various fruit waste

The trend in voltage and current outputs in the present study show a resemblance. As shown in figure 4.12 above, the voltage increased until the 17^{th} day when it started to decline. The banana gave the highest average voltage output at 337.00 ± 0.42 mV and a mixture of fruit waste gave the

lowest average voltage output of 225.30 ± 0.26 mV which could be attributed to the competing for reactive activities inside an assortment of the waste, which hampered voltage production (Agbossou *et al.*, 2004). Other average voltage outputs were 238.70 ± 0.15 mV; 249.30 ± 0.61 mV; 270.70 ± 0.44 mV and 325.6 ± 0.4 mV for tomato, avocado, watermelon, and mango, respectively. The increase in the production, possibly an indication of the continuous microbial activities up to day 17th is because there is enough food for the microbes to feed on hence higher productivity. Kamau *et al.* (2018), indicated that rumen fluid of 350 mL concentration produced the highest voltage output, which was attributed to the bacteria having practically adequate nutrition for the entire research period.

In Figure 4.13, voltage output trend is shown when goat rumen fluid of 500 ml ($1.6\ X\ 10^{15}$cfu) was used for the various fruitwastes (substrate), the average voltage, current density, and power density outputs were in the range of: 92.62 ± 57.08 mV - 161.52 ± 82.3 mV; 1.897-2.779 mA/m^2; 200 - 306 $\mu W/m^2$ many low outputs as compared to both 250 mL and 300 mL goat rumen fluid is used as inoculum; this is because, at higher inoculum concentrations, microbes were competing for food, indicating nutrients were exhausted.

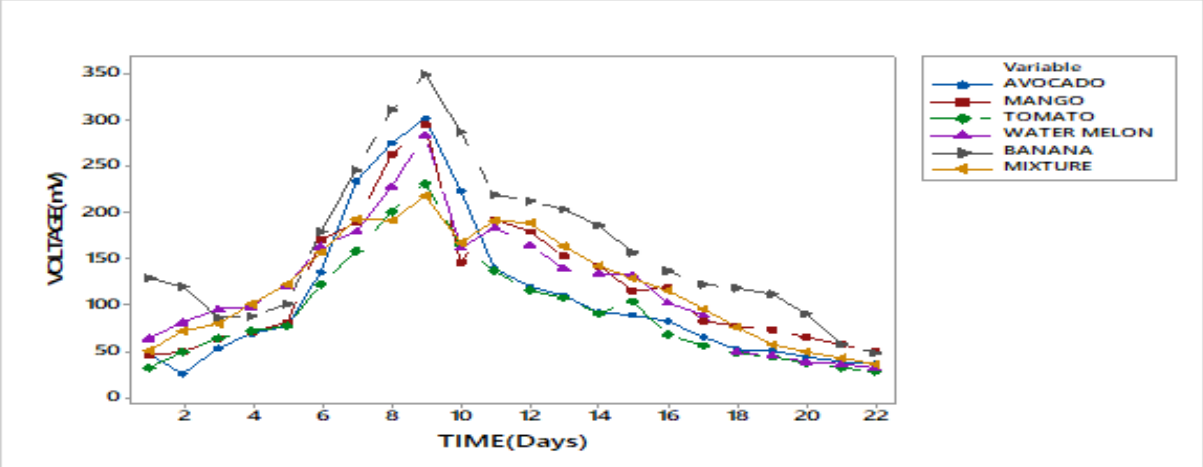

Figure 4.13: Generated Voltage when using 500 mL inoculum from various fruit waste

As shown in Figure 4.13 above, the trend increased until the 9th day when it started to decline till day 22. Banana waste gave the highest average voltage of 349 ± 0.35 mV, while the mixture of fruit waste gave the lowest average voltage of 217 ± 0.45 mV. The high and low values are attributed to the good supply of carbon from banana waste on one hand and the toxicity of different

fruits (mixture) put together (Agbossou *et al.,* 2004). Other average voltage outputs were 231 ± 0.21 mV; 284 ± 0.32 mV; 295 ± 0.15 mV and 300 ± 0.40 mV for tomato, watermelon, mango, and avocado respectively; indicating that the abundant concentration of microorganisms (anaerobic bacteria) content in goat rumen fluid worked effectively in degrading organic waste (substrate). In addition, 500 mL ($1.6\ X\ 10^{15}$ cfu) gave the highest output faster (on the 9th day) while the others gave almost the same result later than the 17th day. An indication that there were enough microorganisms to efficiently catalyze the degradation of organic materials. The concentration of the microorganisms then increased, but that of the substrates decreased, and the toxins produced during this process increased, resulting in a decrease in metabolic rate, as the microbes approached the endogenous phase. Kamau *et al.* (2018) indicated that, after the first 24 hours, the 500 mL ($1.6\ X\ 10^{15}$cfu) cow rumen fluid produced the maximum voltage, which was explained by the bacteria's access to enough substrate, resulting in high-rate electron generation. A study by Andrade and Buitr'on (2004) indicated that, rate of substrate biodegradation was largely affected by inoculum concentration, while Shelton and Tiedje (1984) observed that the amount of time that had passed since the inoculum was sampled did not affect the microbial decomposition of garbage.

4.5.1.2 Current generated by fruitwaste degradation

The current generated from various fruitwastes when different inoculum concentrations were applied is presented in Table 4.5.

Table 4.5: Generated current from various fruit waste and different inoculum concentrations

AVERAGE CURRENT VALUES (mA)			
FRUITS	250 mL	300 mL	500 mL
AVOCADO	0.0197 ± 0.007	0.0178 ± 0.006	0.0133 ± 0.006
MANGO	0.0226 ± 0.008	0.0189 ± 0.007	0.0146 ± 0.005
TOMATO	0.0211 ± 0.008	0.0166 ± 0.006	0.0115 ± 0.006
WATERMELON	0.0185 ±0.007	0.0149 ± 0.007	0.0101 ± 0.006
BANANA	0.0245 ± 0.009	0.0205 ± 0.006	0.0168 ± 0.005
MIXTURE	0.0176 ± 0.006	0.0141 ± 0.005	0.0101 ± 0.006

The study showed that inoculum concentration of 250 mL gave the highest average current output, and 500 mL gave the lowest average current (Table 4.5) irrespective of the fruitwaste used. The banana fruit gave the highest current, and a mixture of fruit gave the lowest current results in the range of $0.0221 \pm 0.0070 - 0.0176 \pm 0.0070$ mA for 250 mL, 300 mL gave a current output in the range of $0.0183 \pm 0.0005 - 0.0141 \pm 0.007$ mA, and 500 mL in the range of $0.0148 \pm 0.005 - 0.0101 \pm 0.006$ mA for all the sampled fruit wastes respectively. The current decreased with increasing inoculum concentration in all the fruit wastes throughout the entire study period of 22 days which suggested that microorganisms competed for food at increasing inoculum concentrations, indicating nutrient depletion, resulting in decreased current outputs. The decrease was attributed to the production of electrons from all fruitwastes that made the microbes inactive. Hence the optimization study revealed that there is optimal inoculum concentration $7.9\ X\ 10^{14}$ cfu (250 mL) at which the current is generated to facilitate the production of electricity.

Figure 4.14 shows that a volume of 250 mL ($7.9\ X\ 10^{14}$ cfu), formed the optimum inoculum concentration, conducive for the microbes to feed on the substrate and donate more electrons to generate high current. When the volume was increased to 500 mL, the inoculum concentration provided an environment that was toxic since the microrobes competed for food and rapidly reached the endogenous phase.

Further more, the food to microorganism ratio in this system is envisaged to be quite low and may not be favourable for the growth of microorganisms, and therefore the recorded current and voltage generation is also low.

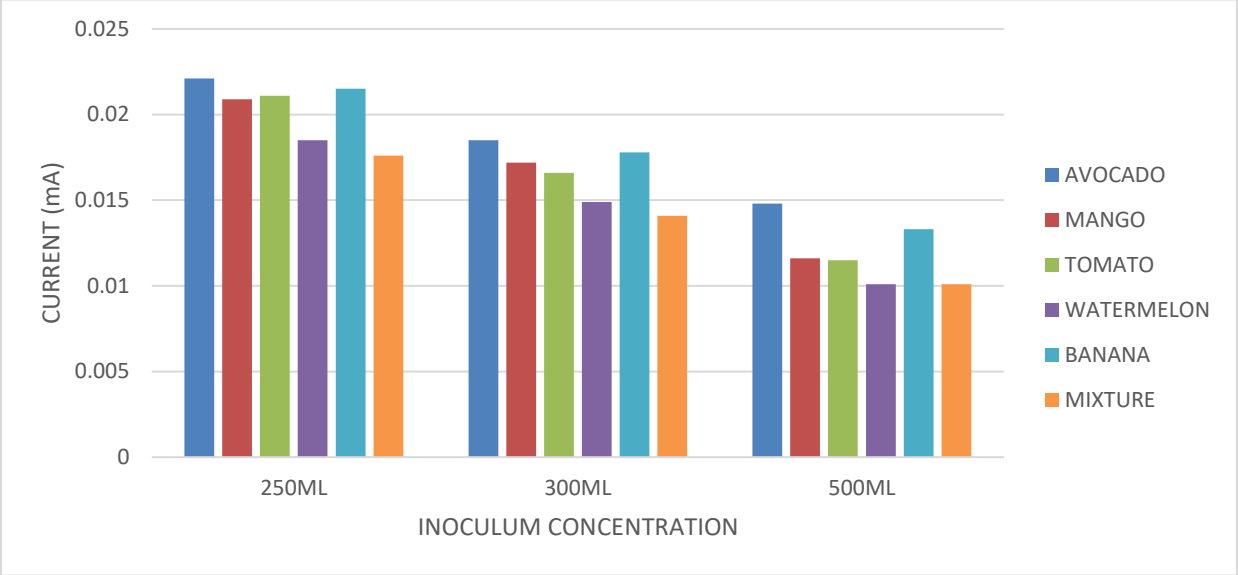

Figure 4.14: Generated current of 250 mL, 300 mL and 500 mL inoculum from fruit waste

The bar graph in Figure 4.14 showed that the current output was highest in avocado while the low current was observed in watermelon and the fruitewaste mixture in all the inoculum concentration. This is attributed to high crude fiber content levels, as well as lignin, cellulose, and hemicellulose according to Azuoma, *et al.* (2018) who reported that high level cellulose fibers limit the microorganisms' ability to degrade organic waste. This became clear on the last day of the experimental period (22^{nd} day), while the other fruit waste samples in their MFCs greatly diminished, leaving more water and a small amount of biodegraded substrate, watermelon and fruit waste mixture had more undecomposed substrate, resulting in lower current outputs.

4.5.1.3 Generated Power by market fruitwaste

In Figure 4.15, a plot of power for the various fruit waste is represented. The power values were obtained using equation 4.2. The outputs were in the range of: 3.95 ± 0.3 µW; 2.89 ± 0.2 µW, and 1.41 ± 0.2 µW for 250 mL, 300 mL, and 500 mL, respectively, suggesting that, at higher inoculum concentration, microbes were competing for food as the nutrients were being exhausted hence low voltage and current outputs resulting in low power output.

Power generated from market fruit waste (Figure 4.15), resulting from 250 mL ($7.9\ X\ 10^{14}$ cfu), goat rumen fluid, was in the average range of $3.62\ \mu W - 4.41\ \mu W$ It was observed that when the inoculum concentration was increased to 300 mL and 500 mL, the power decreased to the range of $2.53\ \mu W - 3.24\ \mu W$ and $1.07\ \mu W - 1.63\ \mu W$ respectively.

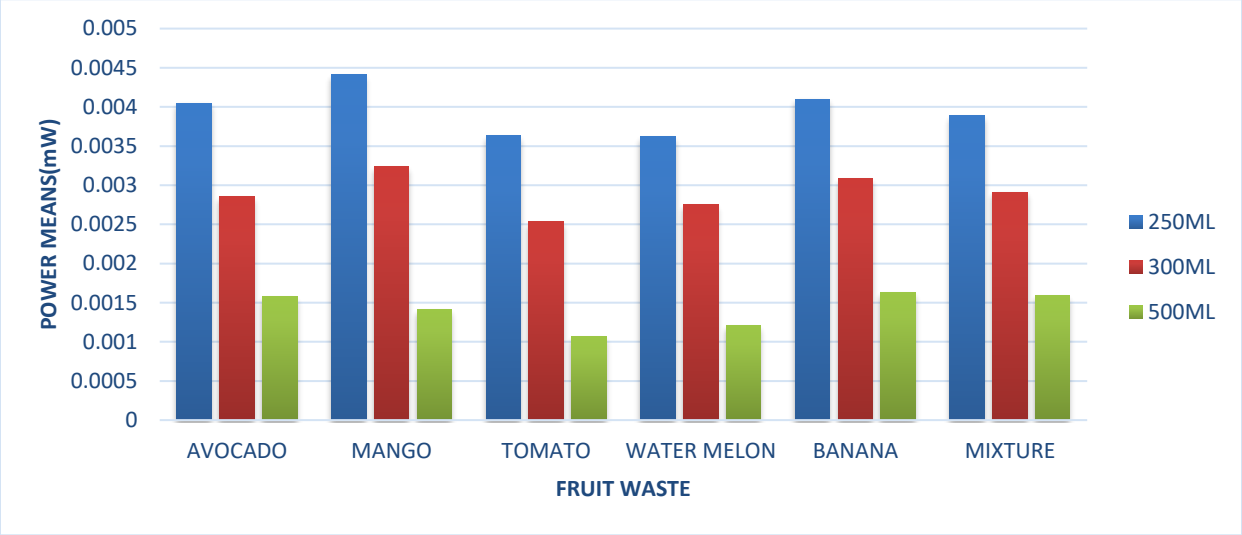

Figure 4.15: Generated power from various inoculum concentrations

There was a gradual increase of power output, after which there was a decline in all the inoculum concentrations. Studies by Meignanalakshmi and Kumar (2016) on influence of inoculum concentration on power generation by the MFC series showed that power increased progressively up to 192 hours, after which it decreased.

4.5.1.4 Generated Power density by market fruitwaste

Figure 4.16 illustrates a plot of power density averages. The power density values were obtained using equation 4.4. The outputs were in the range of: $0.742 \pm 0.056\ \mathrm{mW/m^2}$; $0.544 \pm 0.046\ \mathrm{mW/m^2}$ and $0.266 \pm 0.044\ \mathrm{mW/m^2}$ for 250 mL, 300 mL, and 500 mL respectively. It is shown that at higher inoculum concentration, microbes competed for food, thus exhausting the nutrients and resulting in low voltage, current and power density outputs.

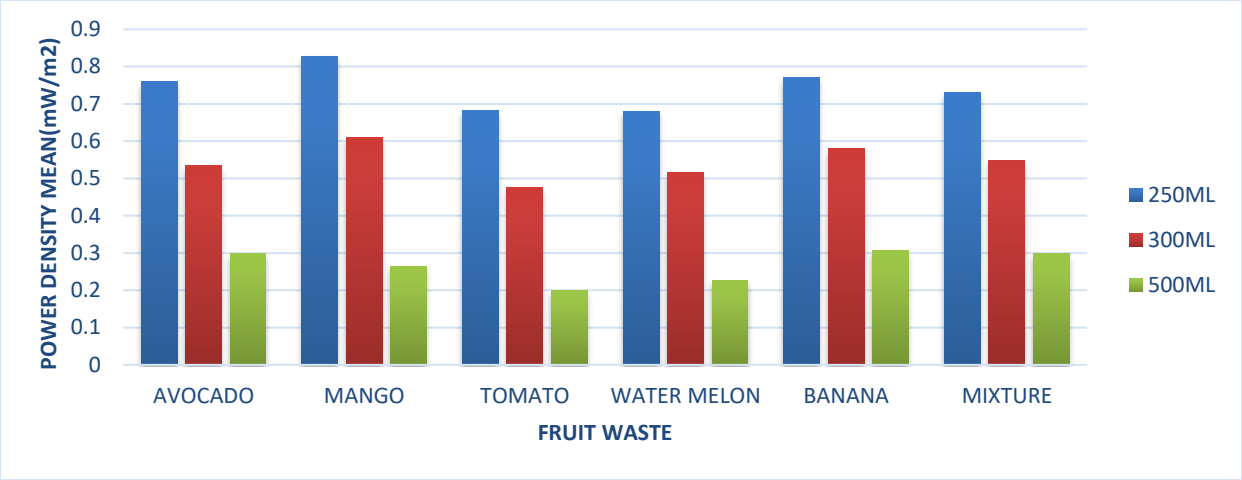

Figure 4.16: Generated power density from various inoculum concentrations

High concentration of the microbes saturates the anode and impede chemical reaction at the cathode, a situation that inhibits the power density as observed in Figure 4.16 above. The power density output was decreasing with an increasing inoculum concentration, which shows how the microbial activities with substrate used influence the output in double chamber MFC. Javed *et al.* (2017) observed that maximum power density achieved was 88990 mW/m^2 which is a higher power density output than prior studies in similar research (Cao *et al.*, 2021; Yong *et al.*, 2013). Higher power output was obtained in their tests as a result of lower ohmic losses caused by increased interaction between electrodes and microbes at the bottom of an fuel cell, as well as optimum ionic strength as a result to the use of a phosphate buffer and adequate salt concentration (Clauwert *et al.*, 2008; Li *et al.*, 2013).

4.5.2 External Resistance Influence on electricity generation

In the investigation of how external resistance influences electricity output in a fabricated MFCs, this study showed that the resistors: 1 kΩ, 5 kΩ 10 kΩ, and 15 kΩ improved the efficiency of electricity output when the operating parameters in this case temperature and pH are kept constant. It was found that voltage production increased as external resistance increased after a slight voltage drop in a closed-circuit, an indication that external resistance is a critical factor on the MFC performance, including electricity production and microorganism population evolution.

4.5.2.1 Voltage generated by market fruitwastes

A plot of daily voltage outputs versus time (days) given in Figure 4.17 showed that voltage increased proportionally with an increase in time from day 1 to 17 and then dropped. Results showed that the mean voltage output was highest in bananas which were 109.33 ± 59.99 mV, and lowest in the mixture of fruits, having a value of 67.31 ± 19.94 mV. The other fruit wastes had mean voltage outputs of: 78.28 ± 34.89 mV, 101.50 ± 44.48 mV, 103.96 ± 52.66 mV, and 102.16 ± 54.99 mV for tomato, watermelon, avocado, and mango, respectively, when a 1 kΩ resistor was applied.

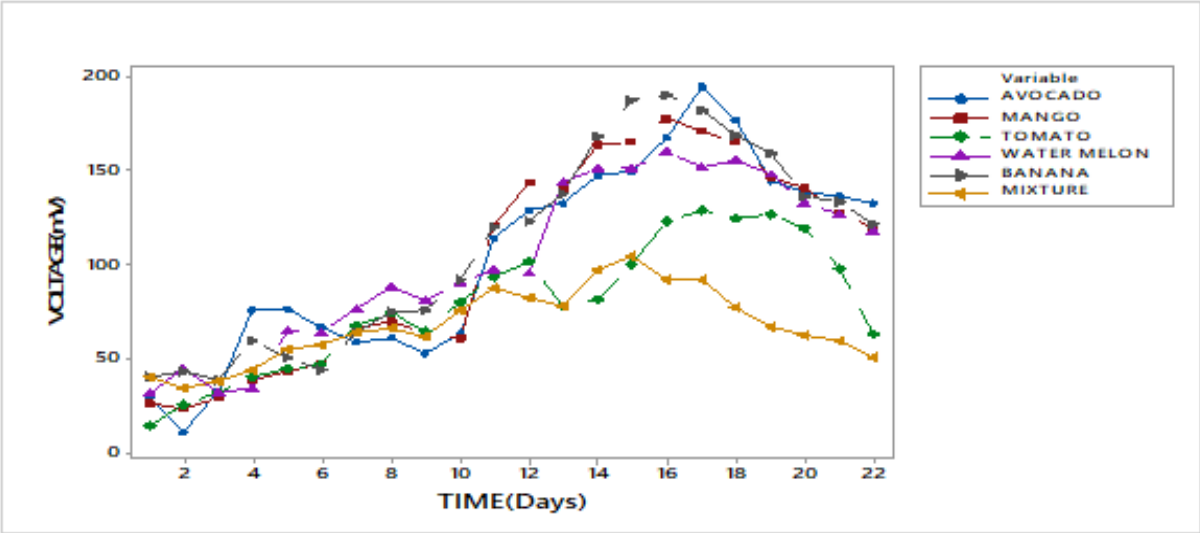

Figure 4.17: Generated Voltage from the fruit wastes when 1kΩ External Resistance was applied

The plot on voltage obtained when 1 kΩ external resistance was applied for the market fruit wastes increased with time until day 17 thereafter it started to taking a downward trend (Figure 4.17). The avocado gave the highest recording in voltage of 194.6 mV, which may be due to energy generated during the denaturation of avocado's high fat content. Highest voltage generated for the other fruit wastes were as follows: 170.9 mV, 128.4 mV, 151.9 mV, 181.7 mV, and 92.03 mV for mango, tomato, watermelon, banana, and mixture, respectively, across the 1 kΩ resistor. Results obtained in this study (that low voltage output was obtained when using a small external resistance (1 kΩ)) compared well with the previous studies. For example, Menicucci *et al.* (2006) who used varied external resistance (6 kΩ to 0.125 kΩ) in an MFC observed that cell potential decreased as the

external resistance reduced. They attributed this to a current-limiting electrode's restrictions on the kinetics of electrodes reactions, the mass-transfer, as well as on the charge-transfer processes.

The plot of daily voltage outputs for the twenty-two days (Figure 4.18) showed that the mean voltage output was lowest in the mixture (105.25 ± 37.03 mV) and highest in banana (158.42 ± 71.85 mV), while in the other fruit waste, the mean voltage outputs were: 114.09 ± 53.82 mV, 144.19 ± 56.75 mV, 137.74 ± 72.49 mV, and 142.42 ± 76.10 mV for tomato, watermelon, avocado, and mango, respectively, across a 15 kΩ resistor.

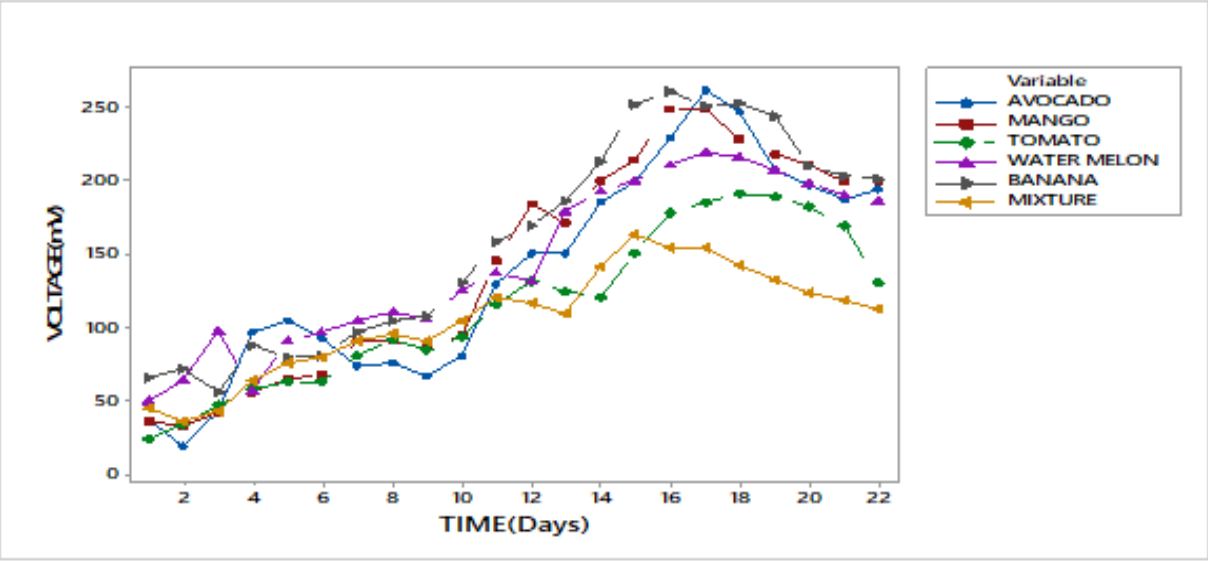

Figure 4.18: Generated Voltage from the fruit waste using 15 kΩ External Resistance

A plot of daily voltage outputs (Figure 4.18) showed that the maximum voltage occurred on day 17 with the highest being 262 mV in banana while for the other fruit waste outputs, the voltages were: 249 mV, 184.9 mV, 219 mV, 251 mV, and 154.6 mV for mango, tomato, watermelon, avocado, and mixture respectively, across the 15 kΩ resistor. High voltage output is due to energy generated during the avocado's high-fat content breakdown, while for bananas fruitwaste high number of calories, was attributed to the high voltage values. According to Ghangrekar and Shinde (2007), cell voltage output increased proportionally with a significant increase in the respective external resistance of between 0 Ω - 4,000 Ω while maximum potential of 358 mV resulted in high external load. Similarly, Rismani *et al.* (2011) recorded identical cathode voltage when using various resistances. Higher anodic potentials were achieved using double chambered MFCs with

decreased external resistance. Previous study by Song *et al.* (2010), who employed a MFC made out of sediment (SMFC), also observed the same results. High current resulted from the high electron movement from anodic side to cathodic area of microbial fuel cell chambers.

Figure 4.19, a plot of daily voltage outputs for banana fruit waste, showed that the highest mean output was 218.89 ± 86.47 mV when no resistor was connected (open-circuit) and lowest when external resistor (1 kΩ) was connected to the circuit with an output of 109.33 ± 52.99 mV. Resistor 15 kΩ recorded a result of 158.42 ± 71.85 mV, resistor 5 kΩ, outputs mean was 124.60 ± 59.49 mV, and 143.28 ± 66.93 mV, for resistors 10 kΩ, respectively.

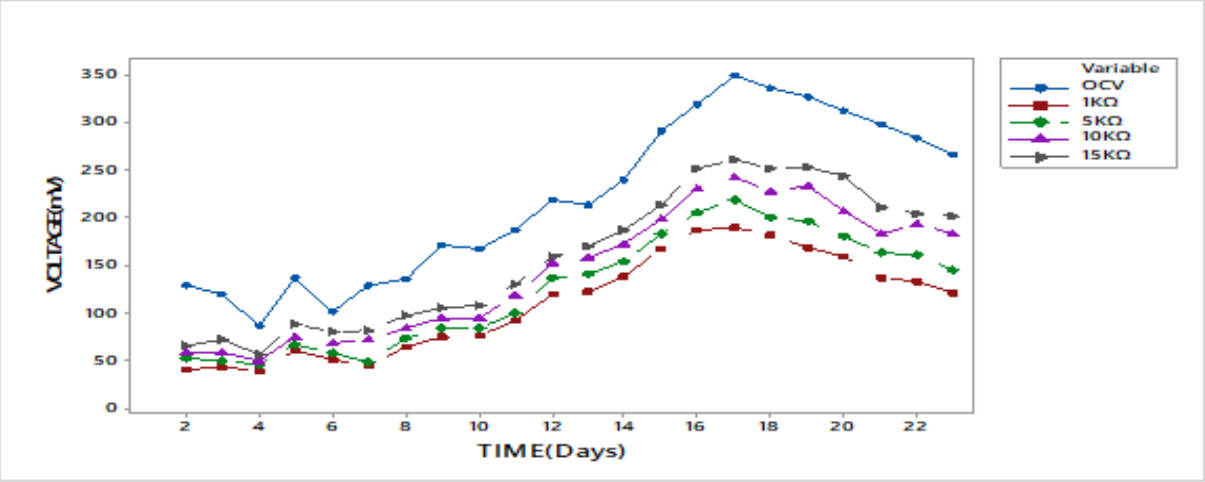

Figure 4.19: Generated Voltage from Banana waste when using various External Resistors

A daily plot of voltage outputs for the banana fruit waste (Figure 4.19) showed that maximum potential output was on day 16 with the highest production of 349 mV in an open circuit voltage (OCV), and with external resistance outputs of 190 mV, 218.3 mV, 242 mV, and 260 mV, for 1 kΩ, 5 kΩ, 10 kΩ, 15 kΩ resistors respectively. The trend showed open circuit voltage giving the highest voltage output, with the lowest external resistance giving the lowest voltage output. In comparison to other employed resistors, a 15 kΩ resistor produced highest voltage readings. These findings support Ohm's law, which states that voltage and resistance are directly proportional (Kamau *et al.*, 2017). Previous research (Menicucci *et al.*, 2016) revealed that when external resistance decreased, voltage fell, which was also found in this investigation.

Figure 4.20 shows a trend plot of voltage data outputs for the various fruit waste components. The open-circuit voltage recorded the highest average voltage output for fruit waste in the range of 155.85 ± 56.50 mV. The lowest voltage was recorded in resistor 1 kΩ (67.31 ± 19.95 mV), followed by resistor 15 kΩ recording an output of 105.25 ± 37.03 mV, while resistors 5 KΩ and 10 kΩ, gave voltage outputs of 80.46 ± 25.79 mV, and 92.63 ± 31.42 mV, respectively.

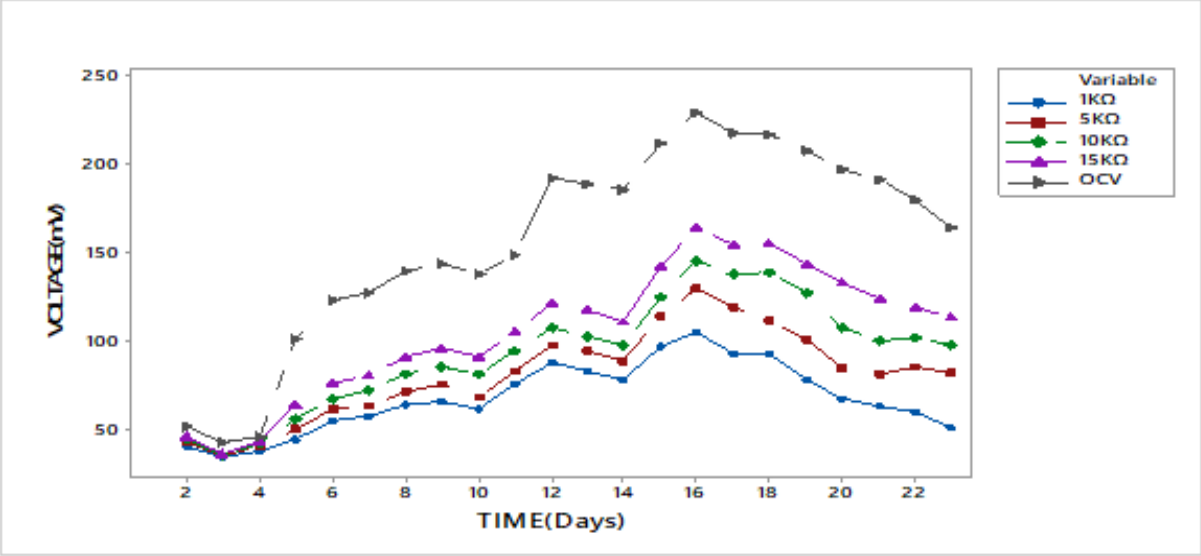

Figure 4.20: Generated Voltage of mixture waste from various External Resistors

The results in Figure 4.20 show that maximum voltage output was on day 15 with the highest output of 228.7 mV in an open circuit voltage (OCV), and with external resistance outputs of 104.6 mV, 129.5 mV, 144.6 mV, and 163.8 mV, for 1 kΩ, 5 kΩ, 10 kΩ, 15 kΩ respectively. The open circuit recorded the highest voltage output which initially increased for the first 16 days and then dropped. This was an indication that microbes in the goat rumen fluid were activated and were consuming the available substrates from fruit waste thus the rising tendency. As new rumen fluid becomes scarce, microorganisms begin to die, resulting in a negative voltage trend. This is in accordance with Kamau *et al.* (2018) who observed that microorganisms in the cow-dung competed for the available substrates, which caused the voltage to rise for the first three days before declining. As the dung is exhausted, the bacteria begin to perish, causing a downward voltage trend.

4.5.2.2 Current generated by fruit waste degradation

The possible effect of external load on current generated by microbial fuel cells was also investigated. The obtained data in Table 4.6 shows average current generated from fruit wastes catalyzed by goat rumen fluid in the range of $(0.0152 \pm 0.006\ \text{mA} - 0.0198 \pm 0.008\ \text{mA})$, $(0.0125 \pm 0.006\ \text{mA} - 0.0169 \pm 0.007\ \text{mA})$, $(0.0089 \pm 0.005\ \text{mA} - 0.0138 \pm 0.006\ \text{mA})$, and $(0.0068 \pm 0.005\ \text{mA} - 0.0115 \pm 0.006\ \text{mA})$ for 1 kΩ, 5 kΩ, 10 kΩ and 15 kΩ respectively.

Table 4.6: Generated current from various External Resistance

AVERAGE CURRENT (mA) VALUES				
FRUITS	1 kΩ	5 kΩ	10 kΩ	15 kΩ
AVOCADO	0.0189 ± 0.008	0.0143 ± 0.007	0.0128 ± 0.006	0.0090 ± 0.006
MANGO	0.0194 ± 0.008	0.0152 ± 0.007	0.0131 ± 0.007	0.0105 ± 0.006
TOMATO	0.0181 ± 0.008	0.0131 ± 0.007	0.0121 ± 0.007	0.0086 ± 0.006
WATERMELON	0.0187 ± 0.008	0.0139 ± 0.007	0.0127 ± 0.006	0.0083 ± 0.005
BANANA	0.0198 ± 0.007	0.0169 ± 0.006	0.0138 ± 0.006	0.0115 ± 0.006
MIXTURE	0.0152 ± 0.006	0.0125 ± 0.006	0.0089 ± 0.005	0.0068 ± 0.005

In Table 4.6, the average current generated by fruit wastes from other markets showed a decrease in current as the external resistance increased. This was observed when external resistance in MFC increased from resistor 1.0 kΩ - 15.0 kΩ, and current output decreased down from 0.034 mA to 0.022 mA on day 9. Kamau *et al.* (2017) reported a similar observation that when the external resistance increased, the resulting current output in micro-ampere dropped to 0.0020 mA from initial 0.0024 mA on day 6.

This study agreed with previous studies by Jang *et al*. (2004), suggesting that high electron movement from the anodic chamber through the switch (digital multimeter) to cathode chamber leads to high current output, as evidenced on market fruit wastes with small external resistance. Zhang *et al*. (2011) observed in their study a conventional double chamber MFC with a lower external load generated more current after start-up; the study further revealed that microorganisms could not transport their electrons to unfavourable electron-acceptor when functioning at a high

external resistance that resembled an open circuit. Earlier studies by Aelterman *et al.* (2008) found that when resistance decreased from 50 Ω to 10.5 Ω, there was a significant increase in the current generation. According to Lyon *et al.* (2010), the high external resistance could limit current passing from anode to cathode, thereby impacting microorganisms that colonize the anode. Ghangrekar and Shinde (2007) observed in a similar work, when external load was very high, current output was at its minimum level and nearly to a constant value.

Furthermore, the external resistance was regarded as the limiting element (Katuri *et al.*, 2011). Current output was independent of other factors, such as the distance in between the anode and cathode electrodes and anode surface. This study showed that the ideal external resistance for the current generation in the optimization study was 1 kΩ to facilitate high electricity production.

4.5.2.3 Power generated from market fruit waste.

The power outputs generated by market fruit wastes for all resistors (1 kΩ - 15 kΩ) were in the following ranges: Mango: 1.3 – 1.9 µW; tomato: 1.0 - 1.4 µW; watermelon: 1.5 - 2.0 µW, banana: 1.1- 1.7 µW while for the mixture of fruits, the range was: 1.0 - 1.3 µW (Figure 4.21).

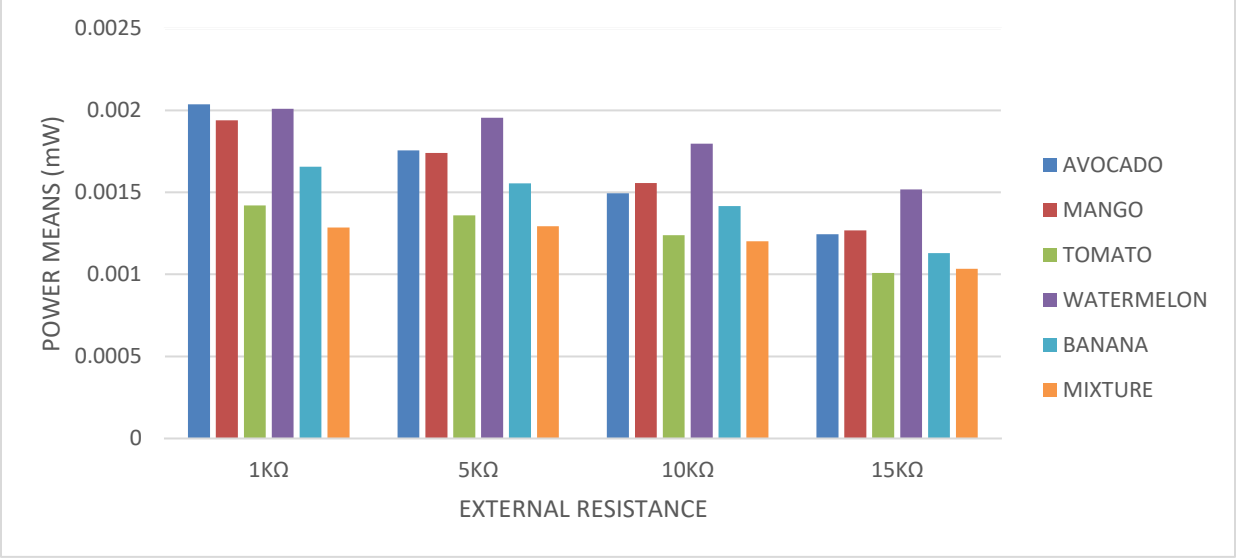

Figure 4.21: Generated power from various External Resistance

The mean power generated by each market fruit waste decreased with increasing external resistance within the MFC as observed increased across the resistors (Figure 4.21). Resistor 1 kΩ

gave the highest power output in all the fruit waste (1.3 - 2.0 µW), while resistor 10 kΩ gave power in the range of (1.2 - 1.5 µW), as resistor 15 kΩ gave the lowest power in all the market fruit waste in the range of (1.0 - 1.2 µW). The power output depended on the resistance of the resistors which could be due to the substantial effort needed to overcome the higher resistance. Therefore, when an electrical energy source equals the internal load (R_{int}) of a power source, cell's potential adjust to external resistance (R_{ext}). Suggesting that power produced by microbial fuel cell (MFC) is highly dependent on recorded current output, as indicated in Equations 4.5 – 4.8.

$$I = \frac{V}{R_{int} + R_{ext}} \tag{4.5}$$

And hence,

$$P = I^2 \ * \ R_{ext} = \frac{V^2}{(R_{int}+R_{ext})^2} * R_{ext} = \frac{V^2}{\frac{R^2}{R_{int}} + 2R_{int} + R_{ext}} \ * \ R_{ext} \tag{4.6}$$

Note: P - is at maximum particularly when the denominator is at the minimum. In differentiating the denominator to R_{ext}

$$\frac{d\left[\frac{R_{int}^2}{R_{ext}} + 2R_{int} + R_{ext}\right]}{dR_{ext}} = -\frac{R_{int}^2}{R_{ext}} + 1 \tag{4.7}$$

For maximum or minimum, the first derivative is zero, so

$$-\frac{R_{int}^2}{R_{ext}^2} = 1 \tag{4.8}$$

Therefore, the power output is maximum when,($R_{ext} = R_{int}$).

When external resistance is more than or less than internal resistance, power generated is low as compared to when they are equal. Studies by Gonza´lez *et al.* (2016) on the influence of external resistance indicated that reducing a load (from 2.7 kΩ down to 2.2 kΩ) resulted in a decrease of power output to 1.27 µW from 1.69 µW. It was found that, power output rose from 0.02 µW to 3.131 µW when in this case external resistance was varied from lower resistance of 1 kΩ to a higher resistance of 33 kΩ as per day 6. Lyon *et al.*, (2010) had reported that when using internal

resistance of 300 Ω, there was high power generation when external resistance of 470 Ω was applied, followed by 1,000 Ω, 100 Ω, 10 kΩ, and finally 10 Ω. The external resistance of 10 Ω was observed to produce the lowest power, which was attributed to the low external resistance compared to the internal resistance of 300 Ω (Lyon *et al.*, 2010).

4.5.2.4: Generated Power density from market fruit waste.

The bar chart (Figure 4.22) below shows power density outputs generated by market fruit waste. Obtained results indicated a general decrease for power density with increasing external resistance from 1 kΩ to 15 kΩ. Mango waste gave a result of $0.238 - 0.364\ \mathrm{mW/m^2}$, tomato ranged from $0.189 - 0.267\ \mathrm{mW/m^2}$, watermelon ranged from $0.285 - 0.377\ \mathrm{mW/m^2}$, banana ranged from $0.212 - 0.311\ \mathrm{mW/m^2}$ and mixture in the range of $0.194 - 0.242\ \mathrm{mW/m^2}$.

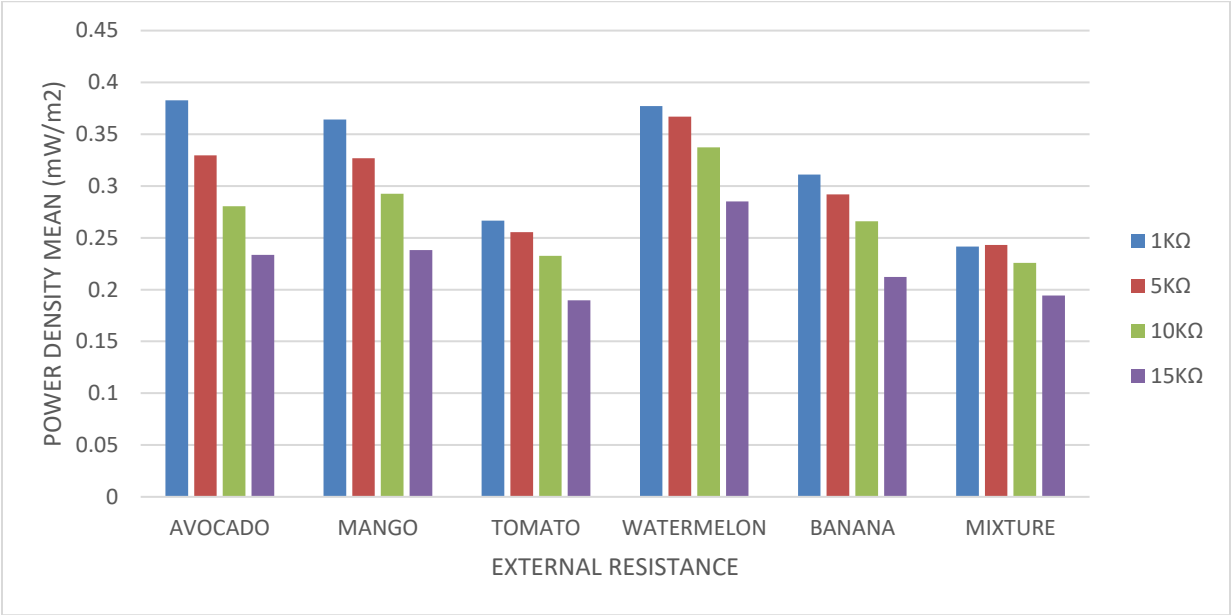

Figure 4.22: Generated power density of fruit wastes from various External Resistors

The power densities average generated values were in the range of $(0.242 - 0.383\ \mathrm{mW/m^2})$, $(0.243 - 0.367\ \mathrm{mW/m^2})$, $(0.226 - 0.337\ \mathrm{mW/m^2})$, and $(0.194 - 0.285\ \mathrm{mW/m^2})$ for 1 kΩ, 5 kΩ, 10 kΩ and 15 kΩ respectively. Earlier studies by Ren *et al.* (2011) showed higher power density values when external resistances were changed from high to low resistance (5,000 to 10 Ω) and, therefore, suggested that to achieve a maximum power density output low resistors should be employed when using the microbial fuel cell technology. Further, membranes in MFC increase

electrolyte resistance and may lead to the formation of a pH gradient. Fouling of the membrane due to biofilm deposition and development of extracellular polymers, as well as replacement of proton binding sites by other cations after a long-term operation, both lead to decreased electrical conductivity and ion-exchange capacity (Christgen *et al.*, 2015). Consequently, the fuel cell's performance is impacted since it is sensitive to the flow rate of the reactants from the anode inhibiting reaction at the cathode.

4.5.3 The effect of varous pH on electricity generation

pH is regarded as a crucial variable that could have an impact on generation of bioenergy in microbial fuel cells. In general, pH affects microorganism activity and therefore may influence the electricity generation output in MFCs. With this in mind, the effect of pH on the various electrochemical parameters in the MFC was investigated, in a bid to determine the optimal pH and proton carrier for the process using bicarbonate as a pH buffer and vinegar as an acid. The additional factors, including operational temperature, inoculum concentration, electrodes surface area, and electrode material were kept constant. In this study, basic pH 11 gave the lowest output followed by acidic pH 2 and a neutral pH (pH 7) gave the highest output in all the fruit waste as shown in figures 4.23, 4.27, and 4.28 below.

4.5.3.1 Generated voltage by market fruit wastes at various pH values

Figure 4.23 shows the results of the market fruit wastes at various pH values. Banana gave the highest average voltage results while the fruit waste mixture gave the lowest . The average voltage production at pH 7 was in the range of 116.44 ± 0.11 mV - 175.35 ± 0.05 mV, pH 2 gave 105.22 ± 0.46 mV - 156.08 ± 0.07 mV and pH 11 gave a range of 92.65 ± 0.04 mV - 140.23 ± 0.05 mV, (Figure 4.23).

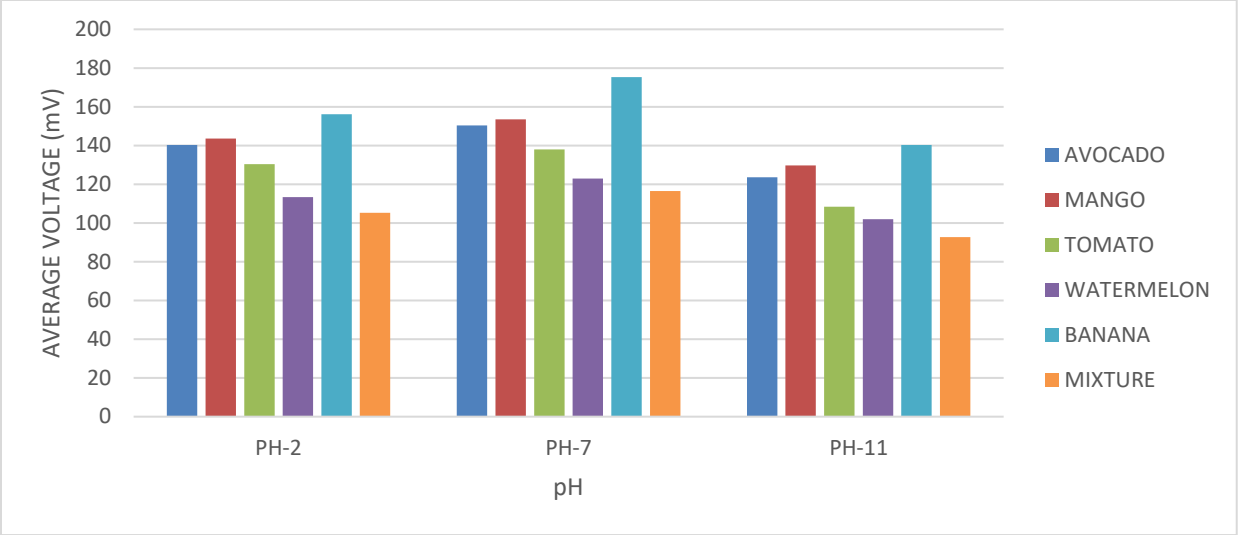

Figure 4.23: Average Generated Voltage at various pH values from the fruit wastes

Figure 4.23 demonstrates the behaviour of microbes in different pH conditions. The bar graphs trend is an indication that bacterial survival is pH dependant and that at high and low pH values, the mortality rate is higher than at a neutral pH value, which is attributed to the microbial activity being strained due to the difficult conditions. At a value less than pH 5.7 and greater than pH 7.8, there is a large decrease in proton motive force (PMF) and this decrease normally corresponds to the inhibition of microbial activities (Jiang *et al.*, 2020). In addition, pH condition of electrolyte solution in MFC is a critical factor in terms of electrical output (Halim *et al.*, 2021). For instance pH 2 can either promote faster electron and proton transfer from anode to cathode due to increased proton concentration or cause the biological mortality to the bacteria due to acidic media (Noori *et al.*, 2019).

A trend of daily average voltage outputs (Figure 4.24) shows the average voltage production under acidic conditions of pH 2 of the various market fruit wastes in acidic pH 2 environment.

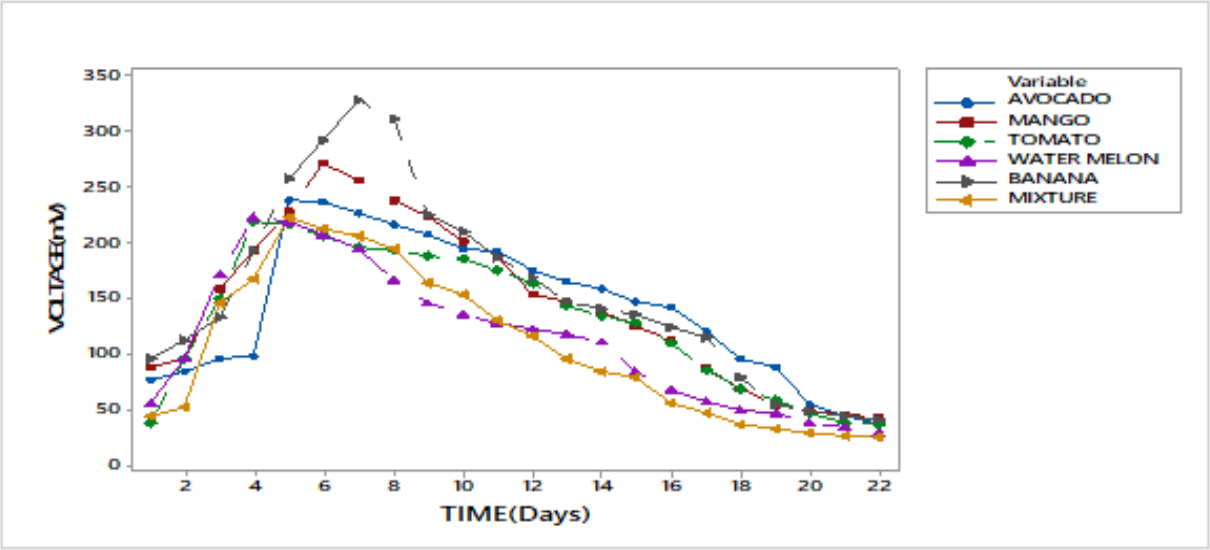

Figure 4.24: Generated Voltage at pH 2 from the various fruit wastes

Figure 4.24 above shows plots of daily generated voltage values of market fruit waste for 22 days. The values peaked on day six for most of the fruit wastes then started to decline. Tomato gave the lowest peak at 205 ± 1.0 mV, while banana gave the highest rise at 291 ± 0.6 mV; the other voltage values obtained include 208 ± 0.5 mV, 213 ± 1.1 mV, 236 ± 1.2 mV, and 272 ± 0.6 mV for watermelon, fruit mixture waste, avocado, and mango, respectively. The present study observed that pH 2 gave a slightly better result regarding the extent of voltage output than the condition at pH 11 environment.

A crucial intermediate in MFCs is thought to be the volatile fatty acids, which are formed during anaerobic digestion. In actuality, VFAs are frequently employed to detect instability or process failure (Boe *et al.*, 2010; Behera *et al.*, 2010). This is due to the strong syntrophic interaction between the methanogenic and fermentative microbes in AD, with the latter using the hydrogen and acetate produced by the former for methane synthesis (Kretzschmar *et al.*, 2017). Because of this connection, there may be a kinetic decoupling between the downstream methanogenesis and the upstream fermentation and acetogenesis, which may be a sign of stress in an AD process. Because of this, VFA concentration is a crucial early state indicator of AD process problem (Falk *et al.*, 2015). Acetic, propionic, butyric, and valeric acids are the four principal VFAs detected in the AD process. The major VFA species varies depending on the particular digester activities (Franke-Whittle *et al.*, 2014). An increasing prominence of propionic and higher acids levels can

occur under the unstable anaerobic digestion conditions (Boe *et al.*, 2010). Once unstable conditions are stabilized, the amounts of acetate and butyrate drop rather fast, but the levels of higher acids can keep rising (Boe *et al.*, 2010). VFAs in raw (untreated) slaughterhouse discharge can typically range from 175 - 400 mg L^{-1} Harris and McCabe (2015) with some slaughterhouse discharge reaching VFA concentrations level of 1020 - 1980 mg L^{-1} (McCabe *et al.*, 2013). However, AD can become unstable if VFAs are allowed to build up. The outcome is a decrease in pH (pH < 6.3), which can prevent bacteria from growing because they are more sensitive to low pH values (Amani *et al.*, 2010).

Figure 4.25 outlines average voltage readings when various market fruit wastes were investigated at a neutral condition pH 7. It is observed that at this environment, there were higher results on voltage output in the range of 116.44 ± 68.89 mV, 122.92 ± 63.77 mV, 138.01 ± 60.89 mV, 150.31 ± 64.69 mV, 153.44 ± 74.55 mV, and 175.15 ± 89.90 mV for the fruit waste mixture, watermelon, tomato, avocado, mango, and banana, respectively.

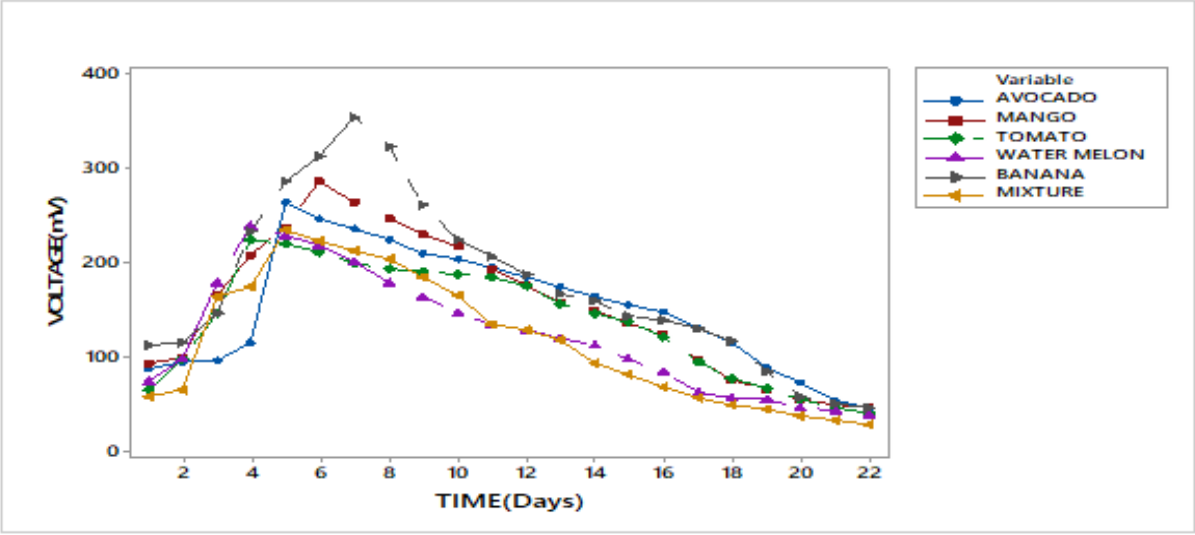

Figure 4.25: Generated Voltage at pH 7 from various fruit wastes

At pH 7 just like at pH 2 resulting voltage values increased upwards until day six and then started declining downwards. The banana waste still recorded the highest voltage value at 312 ± 1.53 mV while tomato waste had the lowest voltage (211 ± 0.58 mV) (figure 4.25). Behera *et al.* (2010), realized that with an influent pH of 8.0, MFCs performed best in organic matter removal as well as in the electricity harvesting when treating such wastewater.

Figure 4.26, outlines a plot of daily average voltage (potential) output from various market fruit wastes at pH 11. At this pH, average potential values of 140.23 ± 82.62 mV, 129.72 ± 69.83 mV, 123.63 ± 62.84 mV, 108.42 ± 53.91 mV, 101.89 ± 58.26 mV, and 92.65 ± 63.56 mV were obtained for banana, mango, avocado, tomato, watermelon, and fruit waste mixture, respectively.

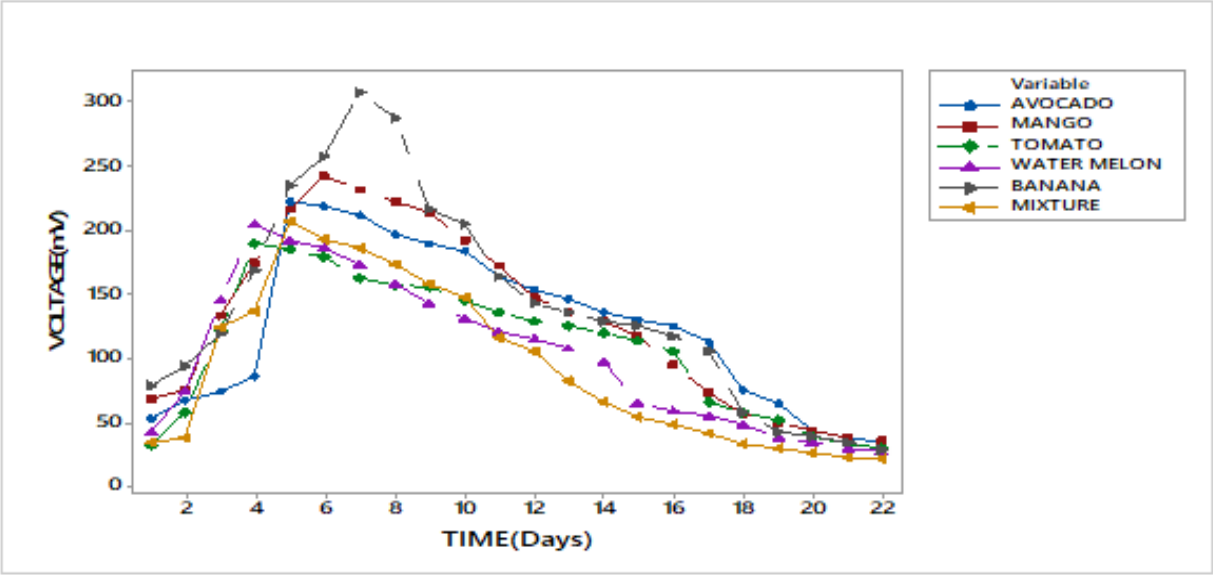

Figure 4.26: Generated Voltage at pH 11 from various fruit wastes

From the results obtained in Figure 4.26, banana gave the highest average voltage output of 308 ± 0.57 mV, while the fruit mixture and tomato peaked at 185.5 ± 0.25 mV and 163.03 ± 0.04 mV respectively. Sebastia *et al.* (2010), observed that at pH values that were higher than the ideal value, the growth of bacteria was inhibited, lowering the voltage generated. In another study, Yong *et al.* (2013) observed that alkaline medium boosted riboflavin biosynthesis from Shewanella, improving bio-anode performance. In this study, at pH 11, the findings indicated a decrease in voltage generation attributed to low electron transfer from the Anodic to Cathodic chambers giving voltage, power, and power density outputs.

A steady rise in voltage output over time was noticed, followed by a fall, possibly due to low microbial activities in all the experimental variations studied. This might be attributed to the adaptability of the inoculated microflora to the anodic microenvironment.

4.5.3.2 Current generated by Market fruit waste at various pH values

Table 4.7 below shows average current outputs from the various wastes at pH values of 2, 7 and 11. Banana waste gave the highest average output in the range of (0.0291 ± 0.0170 mA $-$ 0.0347 ± 0.021 mA) and lowest average output was recorded in mixture range of (0.0208 ± 0.0110 mA $- 0.0244 \pm 0.0130$ mA). Watermelon gave range of (0.0218 ± 0.0110 mA $-$ 0.0256 ± 0.0120 mA), mango ranged between (0.0261 ± 0.0150 mA $- 0.0326 \pm 0.0190$ mA), Avocado ranged between (0.0221 ± 0.0110 mA $- 0.0317 \pm 0.0120$ mA) and tomato at a range of (0.0211 ± 0.0110 mA $- 0.0255 \pm 0.0120$ mA).

Table 4.7: Generated current values at the various pH ranges

	AVERAGE CURRENT		
FRUITS	pH 2	pH 7	pH 11
AVOCADO	0.0273 ± 0.012	0.0317 ± 0.014	0.0221 ± 0.011
MANGO	0.0286 ± 0.017	0.0326 ± 0.019	0.0261 ± 0.015
TOMATO	0.0238 ± 0.012	0.0255 ± 0.021	0.0211 ± 0.017
WATERMELON	0.0256 ± 0.012	0.0270 ± 0.012	0.0218 ± 0.011
BANANA	0.0319 ± 0.019	0.0347 ± 0.014	0.0291 ± 0.015
MIXTURE	0.0221 ± 0.012	0.0244 ± 0.013	0.0208 ± 0.011

From the results obtained in Table 4.7, pH 7 showed the highest average current output. In the assessment of the effect of pH on current from the MFCs, it was noted that experiments performed in alkaline medium gave higher current output than those in acidic medium, probably because acidification of the anode inhibited microbial activity. In this study, banana fruit waste had the highest current, probably due to amount of carbon supplied by the substrates to the microorganisms. Chibueze and Chima (2018) observed an overall effect of pH on MFCs and opined that the amount of carbon given by the substrates at a pH value near neutrality (7.2 – 7.6), produced slightly higher current values. Behera *et al.* (2009) reported that a high current output at pH 8.0 could be efficient extracellular electron transport in this media condition, favouring electrogenic microorganism growth. The bacteria (microorganisms) at the anode have been discovered to be affected by the substrate utilized, which in turn affects the current generated (Zhang *et al.,* 2011). In terms of current measurement, banana and mango gave the lowest values.

According to reporting by Nurhayati (2013) and Azuoma *et al.* (2018), this could be due to the high amount of crude fiber. These low values were also observed in Miran *et al.* (2016), who claimed, that greater cellulose fibers in plants impede bacteria' capacity to degrade.

4.5.3.3 Generated Power and Power density by market fruit waste

In Figures 4.27 and 4.28, graphs of power and power density generated by market fruit waste at various pH values have been recorded. The values were in the range of (2.97 µW - 4.98 µW) and (503 µW /m^2– 935 µW /m^2) for pH 2, (3.53 µW - 6.14 µW), and (577 µW/m^2- 1153 µW/m^2) for pH 7, and (2.29 µW - 4.02 µW) and (417 µW/m^2- 755 µW/m^2) for pH 11 (Figures 4.27 and 4.28).

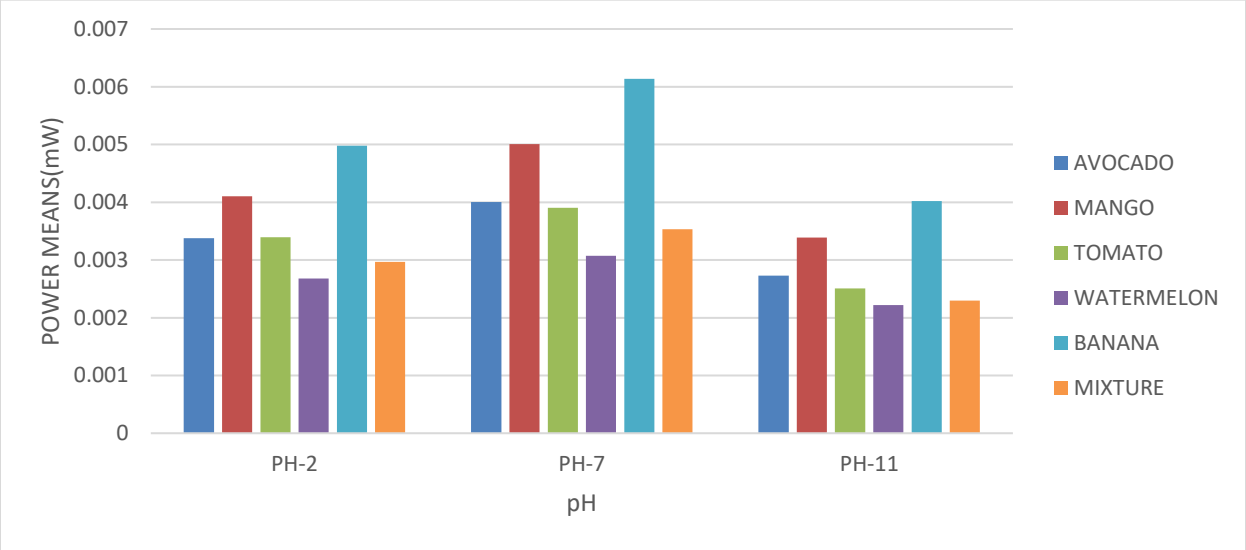

Figure 4.27: Generated Power at the various pH values

From the results (Figure 4.27) pH 7 gave the highest power mean of 4.3 ± 1.1 µW and it was taken as the Optimum operating pH for the MFC. At pH 2, the power output was slightly lower at 3.6 ± 0.8 µW, and this was attributed to the presence of acidic conditions which are hostile and possibly fatal to the microbes. At pH 11, the power output was lowest at 2.9 ± 0.7 µW, which is attributed to poor electron and proton transfer. The pH of the electrolyte in an MFC is a critical factor in its electrical output since low pH can either promote faster transport to both chambers due to increased proton concentrations or it can cause biological mortality of micro-organisms due to their lack of survival in a highly acidic environment (Puig *et al.*, 2010).

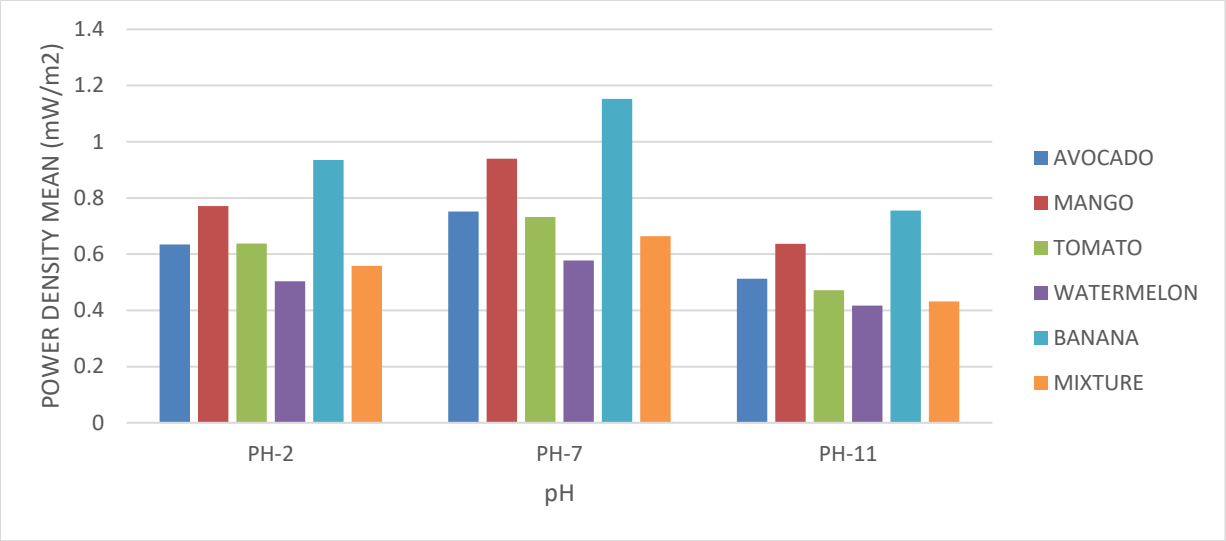

Figure 4.28: Power density values at various pH values

Figure 4.28 demonstrates the influence of pH on power density output. Neutral conditions gave the highest result $(0.803 \pm 0.209\ \mathrm{mW/m^2})$ the alkaline medium of pH 11 gave the lowest findings of $0.537 \pm 0.133\ \mathrm{mW/m^2}$, while the acidic condition of pH 2 gave a result of $0.673 \pm 0.157\ \mathrm{mW/m^2}$ a value that was slightly above those of alkaline conditions but lower than those of the neutral pH. Gil *et al.* (2003) observed that pH has a significant impact on power and power density generation in MFCs. A pH of less than six severely affects the amount of power generated by MFC. Low-pH circumstances had the opposite effect on the electrochemically active bacterial occupants, which result in a significantly low energy and power density output (Jadhav *et al.*, 2013). In other findings, Jadhav and Ghangrekar (2009) reported that pH affects the power generation of a microbial fuel cell. It was suggested that acidification of the anode reduced power generation by suppressing microbial activity (Jung *et al.*, 2011). In conclusion, the optimum operating pH for the MFCs was pH 7, as it resulted in highest voltage, current, power, and power density before it started to decline due to inhibition of microbial activity.

4.5.4 Effects of Temperature on electricity generation

The effectiveness of anaerobic conditions is greatly influenced by temperature. The majority of chemical and biological reactions run faster as they approach a point of deterioration when more

energy is applied to them. Since organisms carry out the digestive process, it was crucial to maintain a precise temperature range during the entire process to maximize reaction time and organism survival. In this research, to maximize MFC output, a suitable temperature was set to allow optimum microbial activity to generate electricity. Three sets of fuel cells were set-up at varied temperatures, namely, 25 °C, 37 °C, and 55 °C in a bid to test the effects of varying temperatures on MFC's output.

4.5.4.1 Voltage generated by market fruit wastes at various temperatures

Figure 4.29 demonstrates a graph of voltage results obtained when potentials of market fruit wastes were examined at different temperatures of 25 °C, 37 °C, and 55 °C. At 25°C, avocado had a slightly higher voltage than banana. Probably the fat in avocado fruit is made up for the lower temperature. Banana waste gave the highest voltage while tomato waste gave the lowest. The average voltage production was observed to be highest at 37°C (133.24 ± 0.23 mV – 215 ± 2.08 mV), followed by 25 °C (121.92 ± 0.34 mV - 174.99 ± 0.27 mV) and 55 °C gave the least voltage in the range of (113.87 ± 0.18 mV - 152.43 ± 0.57 mV) (Figure 4.29).

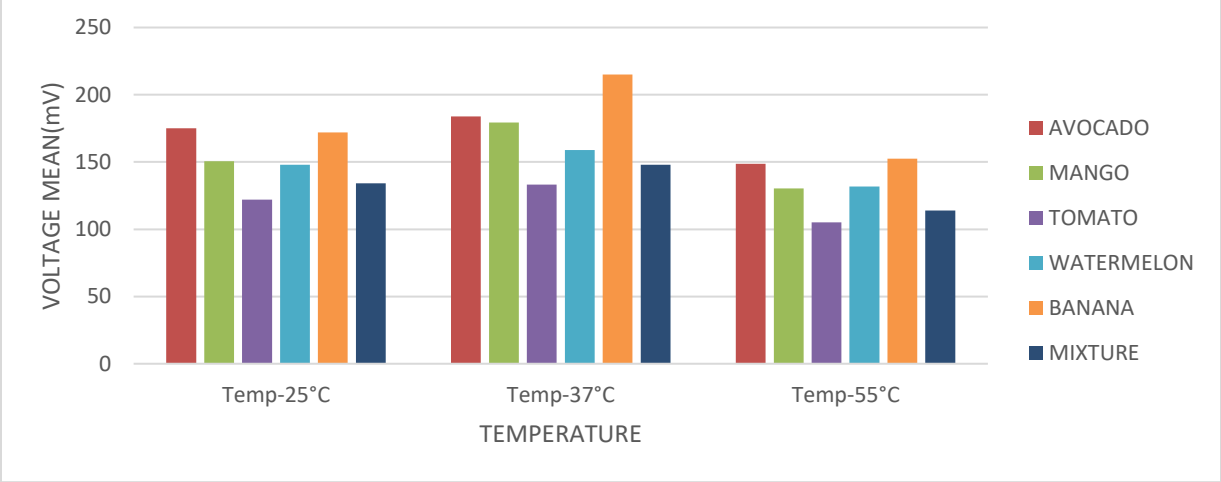

Figure 4.29: Generated Voltage at various Temperatures from various fruit wastes

Figure 4.29 above demonstrates how temperature varies with voltage output. Temperatures of 55 °C gave slightly lower outputs than 37 °C and 25 °C, suggesting that some bacteria involved in

the process of degradation of waste at the anodic chamber might have a higher tolerance to lower level temperatures.

Figure 4.30 below shows a plot of daily average voltage outputs given by MFC at 25 °C. At this temperature, initial MFC average voltage output was considerably low in the ranges of 174.99 ± 64.63 mV, 172.09 ± 81.79 mV, 150.45 ± 81.70 mV, 147.99 ± 55.97 mV, 134.06 ± 54.33 mV, and 121.94 ± 62.55 mV for banana, mango, avocado, watermelon, fruit waste mixture, and tomato, respectively.

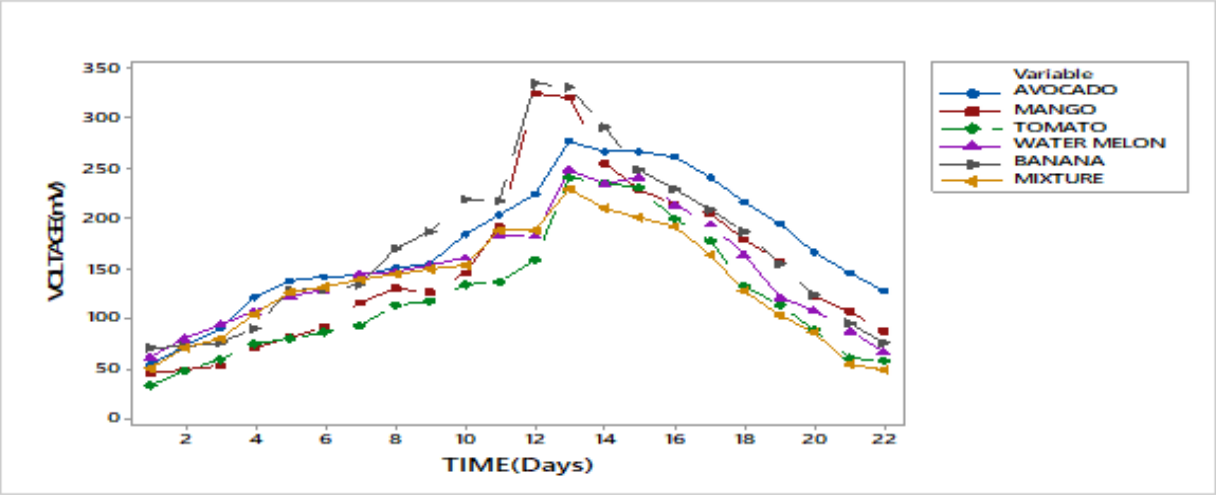

Figure 4.30: Generated Voltage at 25 °C from various fruit wastes

Figure 4.30 above shows that, at 25 °C, the daily voltage from all the market fruit wastes peaked on day 13, with banana giving the highest voltage output of 331 mV followed closely by mango 321 mV. The avocado, watermelon, tomato, and fruit mixture gave voltage outputs of 277 mV, 249 mV, 241 mV, and 230 mV, respectively. In addition, the voltage of the various wastes initially raised up till about day 14 and then declined on subsequent days.

Earlier findings by Bahera *et al.* (2011) when they compared the performance of MFCs at 28 °C, 40 °C, 50 °C, and 60 °C, observed that the initial MFC production at 28 °C was much lower. And this could be because the microorganisms' optimal temperature in the MFC was greater than room temperature. Tee *et al.* (2017) in a similar study, observed voltage output for MFCs operated at temperatures of 15 °C and 20 °C were quite low. The average voltage recorded was 71.74 ± 6.4 mV, 92.48 ± 4.3 mV for 15 and 20 degrees respectively. When they compared these results with

baseline studies conducted at 25 °C, the voltage generation at these temperatures was 20 – 45 % lower. A possible explanation is that higher temperatures made it easier for glucose molecules to spread throughout the sludge, making it more accessible to microorganisms (Larrosa *et al.*, 2010). It's probable that when the temperature rose, the viscosity of the medium decreased and therefore making it easier for the particles to move within the system. Generally, bacteria function well at certain temperatures, and depending on the bacteria involved they may have a more robust tolerance for lower temperatures (Li *et al.,* 2013). The drop-in voltage generation at lower temperatures could be related to microbial activities that are no longer active (Patil *et al.,* 2010), thereby lowering the substrate consumption rate and consequently the bio-energy.

Figure 4.31 below shows a plot of daily voltage readings given by MFC when immersed in a water bath at 37 °C. At this temperature, the MFC average voltage was generally higher than that at 25 °C and 55 °C, with banana waste giving the highest average voltage output of 215.15 ± 103.86 mV. The avocado gave an output of 183.77 ± 63.78 mV, and mango, watermelon, fruit waste mixture, and tomato gave an output of 179.41 ± 81.87 mV, 158.82 ± 54.74 mV, 147.98 ± 58.07 mV, and 133.24 ± 63.60 mV respectively.

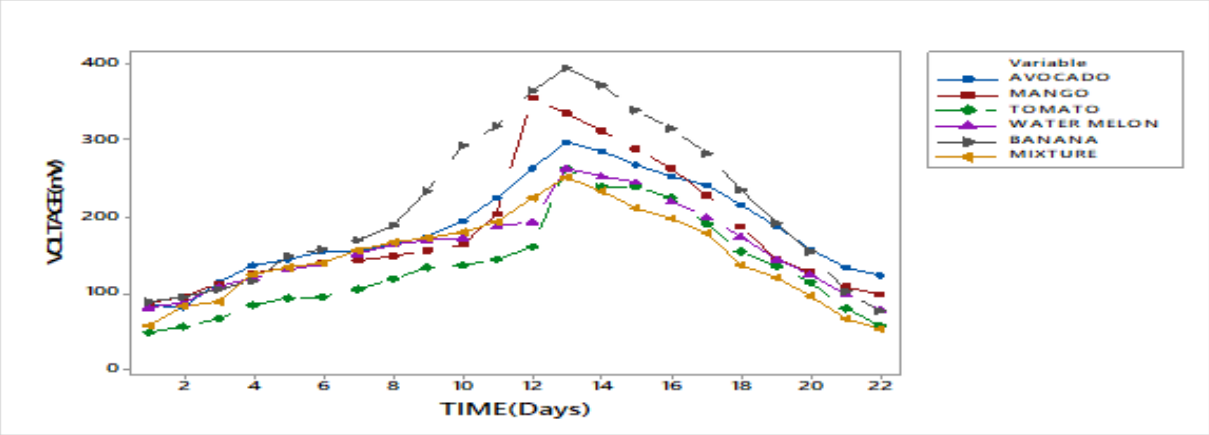

Figure 4.31: Generated Voltage at 37 °C from various fruit waste

Besides other parameters in MFCs optimization, a suitable temperature is crucial for optimal microbial activity in the MFC. At 37 °C temperature, it is observed that highest voltage of the three temperatures investigated is obtained. The results showed that voltage output increased upwards, where it peaked at 339 mV the 13th day, before declining gradually. It is envisaged that at this

temperature, more microbes were able to metabolize the substrate and generate electrons. The high peak observed might be due to the lower resistance in the MFC circuit when compared to MFCs at a higher temperature.

Rahman *et al.* (2021), noted that the most common microbes are mesophiles, which digest materials in a mesophilic manner and function best at temperatures between. 35 °C to 37 °C (95 °F to 98 °F). Bahera *et al.* (2011) and Rahman *et al.* (2021) indicated that an ideal temperature for the microbes in the MFC was greater than room temperature, allowing the microbes to metabolize the substrate, and thus get to consistent voltage output quickly. According to a different study by Pei-Fang et al. (2017), operating temperatures of 30 °C and 35 °C led to the generation of appropriate amounts of voltage, with averages of 115.68 8.2 mV and 125.69 9.1 mV, respectively. These phenomena could be explained by growth in biomass and increased substrate usage when the temperature rises, improving microbial activity and bacterial attachment to the electrode (Grady Jr & Daigger, 1999). As a result, electrons may be successfully transported from the anode, increasing voltage generation.

Figure 4.32 below shows a plot of daily voltage output given by MFC when immersed in a designed water bath conditioned at a temperature of about 55 °C. At this temperature, MFC average voltage output was generally lower than that at the previous temperatures (25 °C and 37 °C). The average voltage values recorded were highest in banana at 152.43±73.71mV, as avocado gave 148.59 ± 59.03 mV, while watermelon, mango, the mixture of fruit wastes, and tomato gave an output of 131.68 ± 52.21 mV, 130.29 ± 74.29 mV, 113.87 ± 51.57 mV, and 105.05 ± 57.79 mV, respectively.

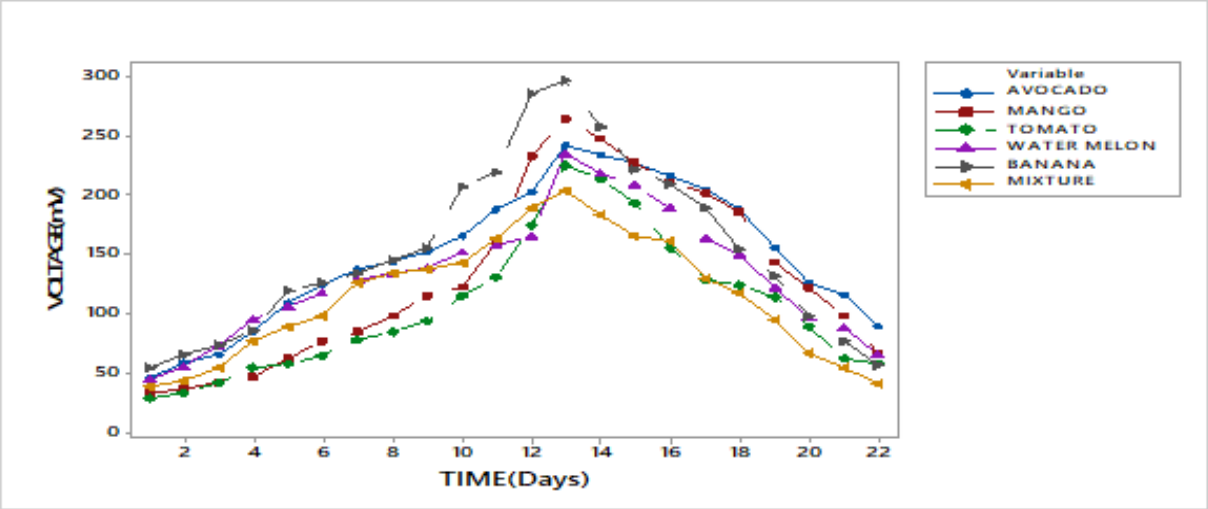

Figure 4.32: Generated Voltage at 55 °C from various fruit wastes

From figure 4.32, it is clear that voltage outputs for all the fruit waste peaked on the 13th day with highest recordings ranging from 203 mV to 296 mV. Microbes are sensitive to changes in temperature, and unfavourable temperatures might lead to a reduction in cellular activity or even death. Tee *et al.* (2017) observed that voltage readings had a declining trend for MFCs operated at varied temperatures of 15 °C, 20 °C, 40 °C and 55 °C. The average voltage recorded was 71.74 ± 6.4 mV, 92.48 ± 4.3 mV, 64.45 ± 9.1 mV, and 62.61 ± 11.5 mV, for 15, 20, 40, and 55 degrees respectively. Low voltage generation at high operating temperatures (> 40 °C) may be caused by enzyme denaturation, which results in poor electron transport to the electrode, resulting in low voltage generation (Kong *et al.*, 2011). Furthermore, when bacteria are repeatedly exposed to high temperatures, critical elements in the cell such as proteins, nucleic acids, and other temperature-sensitive materials may suffer irreparable damage, affecting cell function. Generally, the performance at 37 °C was found better as compared to the MFC-adsorption hybrid system operated at 25 °C which may be because the biofilms grown at 37 °C are more electrochemically active as compared to those grown at 25 °C which in turn helps in the transfer of the electrons to the anode electrode.

4.5.4.2 Current generated by market fruit waste at different temperatures

Current generated in an open circuit by market fruit waste using double chamber MFC at various temperatures was recorded for a period of 22 days. Table 4.8 below shows the tabulated current

average outputs in the range of (0.0182 ± 0.007 mA - 0.0222 ± 0.008 mA), (0.0207 ± 0.007 mA - 0.0241 ± 0.007 mA) and (0.0145 ± 0.006 mA - 0.0198 ± 0.006 mA) for 25 °C, 37 °C and 55 °C respectively.

Table 4.8: Generated current from various Temperatures

	AVERAGE CURRENT (mA)		
FRUITS	Temp 25 °C	Temp 37 °C	Temp 55 °C
AVOCADO	0.0210 ± 0.0070	0.0228 ± 0.0070	0.0176 ± 0.0060
MANGO	0.0216 ± 0.0080	0.0236 ± 0.0080	0.0189 ± 0.0070
TOMATO	0.0192 ± 0.0080	0.0212 ± 0.0080	0.0158 ± 0.0070
WATERMELON	0.0194 ± 0.0080	0.0208 ± 0.0080	0.0169 ± 0.0070
BANANA	0.0222 ± 0.0070	0.0241 ± 0.0070	0.0198 ± 0.0060
MIXTURE	0.0182 ± 0.0070	0.0207 ± 0.0060	0.0145 ± 0.0060

In this study, it was observed that the output was high at 37 °C and lowest at 55 °C. Banana gives the highest range $(0.0198 \pm 0.006\ \text{mA} - 0.0241 \pm 0.007\ \text{mA})$, avocado gave an output range of $(0.0176 \pm 0.006\ \text{mA} - 0.0228 \pm 0.007\ \text{mA})$ and mixture of fruit waste gave lowest output of $(0.0145 \pm 0.006\ \text{mA} - 0.0207 \pm 0.006\ \text{mA})$, this can be attributed to the effect of temperature on-resistance of the circuit. Rahman *et al.* (2021) indicated that higher temperature increased a conductor's resistance, resulting in less current flow. As a result, the efficiency of an MFC dropped when the applied temperature was too high. According to the findings in an earlier study by Tremouli *et al.* (2017), the MFC's increase in effectiveness at relatively high temperatures could be ascribed to the electrogenic bacteria's metabolic activity increases with temperature. The MFC performance did not change considerably when the temperature was varied between 24 °C and 26 °C indicating that the electrogenic bacteria's metabolic activity was not responsive to slight temperature variations in this range.

4.5.4.3 Generated Power and Power density by market fruit waste at different temperature values

Figures 4.33 is a graph of average power generated by various market fruit waste in MFCs and catalyzed by goat rumen fluid. The power observed was in the range of $(3.1 \pm 0.4\ \mu\text{W})$ for 25 °C,

(3.8 ± 0.6 µW) for 37 °C, and (2.3 ± 0.4 µW) for 55 °C. The results showed that the highest outputs were in 37 °C, as shown in Figures 4.33 below.

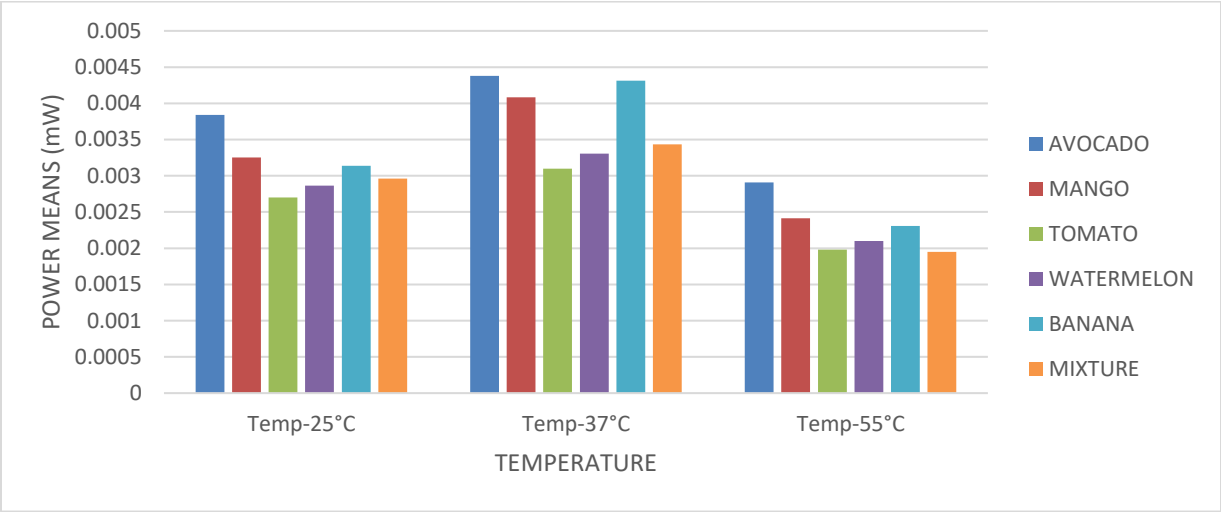

Figure 4.33: Generated power from various Temperatures

The MFC at 37 °C generally showed a stable power output in all market fruit wastes, with avocado giving the highest peak at 4.4 µW and tomato lowest peak at 3.1 µW. There are a few possibilities that might have contributed to this observation. According to studies by Larrosa *et al.* (2010), a conceivable scenario is that higher temperatures increase the distribution of substrate molecules throughout the sludge, making it more accessible to microorganisms and resulting in a significant increase in power output. In the present study, the MFCs established at 37 °C obtained a stable power generation consistent with other studies.

Figure 4.34 is a graph of mean power density values generated by market fruit waste catalyzed by goat rumen fluid. The values were in the range of (587 ± 75 µW/m^2) for 25 °C, (708 ± 104.0 µW/m^2) for 37 °C, and (428 ± 67 µW/m^2) for 55 °C.

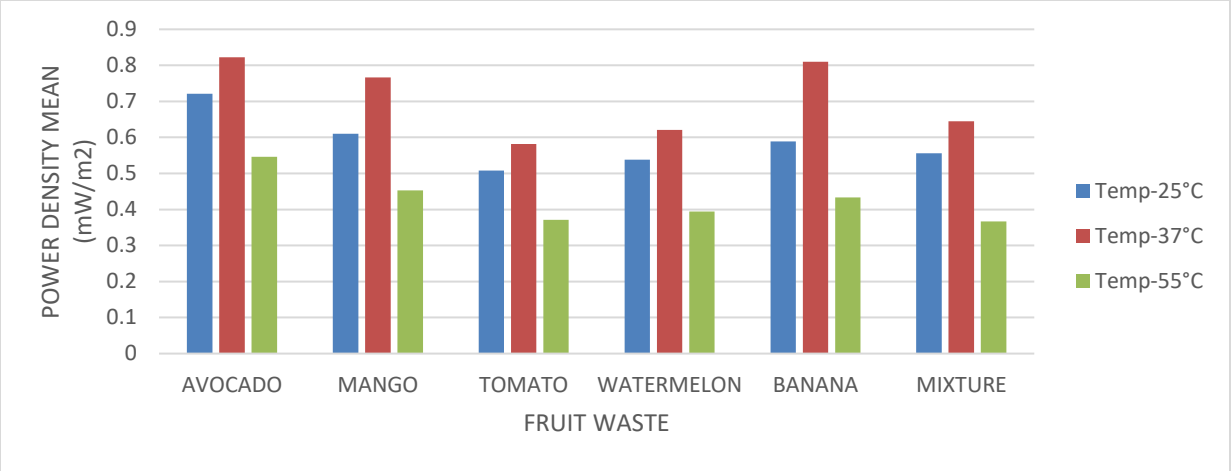

Figure 4.34: Average power density values at Various Temperatures

From figure 4.34, the overall data obtained indicated that the power density output was highest at 37 °C at $708 \pm 104\ \mu W/m^2$, then at 25 °C $587 \pm 75\ \mu W/m^2$) and the lowest at 55 °C ($428 \pm 67\ \mu W/m^2$). These observations are consistent with findings by previous researchers. Li *et al.* (2013), for example, observed that, when temperature of a MFC was raised to 55 °C, there was unstable power generation, which could be linked to the changed bacterial community composition. Tremouli *et al.* (2017) reported power-density rising at a relatively high temperature as compared to low temperatures. In particular, maximum power density remained practically constant ($\sim 36\ mW/m^2$) at 24 °C and 26 °C. It was observed to increase at 30 °C, 33 °C and 35 °C where values of ($49\ mW/m^2, 50.5\ mW/m^2$, and $59\ mW/m^2$) respectively were observed.

In conclusion, therefore, the optimal operating temperature for MFCs in this study was determined to be 37 °C, as it produced the highest voltage, current, power, and power density. In addition, based on the data recorded, the power generated from MFC in all optimized parameters displays a similar trend with the voltage output. This finding agrees with the theory where power output is directly proportional to the voltage output as shown in the power Law equation i.e, (P = IV).

4.6 Modelling of Substrate utilization and Simulation Studies

Modelling studies were used to investigate nature of chemical reactions in MFCs and also to determine the various qualitative and quantitative parameters related to the modeling equations.

4.6.1 Assumptions for the model

Mathematical as well as numerical models normally reflect the influence of varied operational conditions and design parameters on efficient performance of a microbial fuel cell system (Jadhav *et al.,* 2021). As a complicated bioelectrochemical system, numerous assumptions must be made to construct a mathematical model of a complex MFC system into a simple and linear form (Capodaglio *et al.*, 2017; Lari *et al.,* 2019). Some of the most typical assumptions utilized in different models are as follows:

(i) The substrate is assumed to be uniformly mixed under correct mixing conditions, and the substrate concentration gradient in electrode-biofilm matrix is ignored (Gadkari *et al.,* 2019)

(ii) Homogeneity in anolyte and catholyte solutions is assumed throughout the operational duration of MFC (Gadkari *et al.*, 2019)

(iii) Gas generation (CO_2, CH_4 and other minor gases) and transport throughout anodic or cathodic chambers are neglected (Gadkari *et al.*, 2019)

(iv) A non-limiting reaction rate is considered in the cathodic chamber (Luo *et al.,* 2016).

(v) The pH, temperature, and other operating conditions are assumed to be fully controlled to minimize their effect on the microenvironment of MFC (Radeef and Ismail, 2019; Gadkari *et al.,* 2019).

(vi) Most modeling approaches are developed based on one consideration (e.g. electrochemical or biological) while keeping other parameters constant/controlled (Shemfe *et al.* (2018).

(vii) Mathematical or kinetic models are selected based on the behavior of microbial species to boundary conditions Shemfe *et al.* (2018).

(viii) A non-limiting flow of anions and cations in the biofilm maintains electroneutrality; hence, ions moved with no ohmic loss (Su *et al.,* 2018).

4.6.2 Estimation of anode respiration kinetic parameters

The anode respiration kinetic parameters were estimated and calculated as reported in the following sections.

4.6.2.1 Bacterial growth

The Monod model (Equation 4.9a) was used to calculate the kinetic parameters for bacterial growth in the Batch mode MFC because it describes the unstructured and unsegregated phenomenon in the cell. The half-saturation coefficient (K_S) of the substrate in banana fruit waste fed MFC was 99.63 gL^{-1} with a growth yield coefficient of 0.82 h^{-1} after 408 hours (17 days) of microbial activities, calculated using Equation 4.9a - 4.9d (*Appendix* 2*: Monod Model calculations*).

Monod Model:

$$r = r_{max} * \frac{S}{(K_S + S)} \quad (4.9a)$$

Taking the reciprocal of Monod Equation: (y = mx + c). Note: (r = μ)

$$\frac{1}{\mu} = \frac{K_S + S}{\mu_{max} * S} = \left(\frac{Ks}{\mu_{max}}\right) * \left(\frac{1}{S}\right) + \left(\frac{1}{\mu_{max}}\right) \quad (4.9b)$$

$$\mu = \frac{\text{amount of biomass produced}}{\text{time taken}} \quad (4.9c)$$

$$\mu_{max} = \frac{\text{amount of biomass produced}}{\text{initial inoculum volume x time taken}} \quad (4.9d)$$

Where: **S** stands for substrate concentration. **μ** stands for growth yield coefficient. μ_{max} stands for maximum growth rate. K_S stands for half-saturation coefficient

Using the same equations (4.9a - 4.9d) above, the half-saturation coefficient (K_S), growth yield coefficient (μ), and maximum growth rate (μ_{max}) results for all the fruit waste samples collected from markets in Nairobi County, Kenya, in this study were calculated and the results are given in Table 4.9.

Table 4.9: Half-saturation coefficient, growth yield coefficient, and maximum growth rate

No	Sample	μ	μ_{max}	K_S
1	AVOCADO	0.76 h^{-1}	0.003 h^{-1}	99.61±0.03 gL^{-1}
2	MANGO	0.80 h^{-1}	0.003 h^{-1}	99.63±0.03 gL^{-1}
3	TOMATO	0.59 h^{-1}	0.002 h^{-1}	99.66±0.03 gL^{-1}
4	BANANA	0.82 h^{-1}	0.003 h^{-1}	99.63±0.03 gL^{-1}
5	WATERMELON	0.69 h^{-1}	0.003 h^{-1}	99.57±0.03 gL^{-1}
6	MIXTURE	0.53 h^{-1}	0.002 h^{-1}	99.62±0.03 gL^{-1}

μ- stand for growth yield coefficient. μ_{max} – stand for maximum growth rate. K_S- stand for half-saturation coefficient

In the investigation of the results, Table 4.9 showed that banana fruit waste gave the highest output of 0.82 h^{-1} in the growth yield of bacteria and a high half-saturation coefficient of 99.66 ± 0.03 gL^{-1}, which could be attributed to the availability of carbon sources in banana fruit waste. The lowest output in growth yield coefficient of 0.53 h^{-1} was obtained by the fruit mixture sample and the lowest value obtained for the half-saturation coefficient was the one obtained for watermelon at 99.57 ± 0.03 gL^{-1} which is attributable to the high fiber levels and low carbon levels in watermelon substrate, thus inhibiting the degradation process of the substrate eventually lowering the growth yield of the bacteria. Esser *et al.* (2015) and Nasrollahzadeh *et al.* (2010) reported that toxic effects from other vegetables might inhibit the degradation process at high substrate concentrations. According to Kaveh *et al.* (2019), Kinetics of a self-inhibitory substrate's biodegradation was primarily concerned with bacteria's physiological reactions to substrate concentration levels. However, this study has theoretically analyzed the role and interactions between mass transfer limitations and self-inhibition by numerical solutions using a simple model that could have practical relevance.

Furthermore, Monod model only explained microbial growth and activities but not the effect of self-inhibition. This study used other models (Haldane Andrew's Kinetic and Han-Lavenspiel Models) to observe substrate consumption and bacteria growth and estimate substrate degradation's kinetic parameters.

4.6.2.2 Substrate self-inhibitory effect

Haldane Andrew's Kinetic Model (Equation 2.5) was used to calculate the (K_{IH})-self-inhibitory effect coefficient of the substrates. The *Haldane Andrew's Kinetic Model calculations are provided in Appendix* 3:).From the results, the K_{IH} value for the banana fruit waste sample was found to be 50.18 ± 0.04 mL after 408 hours (17 days) of microbial activities using Equations 4.89 - 4.9d and 4.10a - 4.10b. This K_{IH} value was found to be relatively high, a factor that indicated that the inhibitory effect was weak.

Haldane Andrew's Kinetic Model

$$r = r_{max} * \frac{S}{\left(K_S + S + \frac{S^2}{K_{IH}}\right)} \qquad (4.10a)$$

Note: (r = μ)

Taking the reciprocal of Haldane Andrew's Kinetic Equation: ($y = mx + c$)

$$\frac{1}{\mu} = \frac{K_S + \frac{S^2}{K_{IH}}}{\mu_{max}} * \frac{1}{S} + \frac{1}{\mu_{max}} \qquad (4.10b)$$

Where: **S**-Is substrate concentration. **μ**-Is growth yield coefficient. μ_{max} – Is maximum growth rate. K_S -Is half-saturation coefficient. K_{IH} -Is inhibitory effect coefficient

Using the same equations (4.10a - 4.10b) above, the self-inhibitory effect coefficient (K_{IH}) results for the other fruit waste samples collected from markets in Nairobi County, Kenya, in this study were calculated and later tabulated in Table 4.10 below.

Table 4.10: Self-inhibitory effect coefficient for all the fruit waste samples

No	Sample	(K_{IH})
1	AVOCADO	$50.09 \pm 0.04\ gL^{-1}$
2	MANGO	$50.09 \pm 0.04\ gL^{-1}$
3	TOMATO	$50.09 \pm 0.04\ gL^{-1}$
4	BANANA	$50.18 \pm 0.04\ gL^{-1}$
5	WATER MELON	$50.11 \pm 0.04\ gL^{-1}$
6	MIXTURE	$50.09 \pm 0.04\ gL^{-1}$

K_{IH} - inhibitory effect coefficient

The market fruit wastes sampled gave self-inhibitory effect coefficient (K_{IH}) output in a range of $50.18 \pm 0.04\ gL^{-1} - 50.09 \pm 0.04\ gL^{-1}$, a clear indication that the inhibitory effect was weak; since when (K_{IH}) value is high, the inhibitory effect is weak, and the inhibitors are loosely attached to the microbes. When (K_{IH}) value is small, the inhibitor is tightly bound, and the number of active enzymes present will be limited; hence the inhibitory effect will be strong (Chai *et al.,* 2021). The number of active microbes present was high enough to bio-degrade the available substrate in a given period, as was earlier indicated by the Monod model on microbial growth and substrate degradation (Table 4.9). Non-competitive inhibition is that in which the inhibitor does not bind to the active sites of the substrate, giving the substrate space to attach to the bacteria and form a complex that decreases the activation energy of a chemical process. Studies by Jiqiang *et al.* (2013) observed that when the K_{IH} value was high (K_{IH} >10 gL^{-1}), the inhibitory effect was weak and that when K_{IH} value was small (K_{IH} < 10 gL^{-1}) meant the inhibitor was tightly bound. The amount of active enzyme present was small, indicating that the inhibitory effect was substantial. The K_{IH} values obtained in this present study compared well to the previous research work by Seluy and Isla, (2014) on enhanced ethanol production from vinasse fermentation who obtained a. K_{IH} of 67 gL^{-1}.

4.6.2.3 Critical inhibitor concentration

Han-Lavenspiel model (Equation 4.11) was used to calculate the critical inhibitor concentration coefficient (S_m) of the substrate. The amount of substrate degraded by the microbes in the banana fruit waste was up to $100.75 \pm 3.71\ gL^{-1}$ after 408 hours (17 days) of microbial activities using

Equation 4.8a - 4.8d, 4.9a - 4.9b, and 4.10. Suggesting that after consumption of the 100 gL^{-1} substrate and the 0.75 gL^{-1} substrate initially in the rumen fluid, the chemical reaction completely stopped and the production of electrons and protons, indicating the microbes' death and the end of a chemical reaction. (*Appendix* 4*: A sample of the Han-Levenspiel Model calculation*).

Han-Levenspiel Model: Note: $(r = \mu)$ and $(n = m = 1)$

$$r = r_{max} * \frac{S\left(1 - \frac{S}{S_m}\right)^n}{S + K_S * \left(1 - \frac{S}{S_m}\right)^m} \quad (4.11)$$

Where: **S**-Is substrate concentration, **μ**-Is growth yield coefficient. $\boldsymbol{\mu_{max}}$ **–** Is maximum growth rate.$\mathbf{K_S}$ – Is a half-saturation coefficient. $\mathbf{S_m}$**-**Is critical inhibitor concentration coefficient

Using the same Equations (4.11) above, the critical inhibitor concentration coefficient (S_m**)** results for all the fruit waste samples collected from markets in Nairobi County, Kenya, were computed and are tabulated in Table 4.11 below.

Table 4.11 Critical inhibitor concentration coefficient for all the fruit waste samples

No:	Sample	S_m	Time(Hours)	Figure
1	AVOCADO	99.72 ± 3.68 gL^{-1}	408.45 Hrs	Fig. 4.5
2	MANGO	99.75 ± 3.68 gL^{-1}	408.49 Hrs	Fig. 4.5
3	TOMATO	99.85 ± 3.68 gL^{-1}	408.78 Hrs	Fig. 4.5
4	BANANA	100.75 ± 3.67 gL^{-1}	412.57 Hrs	Fig. 4.5
5	WATERMELON	99.60 ± 3.67 gL^{-1}	408.12 Hrs	Fig. 4.5
6	MIXTURE	91.09 ± 3.36 gL^{-1}	373.06 Hrs	Fig. 4.5

It is evident in this study (Table 4.11) that all the experiments stopped after each fruit was biodegraded up to individual fruit waste critical inhibitor concentration coefficient (S_m) at different times as indicated by the different amounts of substrate consumed in (gL^{-1}). Han-Levenspiel models allow for the determination of the critical concentration of substrate that could completely inhibit generation of product as evident from this work. Up to 100 gL^{-1} substrate concentration and the 0.75 gL^{-1} substrates initially in the rumen fluid of the banana fruit waste were exhaustively consumed by the microbes. This indicates that the chemical reaction stopped 5

hours later after peaking at 412.57 hours (17 days). The fruit waste mixture's reaction stopped much earlier after peaking at 373.06 hours (Table 4.11), which could be attributed to the toxicity of individual fruits (Agbossou *et al.*, 2004). The chemical reaction taking place in the MFC chambers loaded with avocado fruit waste as substrate, stopped at 408.45 hrs; mango fruit waste chemical reaction stopped at 408.49 hrs; tomato stopped at 408.78 hrs, and watermelon stopped the reaction at 408.12 hrs which were all attributed to acid inhibition and consequent microbial death. The experiment concluded that, competitive inhibition, where an inhibitor resembling the standard substrate had bound to the enzyme at active site and prevented substrate from binding, or uncompetitive inhibition, where an inhibitor binds only to enzyme-substrate complex and not to free enzyme. Thus, decline in microbial growth, facilitating an end of chemical reaction in the microbial fuel cell.

Jiqiang *et al.* (2013) reported that microbial growth stopped completely when critical inhibitor concentration (S_m) was reached and accounted for different inhibitions using the Han-Levenspiel model. Zhang *et al.* (2013) demonstrated substrate-inhibition by using various models to approximate kinetics-model parameters of substrate degradation using correlation between substrates concentration and substrate breakdown rate as a basis, voltages as well as power densities output in an anodic-denitrification Microbial Fuel Cell (AD-MFC). Their study showed that although high substrate concentrations initially showed high bio-hydrogen production, they dropped to lower levels due to simultaneous acid inhibition and increased partial pressure of hydrogen in the flask (Wang and Wan, 2008). This suggests that bioreactors' optimal carbon source levels are critical during pilot-scale studies and continuous bio-hydrogen production. Failure to do so may affect the microorganism's growth rate, special substrate utilization rate, enzyme activity, and overall process yield. As a result, the substrate concentration in the liquid phase must be kept at appropriate levels to avoid the synthesis of volatile fatty acids (VFAs) and the occurrence of substrate inhibitions (Mullai *et al.*, 2013; Hill *et al.*, 2020).

Moreover, Critical inhibitor concentration (S_m) demonstrated the need to segregate solid waste since each experimental setup stopped at different times depending on fruit waste. Kinetic models are used to investigate and evaluate the metabolic characteristics of defined cultures in general. Optimization studies using various inocula, substrates, process parameters, performance

evaluation, and economics of continuous bio-hydrogen generation systems should be focused on in future research.

4.6.3 Description of Reaction kinetics taking place in MFCs

This section elaborates on kinetics reactions taking place inside microbial cell chambers on sampled market fruit waste.

Using equations (4.12 - 4.14) below, banana fruit waste data recorded from MFC for 528 hours (22 days) was used to identify the order of reaction taking place in this study. *Values for the other substrates were computed as indicated in Appendix* 5*:*

Equation of Zero-Order Reaction (4.12)

$$[\mathbf{A}] = -kt + [A_o] \quad \text{(a)}$$

$$t\frac{1}{2} = \frac{[A_o]}{2k} \quad \text{(b)}$$

Equation of First-Order Reaction (4.13)

$$Ln[A] = -kt + Ln[A_o] \quad \text{(a)}$$

$$t\frac{1}{2} = \frac{0.693}{K} \quad \text{(b)}$$

Equation of Second-Order Reaction (4.14)

$$\frac{\mathbf{1}}{[\mathbf{A}]} = -kt + \frac{\mathbf{1}}{[A_o]} \quad \text{(a)}$$

$$t\frac{1}{2} = \frac{1}{\mathbf{k}[A_o]} \quad \text{(b)}$$

In the equation: (k)– Is Kinetic Rate Constant, [ ]- is Molar concentration, t = Time and ($t\frac{1}{2}$) = Half-life.

Analysis of the dataset ruled out the possibility of Zero-order reaction since the reaction rate in this order is constant, and yet this was not what was observed since in the experiments with MFCs, the potential was observed to increase with time. Comparing results obtained for first-order and second-order reaction kinetics, (Table 4.12) it was noticed that (R^2) values for first-order kinetics were close to a unit, ($R^2 = 0.82$) and the same were significantly lower for second-order kinetic reactions ($R^2 = 0.75$). The outcome of these experiments, favoured first-order kinetics over second-order kinetics, and therefore it was concluded that chemical reactions taking place in various microbial fuel cells in this study followed first-order kinetics.

Figure 4.35 shows natural log (Ln) plot of voltage output against time (days) for 22 days for banana fruit waste using Origin software. The straight line of best-fit had the equation of a line ($y = 0.064x + 4.545$) and correlation coefficient of ($R^2 = 0.82$).

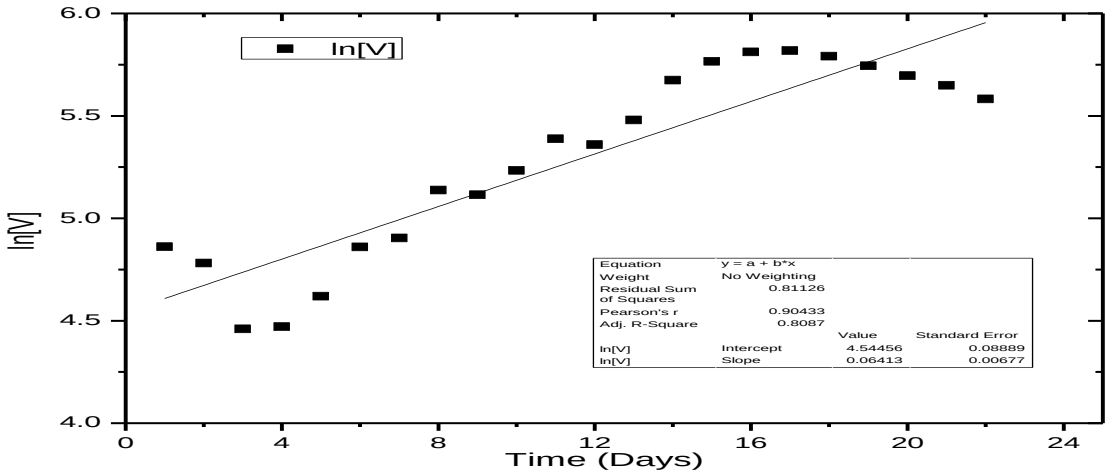

Figure 4.35 A plot of ln(V) versus time (days) for banana

Linear Regression of dataset: Figure 4.35, using the function: A*x+B

R^2= 0.818

Using (Eq. 4.13), the equation of the line obtained, the correlation coefficient (R^2), Kinetic rate (k), and the Half-life ($t\frac{1}{2}$) results for all the fruit waste samples collected in this study were calculated and tabulated in the (Table 4.12) below.

Table 4.12 Results for the First-order kinetic reaction model

FRUITS	EQUATION OF A LINE	R^2	KINETIC RATE(k)	$t\frac{1}{2}$
AVOCADO	$y = 0.093x + 3.916$	0.75	0.0039 hr^{-1}	177.7 hrs.
MANGO	$y = 0.096x + 3.958$	0.87	0.0040 hr^{-1}	173.3 hrs.
TOMATO	$y = 0.083x + 3.891$	0.87	0.0034 hr^{-1}	203.82 hrs.
WATERMELON	$y = 0.064x + 4.402$	0.86	0.0026 hr^{-1}	266.5 hrs.
BANANA	$y = 0.064x + 4.545$	0.82	0.0027 hr^{-1}	256.7 hrs.
MIXTURE	$y = 0.051x + 4.422$	0.68	0.0022 hr^{-1}	315 hrs.

The First-order kinetic model (Eq. 4.13) was found to fit microorganisms' biodegradation of organic materials quite well. The voltage output in the samples when reduced to half of its initial amount (half-life) was shorter in mango samples followed by avocado samples and longer in the fruit mixture samples. This implied that mixture samples would be expected to have a longer life than the individual fruit waste samples concerning biodegradation using goat rumen fluid as inoculum. The results tabulated in Table 4.12, indicate the half-life of all the samples. The banana fruit took 256.7 hours (10.7 days) more after 528 hours (22 days) of the experiment with a proposed first-order model $\mathrm{Ln(A)} = \mathrm{Ln(A_o)} - 0.0027\ \mathrm{t}$. In addition, the results indicate that the kinetic rate constant (k) for banana fruit waste was ($k = 0.0027\ hr^{-1}$) which translated to 0.064 days as observed in the straight-line curve equation for the same (y = 0.064x + 4.545).

A probable mechanism for the reaction, given that the enzymatic microbes [E] react with the substrate (fruit waste) [S]: Reaction: S + E → P would be:

$$[S] \rightarrow [S]^* \text{ (slow, rate-limiting)} \qquad (4.15)$$

$$[S]^* + [E] \rightarrow P \text{ (fast)} \qquad (4.16)$$

Where S* is the reactive intermediate in the reaction, S is the fruit waste being investigated (the substrate, E is the Enzyme (or microorganism) concentration, and (P) is the final product after the reaction is completed.

Hereafter, a rate equation is declared to fit the data well if it provides a higher (R^2) value following the recommendation from a statistician (Di-Bucchianico, 2008). Table 4.12 shows the biodegradation rate constants (k) and half-life durations ($t\frac{1}{2}$) for the various remediation procedures. The greater the biodegradation rate constants, the higher or faster the rate of biodegradation and, as a result, the shorter the half-life. According to Ofoegbu *et al.*, (2015), biodegradation rate has a positive correlation coefficient (R^2) with total hydrocarbon content reduction, with a higher biodegradation rate taking less time. For instance, in the biodegradation of 2% crude oil treatment, it was observed that the polluted soil that is amended with a combination of inorganic fertilizer (NPK) and cow-dung (CD), reveals a higher rate constant (k=0.042 day^{-1}) and at a lower half-life ($t\frac{1}{2}$ =16.5 days); compared to soil amended with inorganic fertilizer (NPK) only, which has a lower rate constant (k = 0.035 day^{-1}) and higher half-life ($t\frac{1}{2}$ = 19.8 days) respectively.

4.7 Multivariate Data Analysis (ANOVA) for market fruit wastes

To further elaborate this dataset, the ANOVA analysis was performed and the effects of microbes as a biocatalyst on various market fruit wastes were investigated. All the statistical analyses were performed with JMP 11 (SAS Institute Inc., NC, USA). The Analysis of Variance (ANOVA) and student's t-test at a 95 % confidence level was conducted, and $p < 0.05$ value was considered significant statistically. On graphs in this section, the term: treatment refers to the fruit waste sample.

4.7.1 Fruit waste (Treatment) against Voltage output

One-way ANOVA was used to examine the significant difference between the data that had been collected. Further, an inspection of the correlation matrix in which the diagonal shows the correlation of each variable with itself, while the off-diagonal shows the correlation at the intersection and scatter plot matrix revealed the correlation coefficients between the variables obtained from the analysis. Figure 4.36 shows a visualized dot-plot and confidence intervals for each treatment for voltage output for market fruit waste. The differences in the fruit mixture,

banana, and tomato samples were significant, indicating that other factors such as temperature, pressure, the preparation of the substrates, etc., were affecting the voltage output.

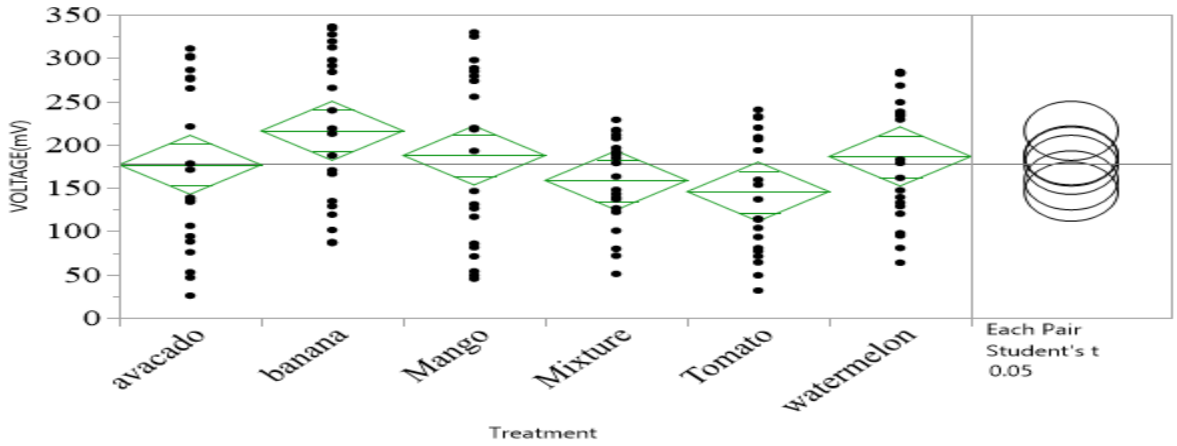

Figure 4.36: ANOVA results for Treatment versus Voltage output

ANOVA findings provided in the Table 4.13 showed a significant difference in banana, tomato and fruits waste mixture (*Appendix* 6 -10*: Multivariate Data Analysis*).

Table 4.13: ANOVA test for market fruit wastes Voltage

Connecting Letters Report

Level			Mean (mV)
Banana	A		215.96 ± 88.26
Mango	A	B	187.56 ± 98.55
Watermelon	A	B	186.38 ± 72.99
Avocado	A	B	176.78 ± 95.16
Mixture		B	158.76 ± 50.96
Tomato		B	145.75 ± 68.72

Level not connected by same letter are statiscally significant

4.7.2 Treatment (Fruit waste) against Current output

Figure 4.37 shows a visualized dot-plot and confidence intervals for each treatment for current output for market fruit waste. Fruit waste mixture and banana alone were significantly different in

terms of the current production. The results illustrated that just like in kinetic modelling, sample mixture generated low output, attributed to the toxicity of individual fruit waste in the mix.

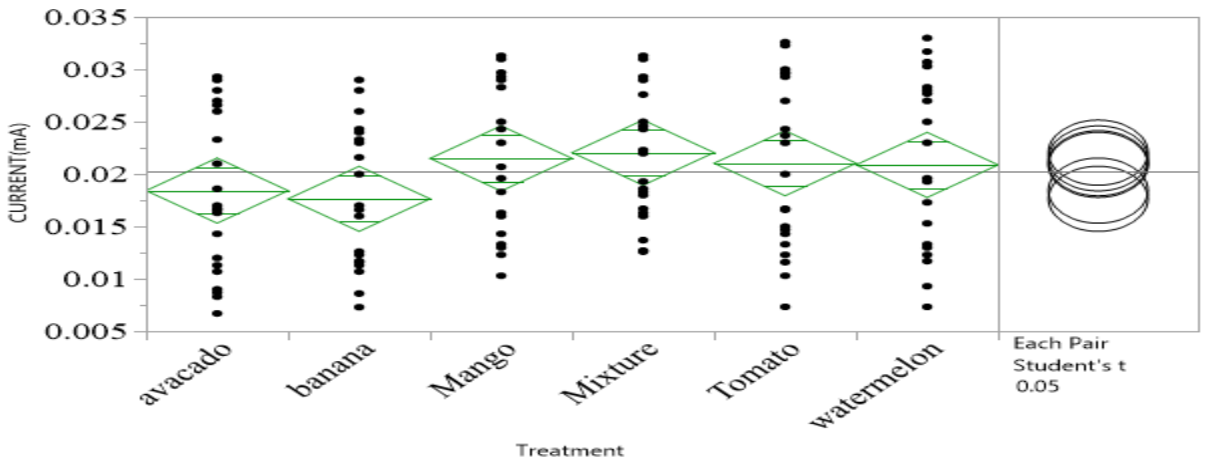

Figure 4.37: ANOVA results for Treatment against Current output

ANOVA findings in Table 4.14 showed that the difference in fruit waste mixture and banana samples was significant, just like in voltage output, indicating that other factors such as temperature, pressure, etc., were affecting the reaction. The results clearly illustrated that segregation of fruit wastes before experiment would be beneficial.

Table 4.14: ANOVA test for market fruit wastes Current

Connecting Letters Report

Level			Mean (mA)
Mixture	A		0.0221 ± 0.006
Mango	A	B	0.0215 ± 0.007
Tomato	A	B	0.0210 ± 0.008
Watermelon	A	B	0.0209 ± 0.008
Avocado	A	B	0.0184 ± 0.008
Banana		B	0.0176 ± 0.007

Levels not linked by the same letters are significantly different

4.7.3 Treatment against Power output

A visualized dot-plot and confidence intervals for each treatment against power output for market fruit waste are shown in Figure 4.38.

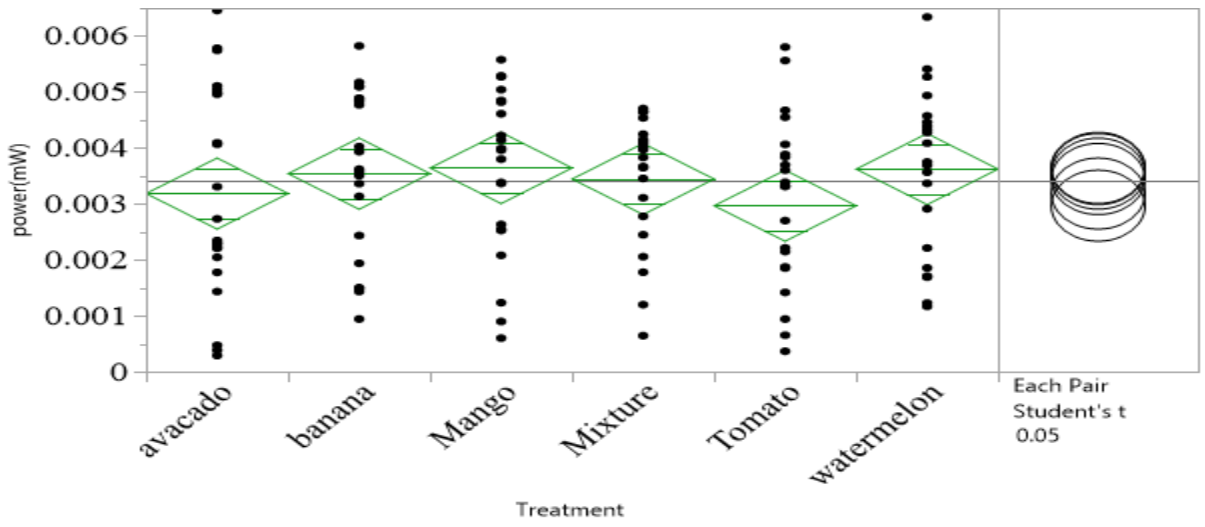

Figure 4.38: ANOVA results for Treatment versus Power output

ANOVA findings in Table 4.15 show no significant difference in all the fruit wastes in power output, suggesting a possibility of bioelectricity generation from fruit waste.

Table 4.15: ANOVA test for market fruit wastes Power

Connecting Letters Report

Level		Mean (mA)
Mango	A	0.0036 ± 0.001
Watermelon	A	0.0036 ± 0.001
Banana	A	0.0035 ± 0.001
Mixture	A	0.0034 ± 0.001
Avocado	A	0.0032 ± 0.002
Tomato	A	0.0029 ± 0.002

Levels not connected by the same letter are significantly different.

Figure 4.39 below shows the Correlation and Scatterplot matrix for Banana fruit waste for voltage, current, power, power density, and current densities output. Values are coloured according to the magnitude of their correlation. For the correlation matrix, diagonal values show the correlation of each variable with itself, while the off-diagonal values are correlated at the intersection of variables. The positive correlation values are bold black colour and negative values are red, indicating that an increase in one variable is associated with a decrease in the other variable. The brown colour shows how close the values are to zero, a correlation with no linear association between the variables within the samples.

Correlation Probability

	DAYS	VOLTAGE(mV)	CURRENT(mA)	Current density(mA/m2)	power(mW)	power density (mW/m2)
DAYS	<.0001	<.0001	0.0499	0.0499	0.1037	0.1037
VOLTAGE(mV)	<.0001	<.0001	0.0357	0.0357	0.0256	0.0256
CURRENT(mA)	0.0499	0.0357	<.0001	<.0001	0.0102	0.0102
Current density(mA/m2)	0.0499	0.0357	<.0001	<.0001	0.0102	0.0102
power(mW)	0.1037	0.0256	0.0102	0.0102	<.0001	<.0001
power density (mW/m2)	0.1037	0.0256	0.0102	0.0102	<.0001	<.0001

Scatterplot Matrix

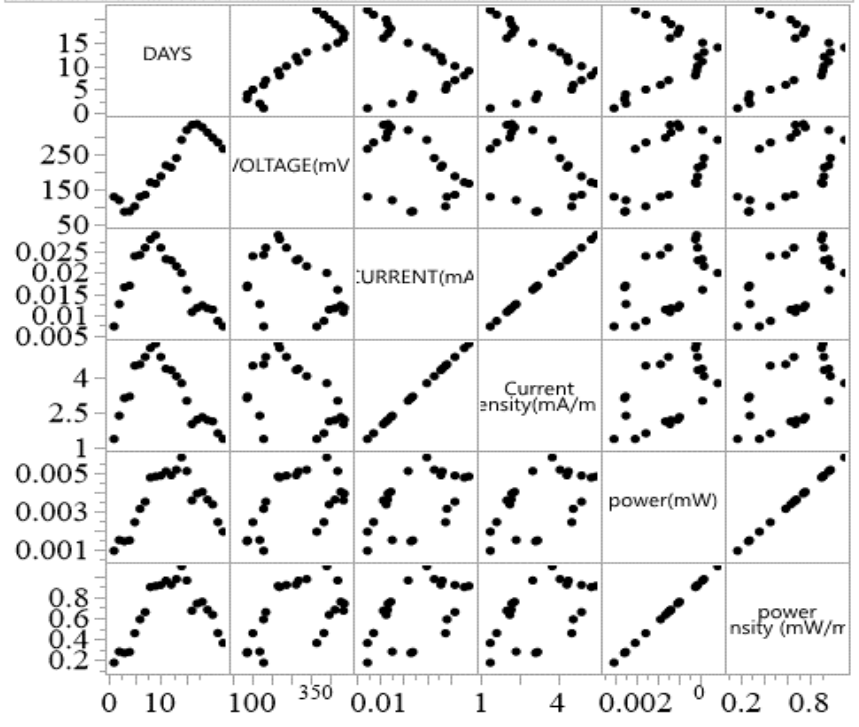

Figure 4.39: Correlation and Scatterplot matrix for Banana fruit waste output

Pearson correlation coefficients (r) were generally poor despite statistical significance, indicating low predictive power of one variable against another but a high probability of linear relationships.

All of the output in this study has a p-value higher than 0.05, which is statistically insignificant when compared to pure error, demonstrating that fitting model accurately matches experimental data (Zhao *et al.*, 2014). These calculations are outlined in (*Appendix* 11a-11f*: Correlation and Scatterplot matrix*).

4.8 Voltage and Current Data Automation

In this study, alternative methods of data recording to save time and reduce voltage and current errors observed in a cheap potential-measuring device (Arduino UNO) were used. These are deemed to be less expensive than the use of the multi-meter for recording the potential and current delivered by a bio-cathode Microbial Fuel Cell.

4.8.1 Microbial Fuel Cell Data Logging using Arduino-Based Sensors

Figure 4.40 below is a trend demonstrating the voltage and current data plot for tomato waste using both the digital multi-meter (DT9201A) and Arduino-based sensor device for comparison purposes. It is observed that the daily voltage recorded in volt (V) ranged between 0.05 – 0.34V, as current output in milliamperes (mA) ranged from 0.002 – 0.05 mA.

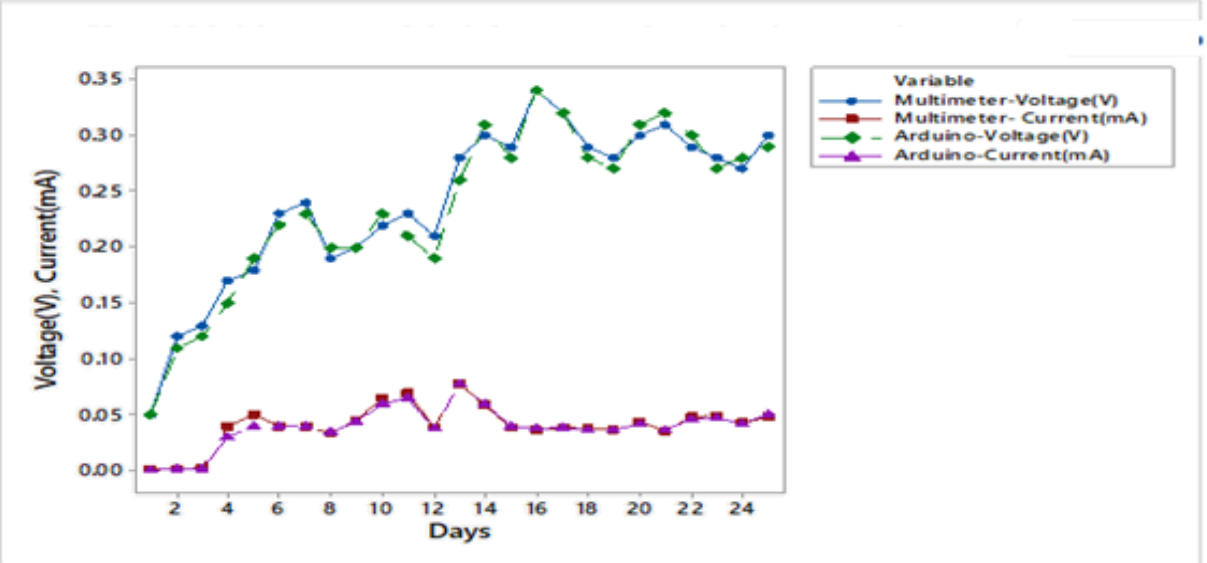

Figure 4.40: Plot of a digital multi-meter and Arduino sensor data for tomato waste

It is observed that the reading of the device (Arduino-UNO) closely followed the multi-meter line, a clear indication that the sensor could be used in place of the multi-meter for data collection. In tomato wastes, a mean voltage of (0.241 ± 0.070 V) and (0.237 ± 0.072 V) were recorded using multi-meter and Arduino-based sensors, respectively at current standards of 0.041± 0.018 mA and 0.040 ± 0.017 mA. Logan (2007), in his study, observed that the Arduino sensor data had an average error reading of 0.75 ± 0.66 mV compared to digital multimeter recordings.

The potential (voltage) and current from Cow-dung waste were monitored using both digital multi-meter and Arduino-based sensors and plotted against time (Figure 4.41). The two techniques of recording data did not significantly differ from one another. The averages were between the range of 0.08 – 0.35 V for voltage (potential) and between the range of (0.001 to 0.041 mA) for current.

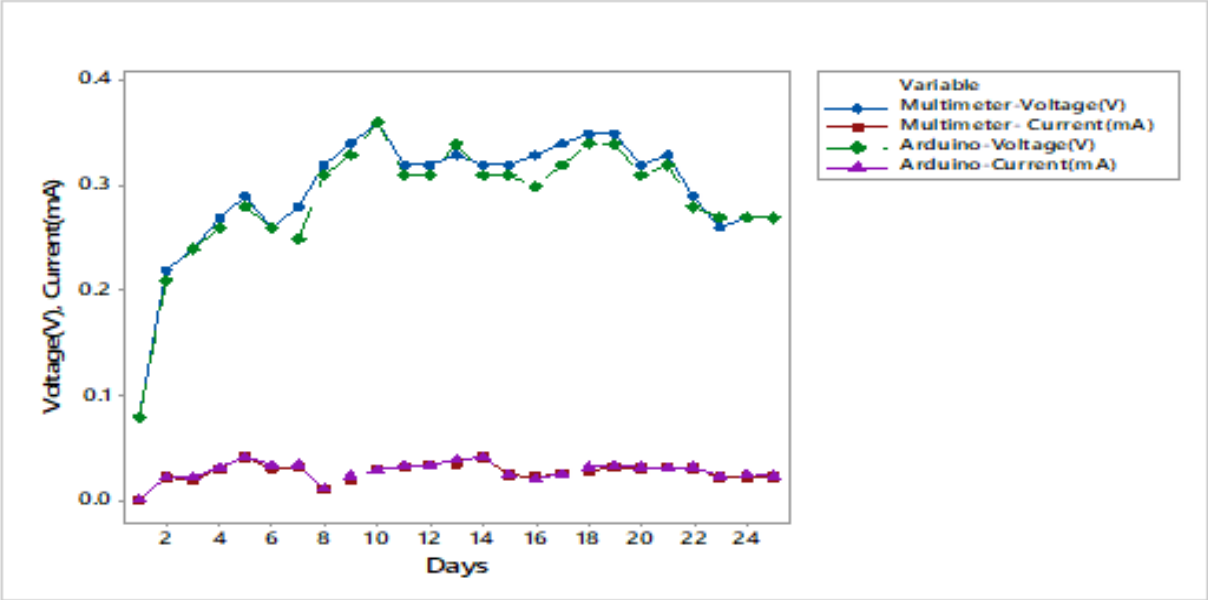

Figure 4.41: Plot of a digital multi-meter and Arduino UNO sensor data for Cow-dung waste

The results obtained in Figure 4.40 showed that the mean voltage and current recorded for cow dung using the two methods were 0.295 ± 0.057 V and 0.027 ± 0.008 mA when using digital multi-meter while 0.287 ± 0.055 V and 0.028 ± 0.008 mA values when using Arduino based sensors respectively. Chalh *et al*. (2020); Haizad *et al.* (2016) indicated that Arduino is an integrated embedded board and a low-cost board which uses a DC power supply or a Universal Serial Bus

(USB) connection with a computer, giving a low percentage of output errors compared to digital multi-meter.

In Figure 4.42, the voltage and current on avocado were monitored using both instruments (digital multi-meter and Arduino-based sensor) and plotted against time. The average avocado recorded data using a digital multi-meter for voltage was 0.215 ± 0.133 V and 0.049 ± 0.033 mA for current readings, while when using Arduino-based sensor the average avocado recorded data for voltage was 0.212 ± 0.135 V and 0.049 ± 0.033 mA for current, respectively.

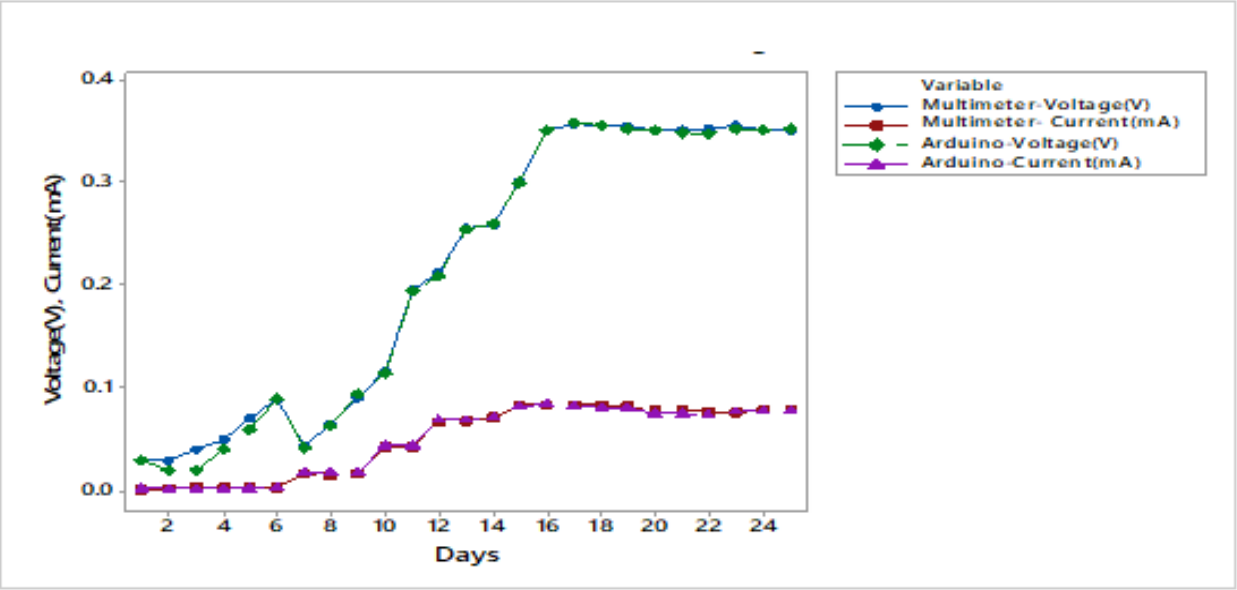

Figure 4.42: Plot of a digital multi-meter and Arduino-based sensor data for Avocado waste

The daily plot of voltage and current for 24 days is presented in Figure 4.42. It is observed that the reading of the Arduino UNO closely followed the digital multi-meter line, a clear finding that the sensor can be used in the place of the digital multi-meter for data collection. Walter *et al.* (2020), observed that, in a potential between 300 mV to 500 mV, maximum power transfer point occurs on a single microbial fuel cell level, depending on design and material used. Furthermore, Ge *et al.* (2014) discovered that, smaller MFCs have higher power density than bigger ones due to diffusion restrictions and increased internal resistance. These two intrinsic characteristics of the technology have pushed microbial fuel cell systems into real-world power applications requiring large power densities.

4.9 Biotransformation of Biodegraded Organic Waste into Organic Fertilizer

The bio-amendment agent (bio-fertilizer) on homemade vermicompost chamber production was set up on biodegraded market fruit waste.

The initial and final Fourier-transform infrared spectroscopy spectra of utilized substrates are shown below in Figure 4.43, where it is observed that, most intense peak at 3400 cm^{-1} belong to O-H stretching bond, while peak at 1000 cm^{-1}, 1625 cm^{-1}, 2750 cm^{-1}, 2875 cm^{-1}, 3375 cm^{-1}, 1625 cm^{-1}belongs to alkane (C-H) bending, alkene (C=C) stretching, carbonyl (C=O) stretching, (H-C=O) stretching bonds

FT-IR spectrum

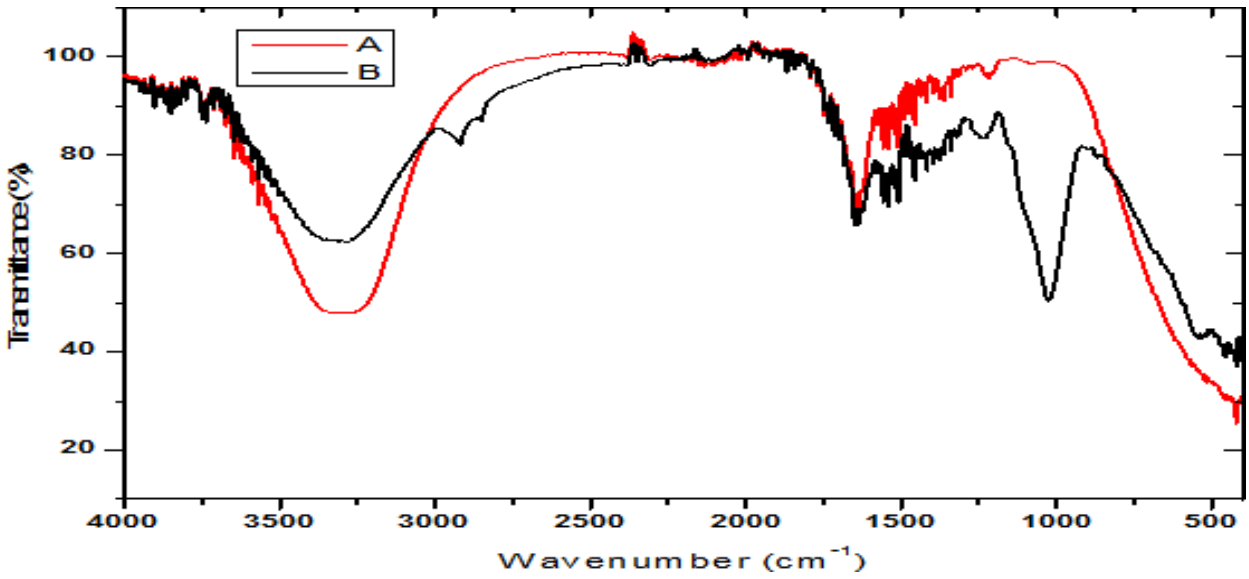

Figure 4.43: FT-IR spectrums of composite and vermicomposite

Above spectra demonstrates functional groupings in two spectrums using an FT-IR-ATR technique. The peak at spectra-A is related to Acetic acid of molecular weight 60.05 g/mol, indicates a rise in the amount of the active group coupled with molecular bond (per unit volume). Spectra-B was connected to butyric acid, which has a molecular weight of 88.11 g/mol. In a similar study by Jin *et al.* (2018) bands that appeared at peaks 3407.6 cm^{-1}, 3435.5 cm^{-1} and 1545.0 cm^{-1} were attributed (N-H) stretching and (C=O) stretching bond vibrations, respectively.

As can be clearly seen on the FT-IR spectrum, that intensity of transmittance peaks decreased compared to initial spectrum, which according to Nora *et al.* (2022) attributed this to degradation of microorganisms in the process of bioelectricity generation and vermicomposting procedure on the biosludge from the microbial fuel cell (Azlim *et al.,* 2022). The Composite (Biosludge) and Vermicast (organic fertilizer) were examined for chemical composition, macro and micro nutrients and the results are tabulated in the Table 4.16 and 4.17 below.

Table 4.16: Properties of the Composite product

Chemical characteristics of the Composite	
EC	0.814 dS/m
pH	8.83 ± 0.05
C/N Ratio	7.1 ± 0.2
(g/kg) OM	179.2 ± 1.0
Macronutrients of the Composite (g/kg)	
Mg	1.3 ± 0.02
P	8.9 ± 0.1
N	32.4 ± 1.4
K	0.003 ± 0.00004
Ca	1.8 ± 0.22
Micronutrients of the Composite (g/kg)	
Mn	ND
Cu	0.17 ± 0.01
Fe	4.85 ± 0.08
Zn	ND

Table 4.17: Properties of the Vermicast product

Chemical properties of the Vermicast	
PH	9.84 ± 0.05
EC	0.552 dS/m
(g/kg) OM	335.2 ± 1.8
C/N Ratio	6.43 ± 0.2
Macronutrients of the Vermicast (g/kg)	
Mg	7.1 ± 0.11
N	87.0 ± 3.8
P	7.6 ± 0.07
K	18.0 ± 0.23
Ca	97.4 ± 11.9
Micronutrients of the Vermicast (g/kg)	
Mn	16.74 ± 0.022
Fe	6.61 ± 0.11
Cu	0.62 ± 0.03
Zn	0.013 ± 0.0001

According to vermicast evaluation result, (Table 4.17), chemical properties tabulated are satisfactory for crops' growth, soil fertility suitable for farming and organic matter is sufficient, having a total organic carbon (TOC) of 384.1 g/Kg up from 20.825 g/Kg initially in a biodegraded organic waste (Imwene *et al.,* 2021). This is because vermicomposting has the higher decomposition rate and nutrient content of the final product (Khatua *et al.,* 2018). In addition, vermicomposting produces a higher concentration of hormones and enzymes that could stimulate plant growth, enhance soil fertility, reduce pH, provides micro and macronutrients, and increase their availability as well as help soil to absorb and retain water (Joshi *et al.,* 2015). The organic matter in fruit waste sample is converted to a dark sludge via an anaerobic digestion process in 30 days, before being bio-amended into a better-quality organic fertilizer by bulking agents (epigeic varieties of earthworms) (Imwene *et al.,* 2021). As a result, enhanced vermicompost may be concluded to promote better plant growth while also improving soil health and fertility. It is

suggested that enhanced vermicompost be researched for its application in agriculture for improvement of crop yield.

CHAPTER FIVE

CONCLUSIONS AND RECOMMENDATIONS

5.1 Conclusions

In this project, the viability of creation of electricity from fruit waste from Kenyan markets using microbial fuel cells was examined. The results indicate that the variability of power production from various fruitwastes using goat rumen fluid was influenced by moisture and the carbohydrate content of the fruitwastes. Waste samples contained high levels output of proximate properties such as moisture content, carbohydrates levels, nitrogen free extract, fat content and crude proteins. The moisture content ranged from $74.3 \pm 2.1\ \% - 95.16 \pm 4.0\ \%$. The carbohydrate compositions in the range of $2.93 \pm 0.09\ \% - 19.24 \pm 1.0\ \%$ influenced the performance of MFC by enhancing the electron transit to the MFC cathode and facilitated mobility of more electrons in the solutions. The average current and voltage generated in a MFC were in the range of 0.018 – 0.022 mA and 145.76 - 215.98 mV respectively.

The highest average output values were in banana fruit waste giving a value of 336mV for voltage and 0.029 mA for current readings respectively, while the lowest was in the fruit waste mixture that produced 216 mV and 0.031 mA for the voltage and current respectively. The optimal temperature was found to be 37 ℃, with the highest voltage reading of 394 mV given by banana waste and lowest in the fruit waste mixture at 250 mV. Optimal pH was at pH 7, with banana waste giving the highest voltage value of 312 mV and the lowest voltage being observed with tomato waste at 211 mV. Kinetic parameters obtained by modelling showed that specific growth rates depended on the types of fruit wastes when their substrate concentrations were kept constant (S = 100 gL^{-1}). The specific growth rate (μ) of the fruit wastes ranged between 0.53 h^{-1} - 0.82 h^{-1}, with a half-saturation coefficient (K_S) in the range of $99.57 \pm 30\ gL^{-1}$ – $99.66 \pm 30\ gL^{-1}$ and the highest was in tomato waste and lowest in watermelon waste when the microbe's substrate digestion was run for 408 hours. The effect of substrate self-inhibition (K_{IH}) ranged between ($50.09 \pm 40\ gL^{-1}$ – $50.18 \pm 40\ gL^{-1}$ indicating that the chemical reaction occurred inside the microbial fuel cells. The Critical inhibitor concentration (S_m) ranged between ($91.09 \pm 3.36\ gL^{-1}$ – $100.75 \pm 3.71\ gL^{-1}$) and reached a point where chemical reaction

completely stopped, as is indicated by the Han-Lavenspiel model, which could be as a result of volatile fatty acids buildup, which makes the anaerobic process unstable. As a result, pH drops ($pH < 6.3$), which can prevent bacteria from growing because they are more susceptible to low pH levels. In all samples, no statistically significant differences were reported in power generation ($P < 0.05$), an indication that fruit waste samples are a better source of electricity generation. In automation of voltage data, readings were observed using the Arduino board and verified using a multi-meter but gave no substantial difference to digital multi-meter. Using Arduino, the highest reading in tomato was 0.237 ± 0.072 V, while in a digital multimeter, the reading was 0.241 ± 0.070 V.

Composting and vermicomposting are regarded as ideal techniques for dealing with organic waste because they not only assist in resolving issue of degradable waste disposal but also yield beneficial bio-fertilizer. However, vermicomposting outperforms composting due to its increased organic matter breakdown capacity and nutrient content. In addition, vermicomposting generates additional hormones and enzymes, which may promote plant growth and prevent illness. However, past research work suggests that a successful combination of this two techniques could be a practical choice for creating a better biofertilizer. The study, therefore, revealed that fruitwastes could be used as substrates to produce electricity. They could form sustainable energy source, which would also address the problems of fruitwaste disposal. Hence the data generated from this study are significant in promoting the use of organic wastes and determining the best time frame for microbial degradation of substrates to produce electricity.

5.2 Recommendation

The recommendations from this study were:

- Research into how electron-donating microorganisms could be enhanced to offer more efficient electron transfer to electrode.
- In order to protect microorganisms and improve effectiveness of microbial fuel cells, we also recommend employing metal electrodes (owing to their great electron-conducting qualities) that have been coated with a non-toxic chemical component. By doing these new

studies, it will become clear whether coated or uncoated metallic electrodes perform better; this can be gauged by the electrical values discovered in subsequent studies.

- In order to maximize bioenergy output and achieve the best anaerobic chamber performance, volatile fatty acid production in MFC is a crucial parameter to monitor.
- The bio-sludge should be bio-amended to be applied in crop production as it is nutritious for crop growth and development.
- The market organic waste should be converted to renewable energy and bio-fertilizer using slaughterhouse waste as a green technology for environmental conservation.

REFERENCES

Abdel-Shafy, H. I., and Mansour, M. S. (2018). Solid waste issue: Sources, composition, disposal, recycling, and valorization. *Egyptian Journal of petroleum*, **27**(4), 1275-1290.

Adzawla, W; Tahidu, A; Mustapha, S; Azumah, SB. (2019). Do socioeconomic factors influence households' solid waste disposal systems? Evidence from Ghana. *Waste. Mngt. Res.* **37**(1): 51 – 57.

Adegunloye, D. V. and Olotu, T. M. (2018). Comparative Measure of Electricity Produced from Benthic Mud of FUTA North Gate and FUTA Junction in Akure, Ondo State, Using Microbial Fuel Cell. *Innov Ener Res*. **7**: 180

Adebule, A.P., Aderiye, B.I. and Adebayo, A.A. (2018) Improving Bioelectricity Generation of Microbial Fuel Cell (MFC) With Mediators Using Kitchen Waste as Substrate. *Annals Of Applied Microbiology and Biotechnology*, **2**(1), 1-5.

Aelterman P, Freguia S, Keller J, VerstraeteW, Rabaey K. (2008). The anode potential regulates Bacterial activity in microbial fuel cells. *Appl Microbiol Biotechnol*. **78**(3), 409–418.

Ahmed, N. A., Miyatake, M., and Al-Othman, A. K. (2008). Power fluctuations suppression of stand-alone hybrid generation combining solar photovoltaic/wind turbine and fuel cell systems. *Energy Conversion and Management*, **49**(10), 2711-2719.

Agbossou, K., Kolhe, M., Hamelin, J. and Bose, T. K. (2004). Performance of a stand-alone renewable energy system based on energy storage as hydrogen. *IEEE Transactions on Energy Conversion*, **19**(3), 633-640.

Akinmusire, O. O. (2011). Fungal species associated with the spoilage of some edible fruits in Maiduguri Northern Eastern Nigeria. *Advances in Environmental Biology*, **5**(1), 157-161.

Akuyea, N. N. A. (2013). Assessing the effects of uncollected waste generated by households in Tema Newtown, Accra. Unpublished masters dissertation, *Institute of Statistical, Social and Economic Research, University of Ghana, Legon, Ghana*.

Akshay D. Tharali, Namrata Sain, and W. Jabez Osborne. (2016). Microbial fuel cells in Bioelectricity production. *Frontiers in life science.* **9** (4), 252-266.

Allison, K., and Von Blottnitz, H. (2010). Solid waste management in Nairobi, a situational Analysis, technical document accompanying the integrated solid waste management plan. UNEP, Nairobi.

Amani, T., Nosrati, M., Sreekrishnan, T.R., 2010. Anaerobic digestion from the viewpoint of microbiological, chemical, and operational aspects — a review. *Environmental Reviews* **18**, 255-278.

Ambar P, Endang S, Rochijan, Nanung A F, Yudistira S and Mochammad F. H (2017), Potential test on utilization of cows rumen fluid to increase biogas production rate and methane concentration in biogas. *Asian J. Anim. Sci.,* **11**: 82-87.

Amo-Asamoah, E., Owusu-Manu, D. G., Asumadu, G., Ghansah, F. A., & Edwards, D. J. (2020). Potential for waste to energy generation of municipal solid waste (MSW) in the Kumasi metropolis of Ghana. *International Journal of Energy Sector Management*, **14**(6), 1315-1331.

Andole, O. H. (2016). The state of solid waste management in Kenya. Jomo Kenyatta University of Agriculture and Technology Kenya.

Arias, A., Feijoo, G., & Moreira, M. T. (2023). Process modelling and environmental assessment on the valorization of lignocellulosic waste to antimicrobials. *Food and Bioproducts Processing*, **137**, 113-123.

Aurah, C. M. (2013). Assessment of extent to which plastic bag waste management methods used in Nairobi City promote sustainability. *American Journal of Environmental Protection*, **1**(4), 96-101.

AOAC (1990) Official Methods of Analysis: Association of Analytical Chemists. 14th Edition, AOAC, 20-34.

Ayad, M. Y., Pierfederici, S., Raël, S., and Davat, B. (2007). Voltage regulated hybrid DC power Source using supercapacitors as an energy storage device. *Energy Conversion and Management*, **48**(7), 2196-2202.

Azlim, N.A.; Mohammadi Nafchi, A.; Oladzadabbasabadi, N.; Ariffin, F.; Ghalambor, P.; Jafarzadeh, S.; Al-Hassan, A.A. (2022). Fabrication and Characterization of a PH-Sensitive Intelligent Film Incorporating Dragon Fruit Skin Extract. *Food Sci. Nutr.*, 10, 597–608.

Azuoma YA, Jegla Z, Reppich M, Turek V, Weib M (2018) Using Agricultural Waste for Biogas Production as a Sustainable Energy Supply for Developing Countries. *Chem Engr Transact* **70**: 445-450.

Babalola, A., Ishaku, H. T., Busu, I., & Majid, M. R. (2010). The practice and challenges of solid waste management in Damaturu, Yobe State, Nigeria. *Journal of Environmental Protection*, **1**(4), 384.

Babu, B. R., Kumar, P. P., and Kuppusamy, P. G. (2019). Arduino Mega-based PET feeding Automation. *IOSR Journal of Electronics and Communication Engineering*, **14**(4), 13-16.

Bagyaveereswaran, V., Ratnakaran, S., Trivedi, R., & Sangeetha, S. (2017, April). Design of low Cost portable DAQ unit for Microbial fuel cells. In *2017 Innovations in Power and Advanced Computing Technologies (i-PACT)* (1-5). IEEE.

Bahera, M., Murthy, S., Ghangrekar, M. (2011), Effect of operating temperature on Microbial Fuel Cell. *Water Science and Technology*, **64**(4), 917-22.

Bazrafshan, E., Kord Mostafapour, F., Farzadkia, M., Ownagh, K. A., and Mahvi, A. H. (2012). Slaughterhouse wastewater treatment by combined chemical coagulation and electrocoagulation process. *PloS one*, **7**(6), e40108.

Behera, M., Jana, P. S., More, T. T., & Ghangrekar, M. M. (2010). Rice mill wastewater treatment in microbial fuel cells fabricated using proton exchange membrane and earthen pot at different pH. *Bioelectrochemistry*, **79**(2), 228-233.

Bowan, P. A., Anzagira, L. F. A. C. A., & Anzagira, C. A. (2014). Solid waste disposal in Ghana: A study of the wa municipality. *Journal of Environment and Earth Science*, **4**(4), 10-16.

Bhale, U. N. (2011). Survey of market storage diseases of some important fruits of Osmannabad District (MS) India. *Science Research Reporter*, **1**(2), 88-91.

Boe, K., Batstone, D.J., Steyer, J.P., Angelidaki, I., 2010. State indicators for monitoring the anaerobicdigestion process. *Water Res.* **44**(20), 5973-5980.

Budzianowski, W. M., Nantongo, I., Bamutura, C., Rwema, M., Lyambai, M., Abimana, C. & Sow, S. (2018). Business models and innovativeness of potential renewable energy projects in Africa. *Renewable Energy*, 123, 162-190.

Braga, M. E., Leal, P. F., Carvalho, J. E., and Meireles, M. A. A. (2003). Comparison of yield, composition, and antioxidant activity of turmeric (Curcuma longa L) extracts obtained using various techniques. *Journal of agricultural and food chemistry*,**51**(22), 6604-6611.

Bruce E. Logan, Bert Hamelers, René Rozendal, Uwe Schröder, Jürg Keller, Stefano Freguia, Peter Aelterman, Willy Verstraete, and Korneel Rabaey. (2006). "Microbial fuel cells: Methodology and Technology," *Environmental Science and Technology*, **40**(17), 5181-5192.

Cao, B., Zhao, Z., Peng, L., Shiu, H. Y., Ding, M., Song, F., ... & Huang, Y. (2021). Silver nanoparticles boost charge-extraction efficiency in Shewanella microbial fuel cells. *Science*, **373**(6561), 1336-1340.

Capodaglio, A. G., Cecconet, D., Molognoni, D. (2017). An integrated mathematical model of microbial fuel cell processes: bioelectrochemical and microbiologic aspects. *Processes*, **5**(4), 73.

Cappucino JG, Sherman N. Microbiology a Laboratory Mannual. 2th Ed. California: The Benjamins Columningn Publishers Company. 1987.

Carneiro J.S, Nogueira R.M, Martins M.A, Valladãod. M, Pires E.M. (2018). The Oven- Drying Method for Determination of Water Content in Brazil Nut, *Bioscience Journal*. **34**(3), 595-602.

Castillo-Gonzáleza, A. R., Burrola-Barrazab, M.E., Domínguez-Viverosb, J. and Chávez-Martínezb, A. (2014). Rumen microorganisms and fermentation. *Arch Med Vet.* **46**:349-361.

Cercado-Quezada, B., Delia, M. L., & Bergel, A. (2010). Testing various food-industry wastes. for electricity production in microbial fuel cell. *Bioresource Technology,* **101**(8), 2748-2754.

Chae, K. J., Choi, M. J., Lee, J. W., Kim, K. Y., & Kim, I. S. (2009). Effect of different substrates on the performance, bacterial diversity, and bacterial viability in microbial fuel cells. *Bioresource technology,* **100**(14), 3518-3525.

Chai, A., Wong, Y. S., Ong, S. A., Lutpi, N. A., Sam, S. T., Kee, W. C., & Ng, H. H. (2021). Haldane-Andrews substrate inhibition kinetics for pilot-scale thermophilic anaerobic degradation of sugarcane vinasse. *Bioresource Technology*, 125319.

Chalh, A., El Hammoumi, A., Motahhir, S., El Ghzizal, A., Subramaniam, U., & Derouich, A. (2020). Trusted simulation using Proteus model for a PV system: test case of an improved HC MPPT algorithm. *Energies,* **13**(8), 1943.

Chang, S.K.C., Zhang, Y. (2017). Protein analysis. Ch. 18, in Food Analysis, 5th ed. S.S. Nielsen (Ed.), *Springer, New York,* 255-386.

Charbel, A. T., Trinchero, B. D., Morais, D. D., Mesquita, H., & Birchal, V. S. (2015). Evaluation of the potential of fruit peel biomass after conventional and microwave drying for use as solid fuel. *In Applied Mechanics and Materials,* **798**, 480-485.

Chaturvedi, V., & Verma, P. (2016). Microbial fuel cell: a green approach for the utilization of waste for the generation of bioelectricity. *Bioresources and Bioprocessing,* **3**, 1-14.

Cheng .S and Bruce E. Longan. (2007). Ammonia treatment of carbon cloth anode to enhance power generation of microbial fuel cells. *Electrochemistry Communications,* **9**(3), 492-496.

Cheng S, H. Liu., and B. E. Logan. (2006). Increased power generation in a continuous flow MFC with adventive flow through the porous anode and reduced electrode spacing. *Environmental science and Technology*. **40**(7), 2426-2432.

Cheng, H.and Hu, Y. (2010). Municipal solid waste (MSW) as a renewable source of energy: Current and future practices in China. *Bioresource Technology*, **101**(11), 3816-3824.

Chibueze, O. U.and Chima, M. I. A. (2018). Application of Different Organic Wastes for Electricity Generation using Double Chambered Microbial Fuel Cell Technology. *Frontiers in Environmental Microbiology,* **4**(4), 94.

Christgen, B., Scott, K., Dolfing, J., Head, I. M., & Curtis, T. P. (2015). An evaluation of the performance and economics of membranes and separators in single chamber microbial

fuel cells treating domestic wastewater. *PLoS One*, **10**(8).

Clauwert, P., Aelterman, P., Pharm, H. T., DeSchamphelaire, L., Carballa, M., Rabaey, K. and Verstraete, W. (2008). Minimizing losses in bio-electrochemical systems: the road to application. *Appl Microb Biotechnol.* **79**: 901.

Cowan I, Steel ST. Cowan and Steel's Manual for the identification of medical bacteria.3rd edn. *Cambridge University Press, London.* 1974.

Chezeau, B., & Vial, C. (2019). Modeling and Simulation of the Biohydrogen Production Processes. *Biohydrogen*, 445–483.

Clauser, N. M., González, G., Mendieta, C. M., Kruyeniski, J., Area, M. C., & Vallejos, M. E. (2021). Biomass waste as sustainable raw material for energy and fuels. Sustainability, **13**(2), 794.

Esser, D. S., Leveau, J. H., & Meyer, K. M. (2015). Modeling microbial growth and dynamics. *Applied microbiology and biotechnology*, **99**(21), 8831-8846.

Devindra, S., Chouhan, S., Katare, C., Talari, A., & Prasad, G. B. K. S. (2017). Estimation of glycemic carbohydrate and glycemic index/load of commonly consumed cereals, legumes and mixture of cereals and legumes. *International Journal of Diabetes in Developing Countries*, **37,** 426-431.

Dewan A., Donoran C, Heo D, Beyenal H. (2010). Evaluating the performance of microbial fuel cells powering electronic devi*ces. J. Power Sources.* **195**(1), 90-96.

Deziel, C 2018, Why do citrus food produce electricity? viewed 10 October 2018, https://sciencing.com/docitrus-fruits-produce-electricity-5167602.html

Dhont, J., & Berghe, E. V. (2003). Analytical Techniques in Aquaculture Research Laboratory of Aquaculture & Artemia Reference Center, Ghent University, Belgium. *Accessed on January*, 12, 2014.

Di Bucchianico, A. (2008). Coefficient of determination (R^2). *Encyclopedia of Statistics in Quality and Reliability*, **1.**

Di Marzo, L., Pranata, J., & Barbano, D. M. (2021). Measurement of casein in milk by Kjeldahl and sodium dodecyl sulfate–polyacrylamide gel electrophoresis. *Journal of Dairy Science*, **104**(7), 7448-7456.

Diskin, S., O. Feygenberg, D. Maurer, S. Droby, D. Prusky, and N. Alkan. 2017. Microbiome alterations are correlated with the occurrence of post-harvest stem-end rot in mango fruit. *Phytobiomes Journal* **1**(3):117–27.

Du Z, Li H, Gu T. (2007). A state of the art review on microbial fuel cells: a promising technology for wastewater treatment and bioenergy. *Biotechnol Adv*. **25**:464–482.

Dykstra, C. M., & Pavlostathis, S. G. (2017). Zero-valent iron enhances biocathodic carbon dioxide reduction to methane. *Environmental Science & Technology*, **51**(21), 12956-12964.

El Hammoumi, A., Motahhir, S., Chalh, A., El Ghzizal, A. and Derouich, A. (2018). Low-cost virtual instrumentation of PV panel characteristics using Excel and Arduino in comparison with traditional instrumentation. *Renewables: Wind, Water, and Solar*, **5**(1), 1-16.

Ezekoye V.A and Ezekoye B.A. (2009). Characterization and storage of biogas produced from the Anaerobic digestion of cow dung spent grains/cow dung and cassava peels/rice husk, *the Pacific Journal of Science and Technology*, **10**(2): 898-904.

Falk, H., Reichling, P., Andersen, C., Benz, R., 2015. Online monitoring of concentration and dynamics of volatile fatty acids in anaerobic digestion processes with mid-infrared spectroscopy. *Bioprocess Biosyst Eng*. **38**(2), 237-249.

Ferreira, P. J., Shao-Horn, Y., Morgan, D., Makharia, R., Kocha, S., and Gasteiger, H. A. (2005). Instability of Pt⁄C electrocatalysts in proton exchange membrane fuel cells: a mechanistic investigation. *Journal of the Electrochemical Society*, **152**(11), A2256.

Forner-Cuenca, A., Penn, E. E., Oliveira, A. M., & Brushett, F. R. (2019). Exploring the role of electrode microstructure on the performance of non-aqueous redox flow batteries. *Journal of The Electrochemical Society*, **166**(10), A2230.

Franke-Whittle, I.H., Walter, A., Ebner, C., Insam, H., 2014. Investigation into the effect of high concentrations of volatile fatty acids in anaerobic digestion on methanogenic communities. *Waste Manag* **34**(11), 2080-2089.

Gadkari, S., Shemfe, M., & Sadhukhan, J. (2019). Microbial fuel cells: a fast converging dynamic model for assessing system performance based on bioanode kinetics. *International Journal of Hydrogen Energy*, **44**(29), 15377-15386.

Gakungu, N. K. Solid waste management; (2011). A case of technical in Kenya; Unpublished MSc. Thesis, University of Nairobi, Kenya.

Gakungu N. K., A. N. Gitau., B. N. K. Njoroge., M. W. Kimani. (2012). Solid waste management in Kenya: A Case study of Public Technical Training Institutions. *ICASTOR Journal of Engineering*, **5**(3),127 – 138.

Galsurker, O., Diskin, S., Maurer, D., Feygenberg, O. and Alkan, N. (2018). Fruit stem-end rot. *Horticulturae,* **4**(4), 50.

Ge Z., LiVJ., XiaoVL., TongVY.R., He Z. (2014). Recovery of electrical energy in microbial fuel ells, *Environ. Sci. Technol. Lett.*, **1**(2):137–141.

Gil GC, Chang IS, Kim BH, Kim M, Jang JK, Park HS, Kim HJ (2003). Operational parameters affecting the performance of a mediator-less microbial fuel cell. *Biosens Bioelectron*, **18**(4), 327–334.

Gitau, GC. (2018). Causes and Effects of Poor Solid Waste Management in the Semi-urban Town of Ongata Rongai in Kenya. *Int. J. Environ. Health Sci*. **1**(1).

González del Campo, A., Cañizares, P., Lobato, J., Rodrigo, M., & Fernandez Morales, F. J. (2016). Effects of external resistance on microbial fuel cell's performance. *Environment, Energy and Climate Change II: Energies from New Resources and the Climate Change*, 175-197.

Ghangrekar MM, Shinde VB (2007). Performance of membrane-less microbial fuel cell treating wastewater and effect of electrode distance and area on electricity production. *Bioresour Technol,* **98**(4), 2879-2885.

Grady Jr, C. P. L., Daigger, G. T. and Lim, H. C. (1999). Rotating biological contactor. *Biological wastewater treatment. Marcel Dekker, New York*, 907-947.

Gutberlet, J., Kain, J.-H., Nyakinya, B., Oloko, M., Zapata, P., & Campos, M. J. Z. (2017). Bridging weak links of solid waste management in informal settlements. Journal of *Environment & Development Policy Review*, 26(1), 106–131.

Haizad, M., Ibrahim, R., Adnan, A., Chung, T. D., & Hassan, S. M. (2016). Development of low-cost real-time data acquisition system for process automation and control. *In 2016 2nd IEEE International Symposium on Robotics and Manufacturing Automation (ROMA)* (1-5).

Halim, M., Rahman, M., Ibrahim, M., Kundu, R., & Biswas, B. K. (2021). Effect of anolyte pH on the performance of a dual-chambered microbial fuel cell operated with different biomass feed. *Journal of Chemistry*, 2021.

Han, S., Liu, Y., Zhang, S., & Luo, G. (2016). Reactor performances and microbial communities of biogas reactors: effects of inoculum sources. *Applied microbiology and biotechnology*, **100**(2), 987-995.

Hasan, N. A., and Zulkahar, I. M. (2018). Isolation and identification of bacteria from spoiled fruits. *In AIP Conference Proceedings*, **2020**(1).

Hill, A., Tait, S., Baillie, C., Virdis, B., McCabe, B. (2020). Microbial electrochemical sensors for volatile fatty acid measurement in high strength wastewaters: A review. *Biosensors and Bioelectronics*, **165**, 112409.

Hossain, M.E., JahangirAlam, M., Hakim, M.A., Amanullah, A.S.M., and Ahsanullah, A.S.M. (2010). An assessment of physicochemical properties of some tomato genotypes and varieties grown at Rangpur. *Bangladesh Research Publications Journal*, **4**(3): 235-243.

Hui Zhou, Aihong Meng, Yanqiu Long, Qinghai Li, and Yanguo Zhang (2014) Classification and comparison of municipal solid waste based on thermochemical characteristics, *Journal of the Air and Waste Management Association,* **64**(5), 597-616.

Imwene K.O., Mbui D.N., Kinyua A.P., Mbugua J.K., Ahenda S and Onyatta J.O. (2021). Biotransformation of Biodegraded Organic Waste from a Batch Mode Microbial Fuel Cell to Organic Fertilizer. *Journal of Bioremediation and Biodegradation an open access journal ISSN: 2155-6199.* **12**(S8).

Jadhav, D. A., Carmona-Martínez, A. A., Chendake, A. D., Pandit, S., & Pant, D. (2021). Modeling and optimization strategies towards performance enhancement of microbial fuel cells. *Bioresource Technology*, **320**, 124256.

Jadhav G.S, Jagtap Y.D, Ghangrekar M.M. (2013), Dual chambered membrane microbial Fuel cell: limitation on potential difference. *International Journal of Engineering Research and Technology,* **2** (4).

Jadhav G, Ghangrekar M (2009) Performance of microbial fuel cell subjected to variation in pH, temperature, external load, and substrate concentration. *Bioresour Technol*, **100**(2), 717-723.

Jaiswal, K. K., Kumar, V., Vlaskin, M. S., Sharma, N., Rautela, I., Nanda, M., & Chauhan, P. K. (2020). Microalgae fuel cell for wastewater treatment: Recent advances and challenges. *Journal of Water Process Engineering*, **38**, 101549.

Jang, J. K., Pham, T. H., Chang, I. S., Kang, K. H., Moon, H., Cho, K. S., and Kim, B. H. (2004). Construction and operation of a novel mediator-and membrane-less microbial fuel cell. *Process Biochemistry*, **39**(8), 1007-1012.

Javed, M. M., Nisar, M. A., Muneer, B., and Ahmad, M. U. (2017). Production of bioelectricity from the vegetable waste extract by designing a U-shaped microbial fuel cell. *Pakistan Journal of Zoology*, **49**(2).

Jiang, D., Curtis, M., Troop, E., Scheible, K., McGrath, J., Hu, B., and Li, B. (2011). A pilot-scale study on utilizing multi-anode/cathode microbial fuel cells (MAC MFCs) to enhance the power production in wastewater treatment. *International Journal of Hydrogen Energy*, **36**(1), 876-884.

Jiang, L. L., Zhou, J. J., Quan, C. S., & Xiu, Z. L. (2017). Advances in industrial microbiome based on microbial consortium for biorefinery. Bioresources and bioprocessing, **4**(1), 1-10.

Jiang, Y., Xie, S. H., Dennehy, C., Lawlor, P. G., Hu, Z. H., Wu, G. X., & Gardiner, G. E. (2020). Inactivation of pathogens in anaerobic digestion systems for converting biowastes to bioenergy: a review. *Renewable and Sustainable Energy Reviews*, 120.

Jin X, Liu Y, Tan J, Owen G, Chen Z (2018) Removal of Cr(vi) from aqueous solutions via

reduction and absorption by green synthesized iron nanoparticles. *J clean prod* 176: 929-936.

Joshi, R., Singh, J., & Vig, A. P. (2015). Vermicompost as an effective organic fertilizer and bio control agent: effect on growth, yield, and quality of plants. *Reviews in Environmental Science and Bio/Technology*, **14**(1), 137-159.

Jung, S., Mench, M. M., and Regan, J. M. (2011). Impedance characteristics and polarization behaviour of a microbial fuel cell in response to short-term changes in medium pH. *Environmental science & technology*, **45**(20), 9069-9074.

Kabeyi, M., & Olanrewaju, O. (2022). Slaughterhouse waste to energy in the energy transition with performance analysis and design of slaughterhouse biodigestor. Journal of Energy Management and Technology, **6**(3), 188-208.

Kaczmarek, M., Avery, S. V., & Singleton, I. (2019). Microbes associated with fresh produce: Sources, types and methods to reduce spoilage and contamination. *In Advances in applied microbiology*, **107**, 29-82.

Kamau, J. M., Mbui, D. N., Mwaniki, J. M., and Mwaura, F. B. (2017). Cow dung to kilowatt using double chamber microbial fuel cell. *International Journal of Scientific Research in Science, Engineering and Technology*, **3**(5), 70-79.

Kamau J.M, Mbui D.N, Mwaniki J.M, Mwaura F.B (2018) Utilization of rumen fluid in production of bio–energy from market waste using microbial fuel cells technology. *Journal of Applied Biotechnology & Bioengineering*, **5**(4).

Kamau JM, Mbui DN, Mwaniki JM, Mwaura FB (2018), Characterization of voltage from food market waste: microbial fuel cells. *Int J Biotech & Bioeng*. **4**:3.

Kamra N.D., (2005). Rumen microbial ecosystem, Current Science, 89(1), 124-135.

Kapoor, R., Ghosh, P., Kumar, M., Sengupta, S., Gupta, A., Kumar, S. S., & Pant, D. (2020). Valorization of agricultural waste for biogas based circular economy in India: A research outlook. *Bioresource Technology*, **304**, 123036.

Katuri, K. P., Scott, K., Head, I. M., Picioreanu, C., and Curtis, T. P. (2011). Microbial fuel cells meet with external resistance. *Bioresource Technology*, **102**(3), 2758-2766.

Kazimierczuk, A. H. (2019). Wind energy in Kenya: A status and policy framework review. *Renewable and Sustainable Energy Reviews*, **107,** 434-445.

Kaymaz, Ç. K., Birinci, S., & Kızılkan, Y. (2022). Sustainable development goals assessment of Erzurum province with SWOT-AHP analysis. *Environment, Development a Sustainability*, **24**(3), 2986-3012

Ketibuah, E., Asase, M., Yusif, S., Mensah, M. Y., & Fischer, K. (2004). Comparative analysis

of household waste in the cities of Stuttgart and Kumasi—Options for waste recycling and treatment in Kumasi. *In Proceedings of the 19th international CODATA Conference*, (1-8).

Kemausuor, F., Kamp, A., Thomsen, S. T., Bensah, E. C., and Østergård, H. (2014). Assessment of biomass residue availability and bioenergy yields in Ghana. *Resources, Conservation and Recycling*, **86**:28-37.

Khandelwal, A. (2021). Development of algae assisted Microbial Fuel Cell for power generation and algae cultivation (Doctoral dissertation, *Indian Institute of Technology Jodhpur).*

Khatua, C., Sengupta, S., Balla, V. K., Kundu, B., Chakraborti, A., & Tripathi, S. (2018). Dynamics of organic matter decomposition during vermicomposting of banana stem waste using Eisenia fetida. *Waste Management*, **79,** 287-295.

Kiprop, E., Matsui, K., & Maundu, N. (2017). Can Kenya supply energy with 100% renewable sources?. In *5th International Conference on Environment and Renewable Energy*. 18-19.

Kituku, W., Odote, C., Okidi, C., & Kameri-Mbote, P. (2020). Title Sectorial Coordination in Kenya's Municipal Solid Waste Management: A Horizontal Assessment. Law Env't & Dev. J., **16**, 55.

Kiyasudeen S.K, Ibrahim M. K and Ismail S.A. (2015), Characterization of Fresh Cattle Wastes Using Proximate, Microbial and Spectroscopic Principles, American-Eurasian J. Agric. & Environ. Sci., **15(**8): 1700-1709.

Kong, W., Guo, Q., Wang, X., and Yue, X. (2011). Electricity generation from wastewater using an anaerobic fluidized bed microbial fuel cell. *Industrial & engineering chemistry research*, **50**(21), 12225-12232.

Kraan, S. (2013). Mass-cultivation of carbohydrate rich macroalgae, a possible solution for sustainable biofuel production. *Mitigation and Adaptation Strategies for Global Change*, 18, 27-46.

Kretzschmar, J., Koch, C., Liebetrau, J., Mertig, M., Harnisch, F., 2017. Electroactive biofilms as sensor for volatile fatty acids: Cross sensitivity, response dynamics, latency and stability. Sensors and Actuators B: *Chemical* **241**, 466-472.

Kumar, S., Smith, S. R., Fowler, G., Velis, C., Kumar, S. J., Arya, S, and Cheeseman, C. (2017). Challenges and opportunities associated with waste management in India. *Royal Society open science*, **4**(3), 160764.

Kumar, S., Kumar, H. D. and Babu K. G. (2012). A study on the electricity generation from the cow dung using microbial fuel cell. *J Biochem Technol.* **3**(4): 442-447.

Kwan TH, Pleissner D, Lau KY, Venus J, Pommeret A, Lin CSK (2015) Techno-economic analysis of a food waste valorization process via microalgae cultivation and co-production of plasticizer, lactic acid and animal feed from algal biomass and food waste.

Bioresour Technol. **198**:292–299.

Lari, K. S., Davis, G. B., Rayner, J. L., Bastow, T. P., and Puzon, G. J. (2019). Natural source zone depletion of LNAPL: A critical review supporting modelling approaches. *Water research*, **157**:630-646.

Larrosa-Guerrero, A., Scott, K., Head, I. M., Mateo, F., Ginesta, A., and Godinez, C. (2010). Effect of temperature on the performance of microbial fuel cells. *Fuel*, **89**(12), 3985-3994.

Lee, Y., Martin, L., Grasel, P., Tawfiq, K., and Chen, G. (2013). Power generation and nitrogen removal of landfill leachate using microbial fuel cell technology. *Environmental Technology*, **34**(19), 2727-2736.

Lee, H. S., Torres, C. I., and Rittmann, B. E. (2009). Effects of substrate diffusion and anode Potential on kinetic parameters for anode-respiring bacteria. *Environmental science & technology*, **43**(19), 7571-7577.

Leicester, D. D., Settle, S., McCann, C. M., & Heidrich, E. S. (2023). Investigating Variability in Microbial Fuel Cells. *Applied and Environmental Microbiology*, **89**(3), e02181-22.

Leton, T; Omotosho O. (2004). Landfill operations in the Niger delta region of Nigeria. *Engin. Geol.* **73**: 171-177

Li, L. H., Sun, Y. M., Yuan, Z. H., Kong, X. Y., & Li, Y. (2013). Effect of temperature change on power generation of the microbial fuel cell. Environmental Technology, **34**(13-14), 1929- 1934.

Lin, T., Bai, X., Hu, Y., Li, B., Yuan, Y. J., Song, H., ... & Wang, J. (2017). Synthetic Saccharomyces cerevisiae-Shewanella oneidensis consortium enables glucose-fed high-performance microbial fuel cell. *AIChE Journal*, **63**(6), 1830-1838.

Liu, H., and Logan, B. E. (2004). Electricity generation using an air-cathode single chamber Microbial fuel cell in the presence and absence of a proton exchange membrane. *Environmental science & technology*, **38**(14), 4040-4046.

Liu, H., Cheng, S., and Logan, B. E. (2005). Production of electricity from acetate or butyrate Using a single-chamber microbial fuel cell. *Environmental science & technology*, **39**(2), 658-662.

Logan, Bruce E.; Hamelers, Bert; Rozendal, René; Schröder, Uwe; Keller, Jürg; Freguia, Stefano; Aelterman, Peter; Verstraete, Willy; Rabaey, Korneel (2006). Microbial Fuel Cells: *Methodology and Technology*. **40**(17), 5181–5192.

Logan, B. E., & Regan, J. M. (2006). Microbial fuel cells—challenges and applications. *Environmental science & technology*, **40**(17), 5172-5180.

López-Bascón, M. A., & De Castro, M. L. (2020). Soxhlet extraction. In Liquid-phase extraction

327-354.

Lovley, D.R., 2012. Electromicrobiology. *Annu. Rev. Microbiol.*, **66**:391-409. Luo, S., Sun, H., Ping, Q., Jin, R., He, Z. 2016. A review of modeling bioelectrochemical systems: engineering and statistical aspects. *Energies*, **9**, 111.

Lyon, D. Y., Buret, F., Vogel, T. M., and Monier, J. M. (2010). Is resistance futile? Changing external resistance does not improve microbial fuel cell performance. *Bioelectrochemistry*, **78**(1), 2-7.

Maier, R. M., & Pepper, I. L. (2015). Bacterial growth. In Environmental microbiology (pp. 37-56). *Academic Press.*

Maldonado-Celis, M. E., Yahia, E. M., Bedoya, R., Landázuri, P., Loango, N., Aguillón, J., and Guerrero Ospina, J. C. (2019). Chemical composition of mango (Mangifera indica L.) fruit: Nutritional and phytochemical compounds. *Frontiers in plant science*, **10**, 1073.

Manchala, K. R., Sun, Y., Zhang, D., & Wang, Z. W. (2017). Anaerobic digestion modelling. In *Advances in bioenergy.* **2**, 69-141.

Masoura, M., & Gkatzionis, K. (2022). The antimicrobial mechanism of Greek thyme honeys against methicillin-resistant Staphylococcus aureus clinical isolates: a case study of comparison with Manuka honey. *International Journal of Food Science & Technology*, **57**(11), 7076-7084.

Mathuriya, A. S. (2013). Eco-Affectionate Face of Microbial Fuel Cells. *Critical Reviews in Environmental Science and Technology*, **44**(2), 97–153.

Mathuriya, A. S. (2013). Inoculum selection to enhance performance of a microbial fuel cell for electricity generation during wastewater treatment. *Environmental technology*, **34**(13-14), 1957-1964.

McCabe, B.K., Harris, P., Baillie, C., Pittaway, P., Yusaf, T., 2013. Assessing a New Approach to Covered Anaerobic Pond Design in the Treatment of Abattoir Wastewater. *Australian Journal of Multi-Disciplinary Engineering.* **10**(1), 81-93.

Meignanalakshmi, S. and Kumar, S. V. (2016). Bioelectricity production by using goat (Capra hircus) rumen fluid from slaughterhouse waste in mediator-less microbial fuel cells. Energy Sources, Part A: *Recovery, Utilization, and Environmental Effects*, **38**(10), 1364-1369.

Menicucci, J., Beyenal, H., Marsili, E., Veluchamy, R. A., Demir, G., and Lewandowski, Z. (2006). Procedure for determining maximum sustainable power generated by microbial fuel cells. *Environmental science & technology*, **40**(3), 1062-1068.

Merem, E. C., Twumasi, Y., Wesley, J., Olagbegi, D., Fageir, S., Crisler, M., & Washington, J. (2019). Analyzing geothermal energy use in the East African Region: The case of Kenya. *Energy and Power*, **9**(1), 12-26.

Mbaki, S. (2019). Towards Resource Recovery, Reuse, Reducing and Recycling of Solid Waste in Nairobi County: a Case Study of Roysambu Sub-County. (http://erepository.uonbi.ac.ke/handle/11295/109413), [Doctoral dissertation, University of Nairobi].

Mbugua, J. K., Mbui, D. N., Mwaniki, J., Mwaura, F., and Sheriff, S. (2020). Influence of Substrate Proximate Properties on Voltage Production in Microbial Fuel Cells. *Journal of Sustainable Bioenergy Systems*, **10**(2), 43.

Mbwilo, E. C., & Mahenge, F. Y. (2022). Municipal Solid Waste Collection Services in Rapidly Growing Cities of Tanzania.*Journal of the Geographical Association of Tanzania*, **42**(1).

Miran, M., Nawaz, M., Jang, J., Lee, D.S. 2016 Conversion of orange peel waste biomass to bioelectricity using a mediator-less microbial fuel cell. *Science of the Total Environment* **547**: 197-205.

Mochache, M., Yegon, R., & Wakindiki, I. I. C. (2020). Market town household solid waste management: A case study of Embu, Kenya. *Journal of Applied Sciences and Environmental Management*, **24**(1), 105-109.

Modak, P; Jiemian, Y; Hongyuan, Y; Mohanty, CR. (2010). Municipal solid waste management: turning waste into resources. *Shanghai manual: a guide for sustainable urban development in the 21st century,* 1-36.

Möller, J. (2014). Comparing methods for fibre determination in food and feed. West Lafayette: *The Association of American Feed Control Officials*.

Mohammed, S. M., Abdurrahman, A. A., & Attahiru, M. (2017). Proximate analysis and total lycopene content of some tomato cultivars obtained from Kano State, Nigeria. *Chem Search Journal*, **8**(1), 64-69.

Monyoncho, G. (2013). Solid waste management in urban areas Kenya: A case study of Lamu town. A thesis submitted to the Department of Real Estate and Construction Management, University of Nairobi, 1-66.

Moukazis, I., Pellera, F. M. and Gidarakos, E. (2018). Slaughterhouse by-products treatment using anaerobic digestion. *Waste Management*, **71**, 652-662.

Mulder, G., De Ridder, F., Coenen, P., Weyen, D. and Martens, A. (2008). Evaluation of an on-site cell voltage monitor for fuel cell systems. *International Journal of hydrogen energy*, **33**(20), 5728-5737.

Mullai, P., Rene, E. R., and Sridevi, K. (2013). Biohydrogen production and kinetic modelling using sediment microorganisms of pichavaram mangroves, India. *Bio-Med research international*, **2013**.

Muiruri, J., Wahome, R., & Karatu, K. (2020). Assessment of methods practiced in the disposal

of solid waste in Eastleigh Nairobi County, Kenya. *AIMS Environmental Science*, **7**(5), 434-448.

Mungai, E. M., Ndiritu, S. W., & Rajwani, T. (2020). Do voluntary environmental management systems improve environmental performance? Evidence from waste management by Kenyan firms. *Journal of Cleaner Production,* **265**, 121636.

Mwangi, H; Sira, F; Kaluli, W. (2017). Sustainable solid waste management strategies in Juja, Kenya. *J. Agric. Sci. Tech*. **13** (1): 79-90.

Mwenzwa, E. M., & Misati, J. A. (2014). Kenya's Social Development Proposals and Challenges: *Review of Kenya Vision 2030 First Medium-Term Plan*, 2008-2012.

Muniafu, M., & Otiato, E. (2010). Solid Waste Management in Nairobi, Kenya. A case for emerging economies. *Journal of Language, Technology & Entrepreneurship in Africa,* **2**(1), 342-350.

Nasrollahzadeh, H. S., Najafpour, G. D., Pazouki, M., Younesi, H., Zinatizadeh, A. A., and Mohammadi, M. (2010). Biodegradation of phenanthrene in an anaerobic batch reactor: Growth kinetics. *Chemical Industry and Chemical Engineering Quarterly/CICEQ,* **16**(2), 157-165.

Nair, L., Agrawal, K., & Verma, P. (2023). The role of microbes and enzymes for bioelectricity generation: a belief toward global sustainability. *In Biotechnology of Microbial Enzymes* (709-751).

Nastro, R. A., Jannelli, N., Minutillo, M., Guida, M., Trifuoggi, M., Andreassi, L., and Falcucci, G. (2017). Performance evaluation of Microbial Fuel Cells fed by solid organic waste: parametric comparison between three generations. *Energy Procedia*, **105**:1102-1108.

National Environment Management Authority (2014) National Management of solid waste Strategy, Nairobi. Kenya.

Njiru, C. W., & Letema, S. C. (2018). Energy poverty and its implication on standard of living in Kirinyaga, Kenya. *Journal of Energy*, **2018.**

Njoroge B.N.K, Kimani M.W. and Ndunge D.A (2014) Review of municipal solid waste management: A case study of Nairobi, Kenya. *International Journal of Engineering and Science*, **4**: 16–20.

Nielsen, S.S. (2010). Food analysis. In S. Suzanne Nielsen (Ed.), (4th ed.). New York Dordrecht Heidelberg London: *Springer*, 85-177

Nitisoravut, R., Thanh, C. N., & Regmi, R. (2017). Microbial fuel cells: Advances in electrode modifications for improvement of system performance. *International Journal of Green Energy*, **14**(8), 712-723.

Nora, A.; Wilapangga, A.; Kahfi, A.; Then, M.; Fairus, A. Antioxidant Activity, Total Phenolic Content, and FTIR Analysis of Fermented Baduy Honey with Pineapple. *Bioedukasi* 2022, **20**, 21–25.

Noori, M. T., Ghangrekar, M. M., Mukherjee, C. K., & Min, B. (2019). Biofouling effects on the performance of microbial fuel cells and recent advances in biotechnological and chemical strategies for mitigation. *Biotechnology advances*, **37**(8).

Nurhayati (2013) Broiler chicken performance feed ration containing pineapple peel meal and supplemented by yoghurt. *J Agripet* **13**: 15-20.

Ofoegbu, R. U., Momoh, Y. O., & Nwaogazie, I. L. (2015). Bioremediation of crude oil contaminated soil using organic and inorganic fertilizers. *Journal of Petroleum & Environmental Biotechnology*, **6**(1), 1.

Ofori-Boateng, C., Lee, K. T., and Mensah, M. (2013). The prospects of an electricity generation from municipal solid waste (MSW) in Ghana: A better waste management option. *Fuel processing technology*, **110**:94-102.

Kuamoah, C. (2020). Renewable energy deployment in Ghana: The hype, hope and reality. *Insight on Africa*, **12**(1), 45-64.

Ogutu, F. A., Kimata, D. and Kweyu, R. (2019). The role of environmental governance in solid waste management, policy implementation in Nairobi County. *Civil and Environmental Research*, **11**, 49-54.

Ogutu, F. A., Kimata, D. M. and Kweyu, R. M. (2021). Partnerships for sustainable cities as options for improving solid waste management in Nairobi city. *Waste Management & Research*, **39**(1), 25-31.

Oliveira, V. B., Falcao, D. S., Rangel, C. M., & Pinto, A. M. F. R. (2007). A comparative study of approaches to direct methanol fuel cells modelling. *International Journal of Hydrogen Energy*, **32**(3), 415-424.

Ondraczek, J. (2014). Are we there yet? Improving solar PV economics and power planning in developing countries: The case of Kenya. *Renewable and Sustainable Energy Reviews*, **30:** 604-615.

Osman, A. I., Elgarahy, A. M., Eltaweil, A. S., El-Monaem, A., Eman, M., El-Aqapa, H. G., & Sillanpää, M. (2023). Biofuel production, hydrogen production and water remediation by photocatalysis, biocatalysis and electrocatalysis. *Environmental Chemistry Letters*, 1-65.

Ozbayram, E. G., Ince, O., Ince, B., Harms, H., & Kleinsteuber, S. (2018). Comparison of rumen and manure microbiomes and implications for the inoculation of anaerobic digesters. *Microorganisms*, **6**(1), 15.

Pandit, S., & Das, D. (2018). Principles of microbial fuel cell for the power generation. Microbial fuel cell: A bioelectrochemical system that converts waste to watts, 21-41.

Parameswaran, P., Torres, C. I., Lee, H. S., Krajmalnik-Brown, R., & Rittmann, B. E. (2009). Syntrophic interactions among anode respiring bacteria (ARB) and Non-ARB in a biofilm anode: electron balances. *Biotechnology and bioengineering,* **103**(3), 513-523.

Parfitt, J., Barthel, M., & Macnaughton, S. (2010). Food waste within food supply chains: quantification and potential for change to 2050. *Philosophical transactions of the royal society B: biological sciences,* **365**(1554), 3065-3081.

Parkash, A., Aziz, S., Abro, M., Soomro, S.A., & Kousar, A. (2015). Design and Fabrication of Microbial Fuel Cell Using Cow Manure for Power Generation, *Sci.Int.(Lahore),***27**(5),4235-423.

Patil, S. A., Harnisch, F., Kapadnis, B. and Schröder, U. (2010). Electroactive mixed culture biofilms in microbial bioelectrochemical systems: the role of temperature for biofilm formation and performance. *Biosensors and Bioelectronics,* **26**(2), 803-808.

Pereira, J. A., Oliveira, I., Sousa, A., Ferreira, I. C., Bento, A., Estevinho, L. (2008). Bioactive properties and chemical composition of six walnuts (Juglans regiaL.) cultivars. *Food Chem Toxicol* **46**, 2103-2111.

Priyadarshini, A., Sahoo, M. M., Raut, P. R., Mahanty, B., & Sahoo, N. K. (2021). Kinetic modelling and process engineering of phenolics microbial and enzymatic biodegradation: A current outlook and challenges. *Journal of Water Process Engineering*, **44**, 102421.

Puig, S., Serra, M., Coma, M., Cabré, M., Balaguer, M. D., and Colprim, J. (2010). Effect of pH on nutrient dynamics and electricity production using microbial fuel cells. *Bioresource Technology*, **101**(24), 9594-9599.

Pushkar, P., and Mungray, A. K. (2016). Real textile and domestic wastewater treatment by novel cross-linked microbial fuel cell (CMFC) reactor. *Desalination and Water Treatment*, **57**(15), 6747-6760.

Qadri, O. S., Yousuf, B., and Srivastava, A. K. (2015). Fresh-cut fruits and vegetables: Critical factors influencing microbiology and novel approaches to prevent microbial risks—A review. *Cogent Food & Agriculture*, **1**(1), 1121606.

Radeef, A. Y., Ismail, Z. Z. 2019. Polarization model of microbial fuel cell for treatment of actual potato chips processing wastewater associated with power generation. *J. Electroanal. Chem.* **836,** 176-181.

Rahman, W., Yusup, S., and Mohammad, S. A. (2021, February). Screening of fruit waste as substrate for microbial fuel cell (MFC). *In AIP Conference Proceedings*, (Vol. **2332**, No.1 p. 020003).

Ram, Y., Dellus-Gur, E., Bibi, M., Karkare, K., Obolski, U., Feldman, M. W., ... & Hadany, L. (2019). Predicting microbial growth in a mixed culture from growth curve data. *Proceedings of the National Academy of Sciences,* **116**(29), 14698-14707.

Ramchandra, P., and Boucar, D. (2011). Green energy and technology. *London Dordrecht Heidelberg New York: Springer.* **10**: 978-981.

Ramluckan, K., Moodley, K. G. and Bux, F. (2014). An evaluation of the efficacy of using selected solvents for the extraction of lipids from algal biomass by the soxhlet extraction method. *Fuel,* **116**, 103-108.

Ramsay, R. R. (2019). Electron carriers and energy conservation in mitochondrial respiration. *ChemTexts*, **5**(2), 9

Rasel, M., Zerin, I., Bhuiyan, S. H., Hoque, K. M. H., Hasan, M., & Alam, M. M. (2019). Industrial Waste Management by Sustainable Way. *European Journal of Engineering and Technology Research,* **4**(4), 111-114.

Rawat, S. (2015). Food Spoilage: Microorganisms and their prevention. *Asian Journal of Plant Science and Research,* **5**(4), 47-56.

Ray, P. (2019). Renewable energy and sustainability. Clean Technologies and Environmental Policy, **21**(8), 1517-1533.

Reddy, A. V. K., Prasad, M. D., Sujatha, V., and Sridevi, V. (2014). A Review on Treatment of Sugar Industry Effluents by Up Flow Anaerobic Sludge Blanket Reactor. i-Manager's *Journal on Future Engineering and Technology*, **9**(3), 31.

Ren, Z., Yan, H., Wang, W., Mench, M. M., and Regan, J. M. (2011). Characterization of microbial fuel cells at microbially and electrochemically meaningful time scales. *Environmental science & technology,* **45**(6), 2435-2441.

Rismani-Yazdi, H., Carver, S. M., Christy, A. D., & Tuovinen, O. H. (2008). Cathodic limitations in microbial fuel cells: an overview. *Journal of Power Sources,* **180**(2), 683-694.

Rismani-Yazdi, H., Christy, A. D., Carver, S. M., Yu, Z., Dehority, B. A., and Tuovinen, O. H. (2011). Effect of external resistance on bacterial diversity and metabolism in cellulose-fed microbial fuel cells. *Bioresource Technology,* **102**(1), 278-283.

Saratale, G. D., Saratale, R. G., Shahid, M. K., Zhen, G., Kumar, G., Shin, H. S., and Kim, S. H. (2017). A comprehensive overview of electro-active biofilms, role of exoelectrogens, and their microbial niches in microbial fuel cells (MFCs). *Chemosphere,* **178**, 534-547.

Sarma, R., Tamuly, A., & Kakati, B. K. (2022). Recent developments in electricity generation by Microbial Fuel Cell using different substrates. *Materials Today: Proceedings*, **49**, 457-463.

Savvidou, M. G., Pandis, P. K., Mamma, D., Sourkouni, G., & Argirusis, C. (2022). Organic Waste Substrates for Bioenergy Production via Microbial Fuel Cells: A Key Point Review. *Energies,* **15**(15), 5616.

Schneider, T., & Lorenz, S. (1993). The United Nations Conference on Environment and Development (UNCED) in Rio de Janeiro in June 1992-Aspects of urgent research in the framework of forest ecology). Zeitschrift fuer Oekologie und Naturschutz (Germany).

Seluy, L.G., Isla, M.A., 2014. A process to treat high-strength brewery wastewater via ethanol recovery and vinasse fermentation. *Ind. Eng. Chem. Res.* **53** (44), 17043–17050
.
Seadon, JK. (2010). Sustainable waste management systems. *J. Cleaner Prdn.* **18**(16-17): 1639-1651.

Shakappa, D., and Talari, A. (2016). Analysis of available carbohydrate fractions from Indian foods by using a modified AOAC total dietary fibre method. *Indian Journal of Scientific Research*, **7**(1), 1-9.

Sharma, Y., and Li, B. (2010). The variation of power generation with organic substrates in single-chamber microbial fuel cells (SCMFCs). *Bioresource Technology*, **101**(6),1844-1850.

Shemfe, M., Gadkari, S., Yu, E., Rasul, S., Scott, K., Head, I. M., Sadhukhan, J. (2018). Life cycle, techno-economic and dynamic simulation assessment of bioelectrochemical systems: A case of formic acid synthesis. *Bioresource Technology,* **255,** 39–49.

Słowik, W., Piątek, P., Dziwiński, T. and Baranowski, J. (2017). Selected current sensing circuits for motor control application. *Pomiary Automatyka Robotyka*, 21.

Simatele, D. M., S. Dlamini, and N. S. Kubanza. 2017. "From Informality to Formality: Perspectives on the Challenges of Integrating Solid Waste Management into the Urban Development and Planning Policy in Johannesburg, South Africa." *Habitat International*, **63**: 122–130.

Singh, A., Kuila, A., Adak, S., Bishai, M., & Banerjee, R. (2012). Utilization of vegetable wastes for bioenergy generation. *Agricultural Research*, **1**(3), 213-222.

Song, T. S., Yan, Z. S., Zhao, Z. W., and Jiang, H. L. (2010). Removal of organic matter in freshwater sediment by microbial fuel cells at various external resistances. *Journal of Chemical Technology & Biotechnology,* **85**(11), 1489-1493.

Song, Z. (2017). Characterization of kinetics and performance in a microbial fuel cell supplied with synthetic landfill leachate. (Publishing No, 2017. 10619477), [Masters Thesis, Michigan Technological University].

Su, S., Cheng, H., Zhu, T., Wang, H., & Wang, A. (2018). Kinetic competition between microbial anode respiration and nitrate respiration in a bioelectrochemical system. *Bioelectrochemistry*, **123**, 241–247.

Sun, M., Zhai, L. F., Li, W. W. and Yu, H. Q. (2016). Harvest and utilization of chemical energy in wastes by microbial fuel cells. *Chemical society reviews*, **45**(10), 2847-2870.

Tai, J., Zhang, W., Che, Y., and Feng, D. (2011). Municipal solid waste source-separated

collection in China: A comparative analysis. *Waste Management*, **31**(8), 1673-1682.

Takase, M., Kipkoech, R., & Essandoh, P. K. (2021). A comprehensive review of energy scenario and sustainable energy in Kenya. *Fuel Communications*, **7,** 100015.

Tee, P. F., Abdullah, M. O., Tan, I. A., Amin, M. A., Nolasco-Hipolito, C., & Bujang, K. (2017). Effects of temperature on wastewater treatment in an affordable microbial fuel cell-adsorption hybrid system. *Journal of environmental chemical engineering*, **5**(1), 178-188.

Tian, Y., Mei, X., Liang, Q., Wu, D., Ren, N., & Xing, D. (2017). Biological degradation of potato pulp waste and microbial community structure in microbial fuel cells. *RSC advances*, **7**(14), 8376-8380.

Torres, C. I., Marcus, A. K., Lee, H.-S., Parameswaran, P., Krajmalnik-Brown, R., & Rittmann, B. E. (2010). A kinetic perspective on extracellular electron transfer by anode-respiring bacteria. *FEMS Microbiology Reviews*, **34**(1), 3–17.

Torres-León, C., Rojas, R., Contreras-Esquivel, J. C., Serna-Cock, L., Belmares-Cerda, R. E., & Aguilar, C. N. (2016). Mango seed: Functional and nutritional properties. *Trends in Food Science & Technology*, **55**, 109-117.

Tremouli, A., Martinos, M. and Lyberatos, G. (2017). The effects of salinity, pH, and temperature on the performance of a microbial fuel cell. *Waste and Biomass Valorization*, **8**(6), 2037-2043.

Tshivhase, S. E., & Mashau, N. S. (2020). A case of household waste management in a rural village in the Limpopo province, South Africa. *The Journal of Solid Waste Technology and Management*, **46**(4), 572-579.

Ueki, T. (2021). Cytochromes in extracellular electron transfer in Geobacter. *Applied and Environmental Microbiology*, **87**(10).

Velenturf, A. P. M., Archer S.A., Gomes, H.I., Christgen, B., Lag-Brotons, A. ., Purnell. P. (2019). Circular Economy and the matter of Integrated Resources. *Science of the Total Environment* **689**, 963 – 969.

Vendruscolo, F. (2015). Starch: a potential substrate for biohydrogen production. *International Journal of Energy Research*, **39**(3), 293-302.

Vergara, SE; Tchobanoglous, G (2012). Municipal solid waste and the environment: a global perspective. Annual Rev. *Environ. Resources***. 37:** 277-309.

Verma N, Bansal NC, Kumar V (2011) Pea peel waste: a lingo cellulosic waste and its utility in cellulose production by Trichoderma reesei under solid-state cultivation. *Bioresources*, **6**:1505–1519.

Walter X.A., Greenman J. and Ieropoulos A.I. (2020). Microbial fuel cells directly powering a Microcomputer, *Journal of Power Sources*, **446**:227-328.

Wang, C. T., Yang, C. M. J., & Chen, Z. S. (2012). Rumen microbial volatile fatty acids in relation to oxidation reduction potential and electricity generation from straw in microbial fuel cells. *biomass and bioenergy*, **37**, 318-329.

Wang, X., Tang, J., Cui, J., Liu, Q., Giesy, J.P. and Hecker, M. (2009) Synergy of Electricity Generation and Waste Disposal in Solid State Microbial Fuel Cell (MFC) of Cow Manure Composting. *International Journal of Electrochemical Science,* **9**:3144-3157.

Wang J and W. Wan. (2008). "The effect of substrate concentration on bio-hydrogen production by using kinetic models," *Science in China B,* **51**(11),1110–1117.

Wang Q, Fan X, Gao W, Chen J (2006) Characterization of bio-sourced cotton fabrics using FT-IR ATR spectroscopy and microscopy techniques. *Carbohydrate Research.* **341**(12): 2170-2175.

Webb D and Møller-Holst S. The Arduino Playground (2018), http://playground.arduino.cc Measuring individual cell voltages in fuel cell stacks, *Journal of Power Sources,* **1**, (2001).

Wei, Y., Zhao, Y., & Yun, H. (2021). Estimating PEMFC ohmic internal impedance based on indirect measurements. *Energy Science & Engineering*, **9**(8), 1134-1147.

Xu, Y., Chen, P., & Peng, H. (2018). Generating electricity from water through carbon nanomaterials. *Chemistry–A European Journal*, **24**(24), 6287-6294.

Yong, Y. C., Cai, Z., Yu, Y. Y., Chen, P., Jiang, R., Cao, B., ... & Song, H. (2013). Increase of riboflavin biosynthesis underlies enhancement of extracellular electron transfer of Shewanella in alkaline microbial fuel cells. *Bioresource technology,* **130**, 763-768.

You S.J., L. Zhao., J.Q. Jiang., J. N Zhang and S.Q. Zhao. (2006). Sustainable approach for Leachate treatment: Electricity generation in microbial fuel cells. *Journal of Environmental science and Health part a-toxic/Hazardous substances and Environmental Engineering.* **41**(12), 2721-2734.

Yurgel, S. N., L. Abbey, N. Loomer, R. Gillis-Madden, and M. Mammoliti. 2018. Microbial communities associated with storage onion. *Phytobiomes Journal.* **2** (1):35–41.

Zain Mumtaz, Saleem Ullah, Zeeshan Ilyas, Naila Aslam, Shahid Iqbal, Shuo Liu 2,Jehangir Arshad Meo and Hamza Ahmad Madni. (2018). An Automation System for Controlling Streetlights and Monitoring Objects Using Arduino. *Open Access* **18**(10), 3178.

Zhang G, Zhao Q, Jiao Y, Wang K, Lee DJ, Ren (2011). Biocathode Microbial Fuel Cell for Efficient Electricity Recovery from Dairy Manure, *Biosensors and Bioelectronics,* **31**(1), 537-543.

Zhang Jiqiang., Ping Zhang., Meng Zhang., Hiu Chen., Tingting Chen., Zuofu Xie., Jing Cai and Ghulam Abbs. (2013). Kinetics of substrate degradation and electricity generation in anodic denitrification microbial fuel cell (AD-MFC). *Bioresource Technology*,**149**:44-50.

Zhang L, Zhu X, Li J, Qiang L, Ye D (2011) Biofilm formation and electricity generation of a microbial fuel cell started up under different external resistances. *J Power Sources,* **196**: 6029-6035.

Zhang Y, Min B, Huang L, Angelidaki I (2011) Electricity generation and microbial community response to substrate changes in microbial fuel cell. *Bioresour Technol***. 102**(2): 1166-1173.

Zhao, G., Ma, F., Wei, L., Chua, H., Chang, C. and Zhang, X. (2012) Electricity Generation From Cattle Dung Using MFC Technology during Anaerobic Acidogenesis and the Development of Microbial Populations. *Waste Management*, **32**:651-1658.

Zhao, Y., Hou, Y., Tang, G., Cai, E., Liu, S., Yang, H., Wang, S. (2014). Optimization of ultrasonic extraction of phenolic compounds from Epimedium brevicornum maxim using response surface methodology and evaluating its antioxidant activities in vitro. *Journal of Analytical Methods in Chemistry*, **2014**, 864654.

Zhou, M., Chen, Y. and Guan, L. L. (2015). Rumen bacteria. In Rumen Microbiology: *From Evolution to Revolution. Springer, New Delhi*. 79-95.

Zhu, L. (2015). Biorefinery as a promising approach to promote microalgae industry: An innovative framework. *Renewable and sustainable energy reviews*, **41,** 1376-1384.

APPENDICES

Appendix 1: Average Voltage output from different fruit waste from day 1-22

	VOLTAGE(mV)					
DAYS	AVOCADO	MANGO	TOMATO	MELON	BANANA	MIXTURE
1	33.6	30.9	31.56	58.15	65.3	50.87
2	25.66	49.13	49.2	80.73	119.27	71.83
3	52.6	53.7	64.13	95.03	86.46	79.8
4	134.1	71.033	71.27	97.7	87.46	100.67
5	137.6	81.53	77.16	120.3	101.5	122.4
6	135.4	85.73	80.53	128.93	129.033	126.53
7	106.3	116.77	93.43	133.13	134.87	139
8	88.16	131.1	113.46	147.27	170.4	143.2
9	75.76	126.63	103.9	139.3	166.53	137.03
10	94.27	146.4	114.5	161.73	187.47	147.83
11	138.83	192.8	136.9	182.97	218.66	191.7
12	171.1	217.67	159.5	178.86	212.67	188.26
13	178.2	219.3	153.76	229	239.66	184.566
14	221	255.33	193.53	235.33	291.33	211
15	277.33	284.67	206.1	269	319.3	228.7
16	300.67	329.7	231.3	284	334.33	217
17	311	325	240.3	282	336.3	216
18	302.33	297.67	232.66	283	327.3	207.4
19	286.33	288.3	231.7	268.33	312.33	196.23
20	275.7	279.33	219.66	249	297.67	190.8
21	265	273.67	208.7	238	284	178.83
22	265.3	255.66	193.5	233.3	265.66	163.3

Appendix 2: Monod Model Calculations

$$r = r_{max} * \frac{S}{(K_S + S)} \quad (4.9a)$$

μ-Lag phase ~ 0, **μ-Log phase** = μ_{max}, **μStat phase** = 0, **μ-Death phase** < 0. Note: $(r = \mu)$

Taking the reciprocal of Monod Equation: (y = mx + c).

$$\frac{1}{\mu} = \frac{K_S + S}{\mu_{max} * S} = \left(\frac{K_S}{\mu max}\right) * \left(\frac{1}{S}\right) + \left(\frac{1}{\mu max}\right) \quad (4.9b)$$

$$\mu = \frac{\text{amount of biomass produced}}{\text{time taken}} \quad (4.9c)$$

Calculations:

Taking the example of the Banana fruit, the maximum voltage produced = 336 mV, and Time taken = 408 hours

μ = [336 mV/408 hrs] = 0.82

Specific growth rate (μ) = 0.82 h^{-1}

$$\mu_{max} = \frac{\text{amount of biomass produced}}{\text{initial inoculum vol x time taken}} \quad (4.9d)$$

The parameters for the experiment with the banana waste are as follows:

Initial biomass = 250 ml, maximum voltage = 336 mV, Time taken = 408 hours

Therefore, the maximum specific growth rate can be calculated as follows:

$$\mu_{max=} \quad \left[\frac{336\ mV}{250\ ml\ x\ 408\ hrs}\right] = 0.003$$

Maximum specific growth rate (μ_{max}) = 0.003 h^{-1}

Using the Monod equation: the equilibrium constant can be calculated:

$$\frac{1}{\mu} = \frac{K_S + S}{\mu max \,.\, S} = \left(\frac{K_S}{\mu max}\right).\left(\frac{1}{S}\right) + \left(\frac{1}{\mu max}\right)$$

$1/0.82\ h^{-1} = Ks/0.003\ h^{-1} * 1/100\ gL^{-1} + 1/0.003\ h^{-1}$ [since, S = 100 ml = 100 gL^{-1}]

$$1/0.82\ h^{-1} = 1/0.003\ h^{-1}\ [K_S/100\ gL^{-1} + 1/1]$$

$$1/0.82\ h^{-1} = 1/0.003\ h^{-1}\ [(K_S + 100\ gL^{-1})/100\ gL^{-1}]$$

$$1/0.82\ h^{-1} = [(K_S + 100\ gL^{-1})/0.3\ gL^{-1}.\ h^{-1}]$$

$$0.3\ gL^{-1}.\ h^{-1} = 0.82\ h^{-1}K_S + 82\ gL^{-1}.\ h^{-1}$$

$$0.3\ gL^{-1} = 0.82K_S + 82\ gL^{-1}$$

$$0.82\ K_S = [82\ gL^{-1} - 0.3\ gL^{-1}]$$

$$0.82\ K_S = 81.7\ gL^{-1}$$

$$K_S = 99.63 \pm 0.03\ gL^{-1}$$

Appendix 3: Haldane Andrew's Kinetic Model Calculations

$$r = r_{max} * \frac{S}{\left(K_S + S + \frac{S^2}{K_{IH}}\right)} \quad (4.10a)$$

Note: ($r = \mu$)

Taking the reciprocal of Haldane Andrew's Kinetic Equation: (y = mx + c)

$$\frac{1}{\mu} = \frac{K_S + \frac{S^2}{K_{IH}}}{\mu max} * \frac{1}{S} + \frac{1}{\mu max} \quad (4.10b)$$

Given: $\mu = 0.82\ h^{-1}$, $\mu_{max} = 0.003\ h^{-1}$, $S = 100\ gL^{-1}$, $K_S = 99.63\ gL^{-1}$

$1/0.82\ h^{-1} = [(99.63\ gL^{-1} + (100\ gL^{-1})^2/K_{IH}))/0.003\ h^{-1}) * 1/100\ gL^{-1} + 1/0.003\ h^{-1}]$

$1/0.82\ h^{-1} = 1/0.003\ h^{-1}[(99.63\ gL^{-1} + (10000\ gL^{-1}/K_{IH}))/100\ gL^{-1} + 1/1]$

$1/0.82\ h^{-1} = 1/0.003\ h^{-1}[((99.63\ gL^{-1}.K_{IH} + 10000\ gL^{-1})/K_{IH})/100\ gL^{-1} + 1/1]$

$1/0.82\ h^{-1} = [((99.63\ gL^{-1}.K_{IH} + (10000\ gL^{-1}/K_{IH}) + 100\ gL^{-1}.K_{IH})\ /0.3\ gL^{-1}.\ h^{-1}]$

$1/0.82\ h^{-1} = [((199.63\ gL^{-1}.\ K_{IH}\ /K_{IH} + 10000\ gL^{-1})/0.3\ gL^{-1}.\ h^{-1}]$

$0.3\ gL^{-1}.\ h^{-1} = [(163.69\ gL^{-1}.K_{IH}.h^{-1} + 8200\ gL^{-1}.\ h^{-1})/K_{IH}]$

$0.3\ gL^{-1}.K_{IH}.h^{-1} = 163.69\ gL^{-1}.K_{IH}.h^{-1} + 8200\ gL^{-1}.h^{-1}$

$163.69\ gL^{-1}.K_{IH} - 0.3\ gL^{-1}.K_{IH} = 8200\ gL^{-1}$

$163.39\ gL^{-1}.K_{IH} = 8200\ gL^{-1}$

$K_{IH} == [(8200\ gL^{-1})/(163.39\ gL^{-1})]$

$K_{IH} = 50.18 \pm 0.04\ gL^{-1}$

Appendix 4: Han-Levenspiel Model:

$$r = r_{max} * \frac{S\left(1-\frac{S}{S_m}\right)^n}{S + K_S * \left(1-\frac{S}{S_m}\right)^m} \quad (4.11)$$

Given: $\mu = 0.82\ h^{-1}$, $\mu_{max} = 0.003\ h^{-1}$, $S = 100\ gL^{-1}$, $Ks = 99.63\ gL^{-1}$

$0.82h^{-1}/1 = [(0.003h^{-1} * 100\ gL^{-1}\ (1– (100\ gL^{-1}/Sm)))/(100\ gL^{-1}+99.63\ gL^{-1}(1-(100\ gL^{-1}/Sm)))]$

$0.82\ h^{-1}/1 = [(0.3\ Sm\ h^{-1} - 30\ gL^{-1}.h^{-1})/ (100\ gL^{-1}+ 99.63\ gL^{-1}Sm- 9963\ gL^{-1})]$

$0.82\ h^{-1}/1 = [(0.3\ Sm.\ h^{-1} - 30\ gL^{-1}h^{-1})/ (99.63\ gL^{-1}.\ Sm- 9863\ gL^{-1})]$

$0.3\ Sm.h^{-1} - 30\ gL^{-1}.h^{-1} = 81.69\ gL^{-1}.Sm.h^{-1} + 8169.7\ gL^{-1}.h^{-1}$

$81.69\ gL^{-1}Sm.h^{-1} - 0.3\ Sm\ h^{-1} = 8169.7\ gL^{-1}.\ h^{-1} + 30\ gL^{-1}.\ h^{-1}$

$81.39\ S_m = 8199.7\ gL^{-1}$

$S_m = 8199.7\ gL^{-1} /81.39$

$S_m = 100.75 \pm 3.67\ gL^{-1}$

Appendix 5: Order of chemical reaction

5.1 Zero-order using banana fruit waste dataset

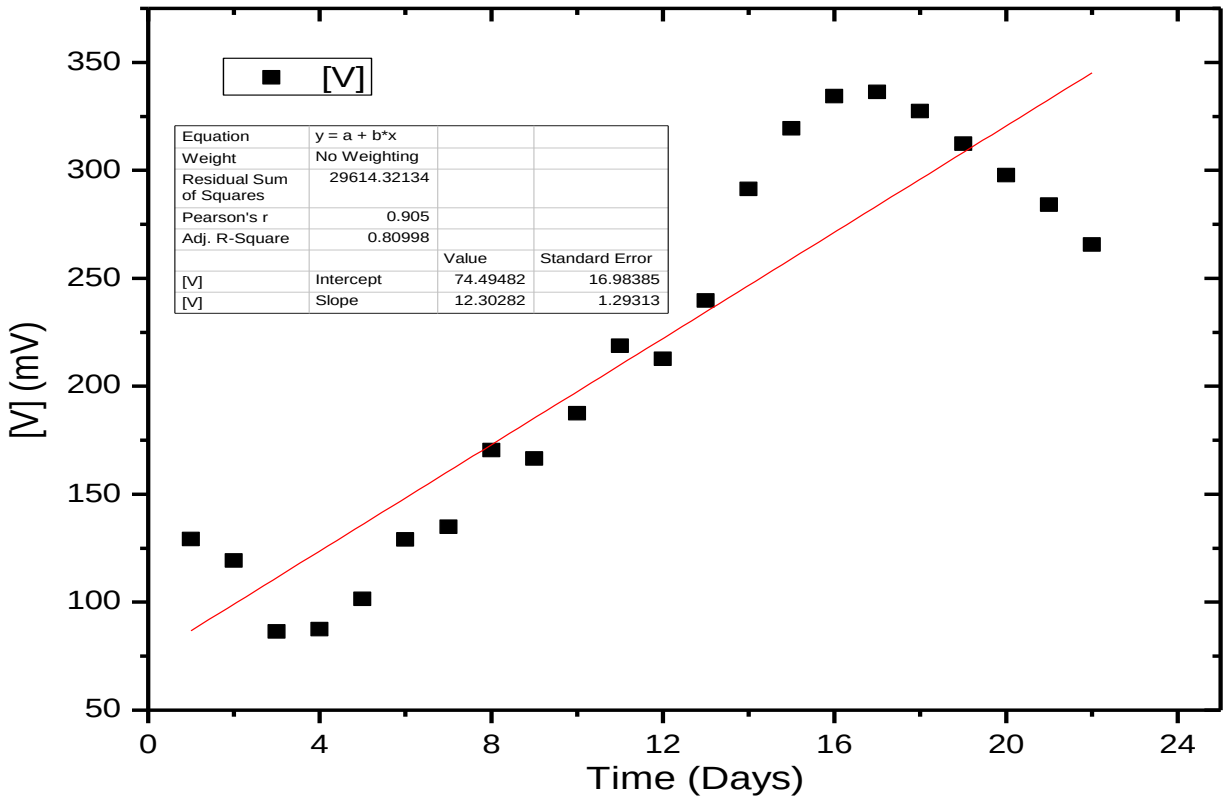

Linear Regression of dataset: Using function: A*x+B

Weighting Method: No weighting

From x = $1.0e^{+00}$ to x = $2.2e^{+01}$

B (y-intercept) = $7.5e^{+01} \pm 1.7e^{+01}$

A (slope) = $1.2e^{+01} \pm 1.3e^{+00}$

$Chi^2/doF = 1.5e^{+03}$

$R^2 = 0.82$

Adjusted $R^2 = 0.80$

RMSE (Root Mean Squared Error) = 38.48

RSS (Residual Sum of Squares) = 29,614.32

5.2 Second-order using banana fruit waste dataset

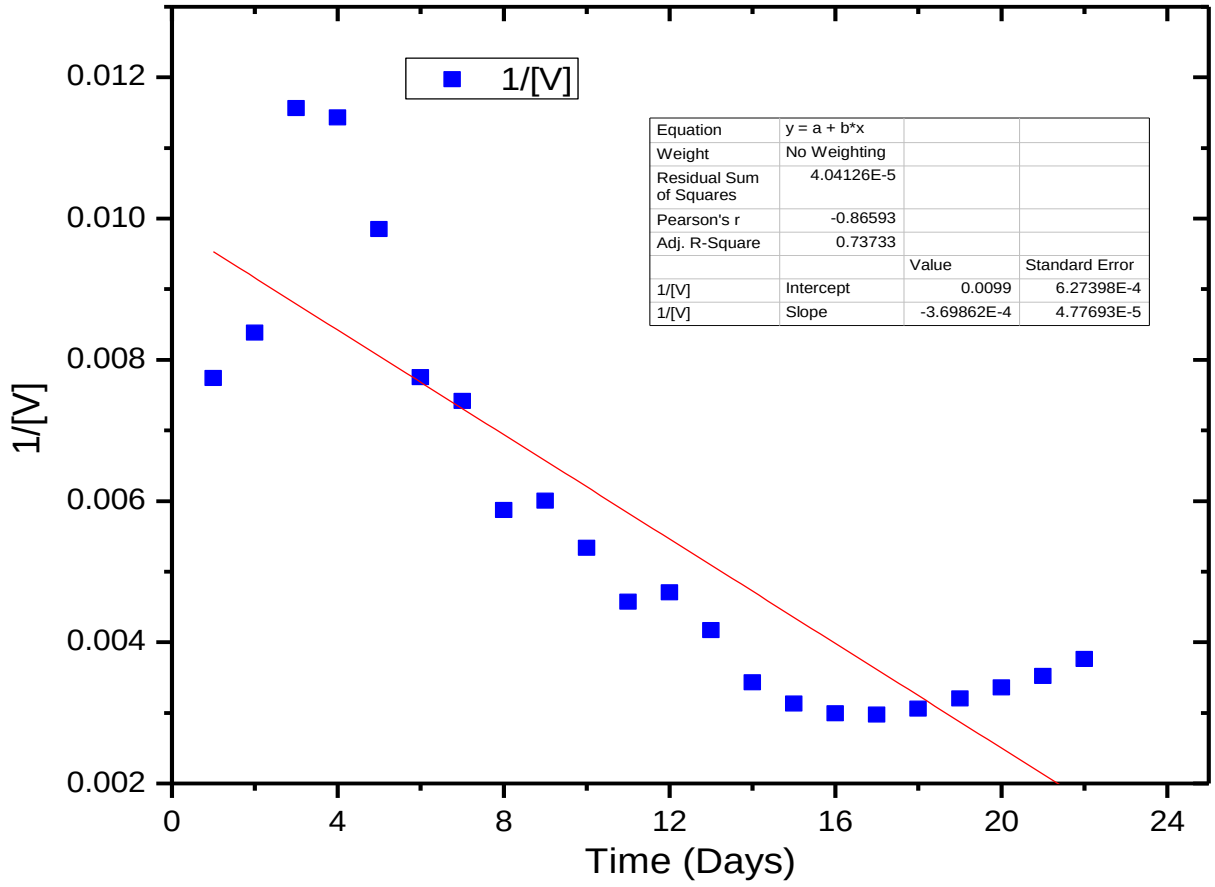

Linear Regression of dataset: Using function: A*x+B

Weighting Method: No weighting

From x = $1.0e^{+00}$ to x = $2.2e^{+01}$

B (y-intercept) = $9.9e^{-03} \pm 6.3e^{-04}$

A (slope) = $-3.7e^{-04} \pm 4.8e^{-05}$

$Chi^2/doF = 2.02e^{-06}$

$R^2 = 0.75$

Adjusted $R^2 = 0.72$

RMSE (Root Mean Squared Error) = 0.0014

RSS (Residual Sum of Squares) = $4.04e^{-05}$

Appendix 6: One-way Analysis of Voltage (mV) By Treatment

Summary of Fit

Rsquare	0.075
Adj Rsquare	0.038
Root Mean Square Error	80.833
Mean of Response	178.534
Observations (or Sum Wgts)	132

Voltage data Analysis of Variance

Source	DF	Sum of Squares	Mean Square	F Ratio	Prob > F
Treatment	5	66277.65	13255.5	2.0287	0.0790
Error	126	823280.34	6534.0		
C. Total	131	889557.99			

Means for One-way Anova

Level	Number	Mean	Std Error	Lower 95%	Upper 95%
Avocado	22	176.780	17.234	142.68	210.88
Banana	22	215.962	17.234	181.86	250.07
Mango	22	187.563	17.234	153.46	221.67
Mixture	22	158.760	17.234	124.66	192.87
Tomato	22	145.754	17.234	111.65	179.86
Watermelon	22	186.385	17.234	152.28	220.49

Standard Error used a pooled estimate of error variance

Means Comparisons
Comparisons for each pair using Student's t
Confidence Quantile

T	Alpha
1.97897	0.05

LSD Threshold Matrix

Abs (Dif)-LSD

	banana	mango	Watermelon	avocado	mixture	Tomato
Banana	-48.232	-19.833	-18.654	-9.050	8.970	21.977
Mango	-19.833	-48.232	-47.053	-37.448	-19.429	-6.422
Watermelon	-18.654	-47.053	-48.232	-38.627	-20.608	-7.601
Avocado	-9.050	-37.448	-38.627	-48.232	-30.212	-17.205
Mixture	8.970	-19.429	-20.608	-30.212	-48.232	-35.225
Tomato	21.977	-6.422	-7.601	-17.205	-35.225	-48.232

Positive values show pairs of means that are significantly different.

Appendix 7: One-way Analysis of Current (mA) By Treatment

The Summary of Fit - 7

R-square	0.049
Adj R-square	0.011
Root Mean Square Error	0.007
Mean of Response	0.020
Observations (or Sum Wgts)	132

Analysis of Variance

Source	DF	Sum of Squares	Mean Square	F Ratio	Prob > F
Treatment	5	0.00035097	0.000070	1.2903	0.2722
Error	126	0.00685454	0.000054		
C. Total	131	0.00720551			

Means for One-way Anova

Level	Number	Mean	Std Error	Lower 95%	Upper 95%
Avocado	22	0.018427	0.00157	0.01532	0.02154
Banana	22	0.017645	0.00157	0.01453	0.02076
Mango	22	0.021500	0.00157	0.01839	0.02461
Mixture	22	0.022055	0.00157	0.01894	0.02517
Tomato	22	0.021042	0.00157	0.01793	0.02415
Watermelon	22	0.020883	0.00157	0.01777	0.02400

Std-Error uses a pooled estimate of error variance

Means Comparisons
Comparisons for each pair using Student's t
Confidence Quantile

t	Alpha
1.97897	0.05

LSD Threshold Matrix
Abs (Dif)-LSD

	Mixture	Mango	Tomato	Watermelon	Avocado	Banana
Mixture	-0.00440	-0.00385	-0.00339	-0.00323	-0.00077	0.00001
Mango	-0.00385	-0.00440	-0.00394	-0.00378	-0.00133	-0.00055
Tomato	-0.00339	-0.00394	-0.00440	-0.00424	-0.00179	-0.00100
Watermelon	-0.00323	-0.00378	-0.00424	-0.00440	-0.00195	-0.00116
Avocado	-0.00077	-0.00133	-0.00179	-0.00195	-0.00440	-0.00362
Banana	0.00001	-0.00055	-0.00100	-0.00116	-0.00362	-0.00440

Positive values show pairs of means that are significantly different.

Appendix 8: One-way Analysis of power (mW) By Treatment

The Summary of Fit - 8;

Rsquare	0.027
Adj Rsquare	-0.011
Root Mean Square Error	0.002
Mean of Response	0.003
Observations (or Sum Wgts)	132

Power data Analysis of Variance;

Source	DF	Sum of Squares	Mean Square	F Ratio	Prob > F
Treatment	5	0.00000800	0.0000016	0.7038	0.6216
Error	126	0.00028640	2.273e-6		
C. Total	131	0.00029440			

Means for One-way Anova

Level	Number	Mean	Std Error	Lower 95%	Upper 95%
Avocado	22	0.003186	0.00032	0.00255	0.00382
Banana	22	0.003542	0.00032	0.00291	0.00418
Mango	22	0.003644	0.00032	0.00301	0.00428
Mixture	22	0.003446	0.00032	0.00281	0.00408
Tomato	22	0.002969	0.00032	0.00233	0.00360
Watermelon	22	0.003624	0.00032	0.00299	0.00426

Standard-Error used a pooled estimate of error variance

Means Comparisons
Comparisons for each pair using Student's t
Confidence Quantile

t	Alpha
1.97897	0.05

LSD Threshold Matrix
Abs (Dif)-LSD

	Mango	Watermelon	Banana	Mixture	Avocado	Tomato
Mango	-0.00090	-0.00088	-0.00080	-0.00070	-0.00044	-0.00022
Watermelon	-0.00088	-0.00090	-0.00082	-0.00072	-0.00046	-0.00024
Banana	-0.00080	-0.00082	-0.00090	-0.00080	-0.00054	-0.00033
Mixture	-0.00070	-0.00072	-0.00080	-0.00090	-0.00064	-0.00042
Avocado	-0.00044	-0.00046	-0.00054	-0.00064	-0.00090	-0.00068
Tomato	-0.00022	-0.00024	-0.00033	-0.00042	-0.00068	-0.00090

Positive values show pairs of means that are significantly different.

Appendix 9: One-way Analysis of Current density (mA/m^2) By Treatment

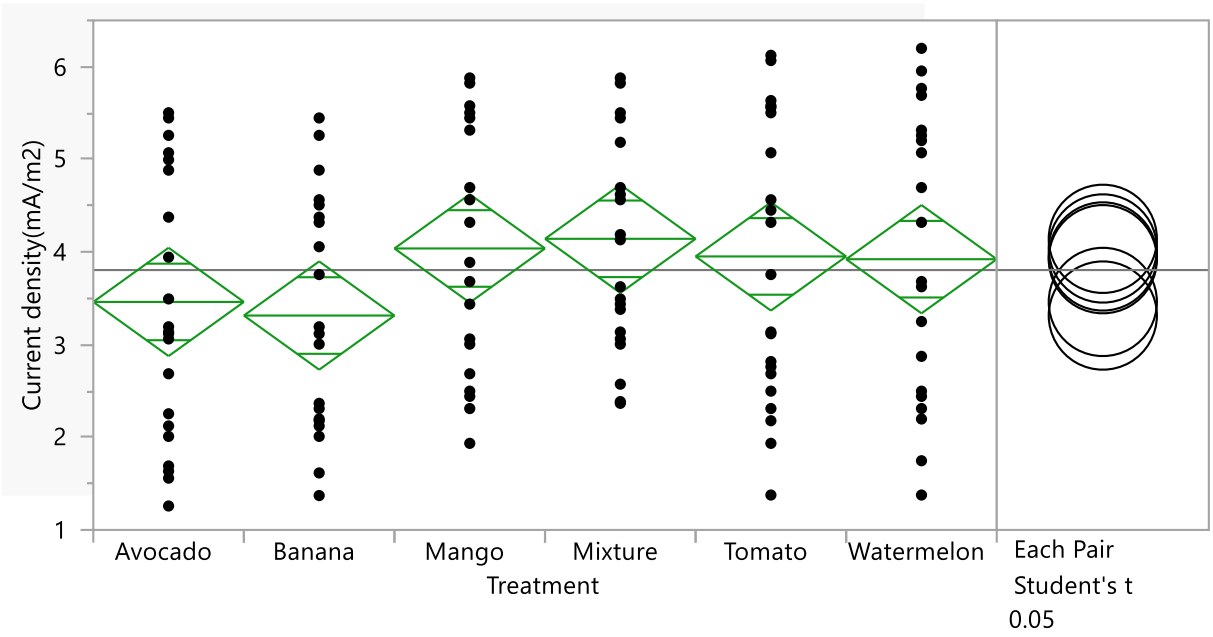

A summary of Fit - 9

R-square	0.049
Adj R-square	0.011
Root Mean Square Error	1.385
Mean of Response	3.805
Observations (or Sum Wgts)	132

Analysis of Variance;

Source	DF	Sum of Squares	Mean Square	F Ratio	Prob > F
Treatment	5	12.38197	2.47639	1.2903	0.2722
Error	126	241.82561	1.91925		
C. Total	131	254.20757			

Means for One-way Anova

Level	Number	Mean	Std Error	Lower 95%	Upper 95%
Avocado	22	3.46117	0.29536	2.8767	4.0457
Banana	22	3.31432	0.29536	2.7298	3.8988
Mango	22	4.03832	0.29536	3.4538	4.6228
Mixture	22	4.14248	0.29536	3.5580	4.7270
Tomato	22	3.95234	0.29536	3.3678	4.5369
Watermelon	22	3.92246	0.29536	3.3379	4.5070

Std Error uses a pooled estimate of error variance

Means Comparisons

Comparisons for each pair using Student's t

Confidence Quantile

t	Alpha
1.97897	0.05

LSD Threshold Matrix

Abs (Dif)-LSD

	Mixture	Mango	Tomato	Watermelon	Avocado	Banana
Mixture	-0.82663	-0.72247	-0.63649	-0.60661	-0.14532	0.00153
Mango	-0.72247	-0.82663	-0.74065	-0.71077	-0.24948	-0.10263
Tomato	-0.63649	-0.74065	-0.82663	-0.79674	-0.33545	-0.18861
Watermelon	-0.60661	-0.71077	-0.79674	-0.82663	-0.36534	-0.21849
Avocado	-0.14532	-0.24948	-0.33545	-0.36534	-0.82663	-0.67978
Banana	0.00153	-0.10263	-0.18861	-0.21849	-0.67978	-0.82663

Positive values show pairs of means that are significantly different.

Connecting Letters Report

Level			Mean± SD
Mixture	A		4.142 ± 1.15
Mango	A	B	4.038 ± 1.29
Tomato	A	B	3.952 ± 1.52
Watermelon	A	B	3.922 ± 1.51
Avocado	A	B	3.461 ± 1.46
Banana		B	3.314 ± 1.33

Levels not connected by the same letter are significantly different.

Appendix 10: One-way Analysis of power density (mW/m^2) By Treatment

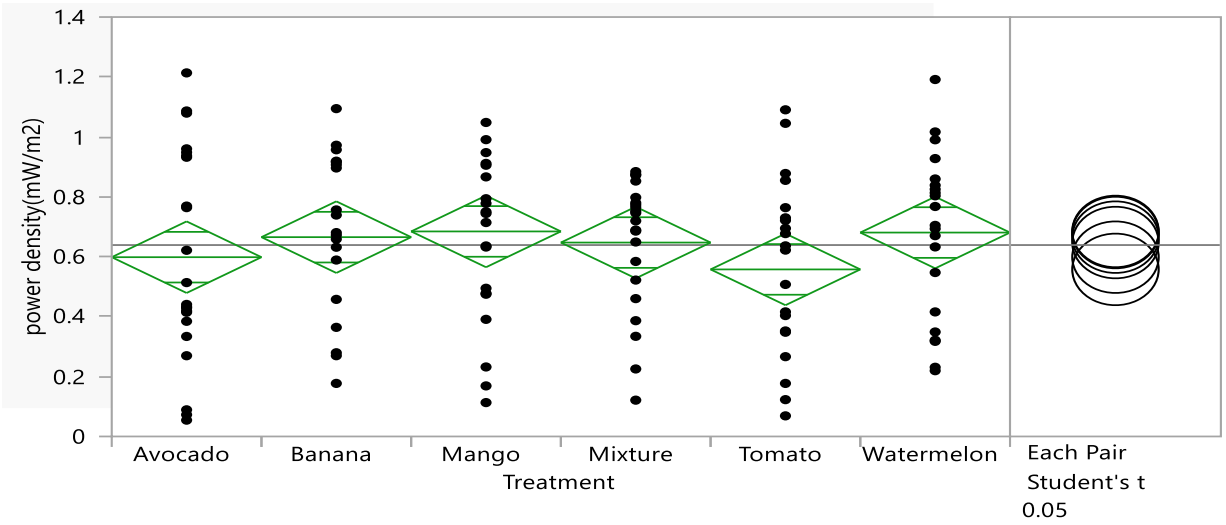

The Summary of Fit:

Rsquare	0.027
Adj Rsquare	-0.011
Root Mean Square Error	0.283
Mean of Response	0.639
Observations (or Sum Wgts)	132

Analysis of Variance

Source	DF	Sum of Squares	Mean Square	F Ratio	Prob > F
Treatment	5	0.282194	0.056439	0.7038	0.6216
Error	126	10.104005	0.080191		
C. Total	131	10.386199			

Means for One-way Anova

Level	Number	Mean	Std Error	Lower 95%	Upper 95%
Avocado	22	0.598411	0.06037	0.47893	0.71789
Banana	22	0.665277	0.06037	0.54580	0.78476
Mango	22	0.684399	0.06037	0.56492	0.80388
Mixture	22	0.647281	0.06037	0.52780	0.76676
Tomato	22	0.557612	0.06037	0.43813	0.67709
Watermelon	22	0.680659	0.06037	0.56118	0.80014

Std Error uses a pooled estimate of error variance

Means Comparisons

Comparisons for each pair using Student's t

Confidence Quantile

t	Alpha
1.97897	0.05

LSD Threshold Matrix

Abs (Dif)-LSD

	Mango	Watermelon	Banana	Mixture	Avocado	Tomato
Mango	-0.16897	-0.16523	-0.14985	-0.13185	-0.08298	-0.04218
Watermelon	-0.16523	-0.16897	-0.15359	-0.13559	-0.08672	-0.04592
Banana	-0.14985	-0.15359	-0.16897	-0.15097	-0.10210	-0.06130
Mixture	-0.13185	-0.13559	-0.15097	-0.16897	-0.12010	-0.07930
Avocado	-0.08298	-0.08672	-0.10210	-0.12010	-0.16897	-0.12817
Tomato	-0.04218	-0.04592	-0.06130	-0.07930	-0.12817	-0.16897

Positive values show pairs of means that are significantly different.

Connecting Letters Report

Level		Mean± SD
Mango	A	0.684 ± 0.281
Watermelon	A	0.681 ± 0.272
Banana	A	0.665 ± 0.273
Mixture	A	0.647 ± 0.217
Avocado	A	0.598 ± 0.351
Tomato	A	0.558 ± 0.287

Levels not connected by the same letter are significantly different.

Appendix 11: Correlation and Scatterplot matrix for Various market fruit wastes

(a) Avocado

Correlation Probability

	DAYS	VOLTAGE(mV)	CURRENT(mA)	Current density(mA/m2)	power(mW)	power density (mW/m2)
DAYS	<.0001	<.0001	0.9687	0.9687	0.0025	0.0025
VOLTAGE(mV)	<.0001	<.0001	0.6530	0.6530	0.0001	0.0001
CURRENT(mA)	0.9687	0.6530	<.0001	<.0001	0.0099	0.0099
Current density(mA/m2)	0.9687	0.6530	<.0001	<.0001	0.0099	0.0099
power(mW)	0.0025	0.0001	0.0099	0.0099	<.0001	<.0001
power density (mW/m2)	0.0025	0.0001	0.0099	0.0099	<.0001	<.0001

Scatterplot Matrix

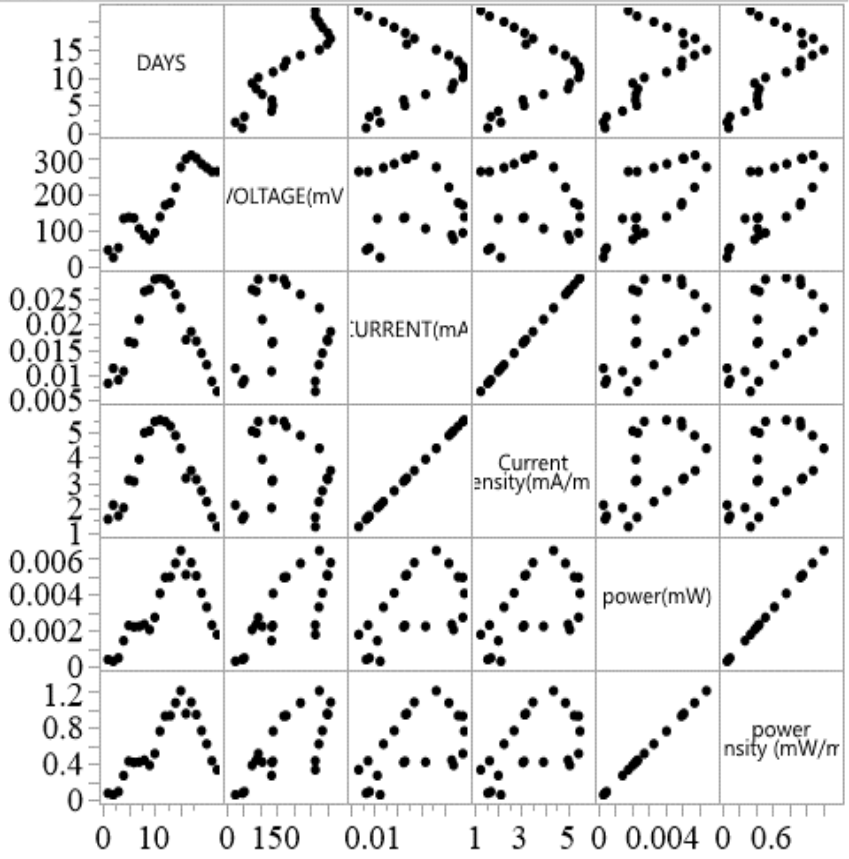

(b) Banana

Correlation Probability

	DAYS	VOLTAGE(mV)	CURRENT(mA)	Current density(mA/m2)	power(mW)	power density (mW/m2)
DAYS	<.0001	<.0001	0.0499	0.0499	0.1037	0.1037
VOLTAGE(mV)	<.0001	<.0001	0.0357	0.0357	0.0256	0.0256
CURRENT(mA)	0.0499	0.0357	<.0001	<.0001	0.0102	0.0102
Current density(mA/m2)	0.0499	0.0357	<.0001	<.0001	0.0102	0.0102
power(mW)	0.1037	0.0256	0.0102	0.0102	<.0001	<.0001
power density (mW/m2)	0.1037	0.0256	0.0102	0.0102	<.0001	<.0001

Scatterplot Matrix

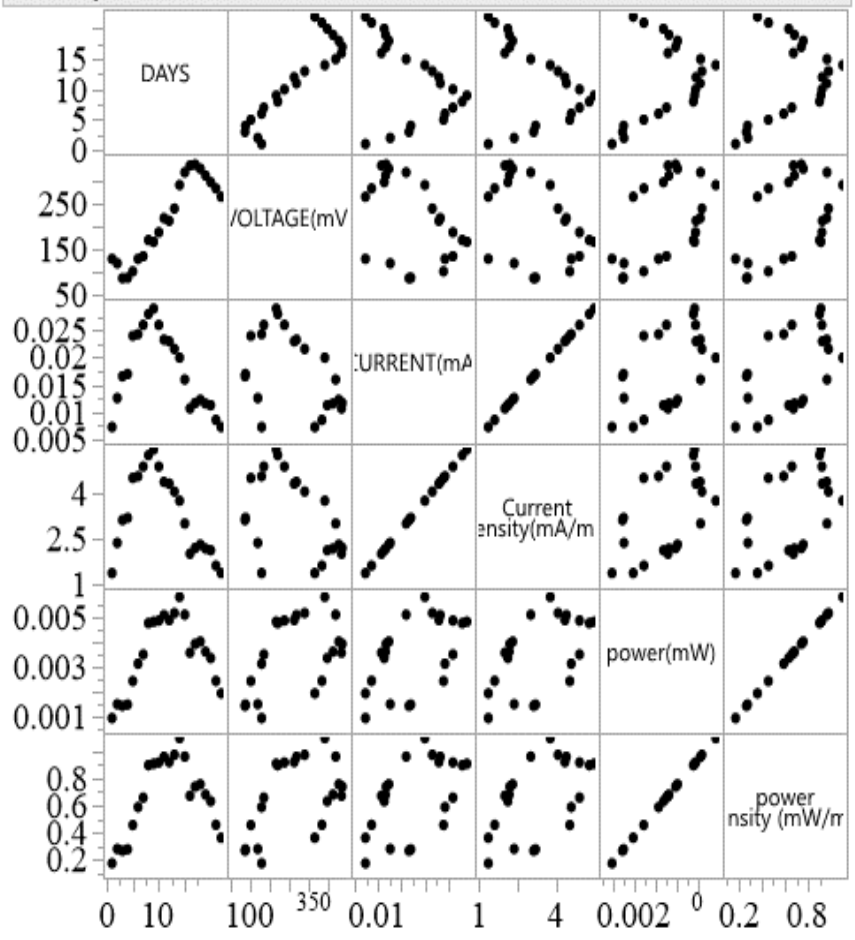

(c) Mango

Correlation Probability

	DAYS	VOLTAGE(mV)	CURRENT(mA)	Current density(mA/m2)	power(mW)	power density (mW/m2)
DAYS	<.0001	<.0001	0.0025	0.0025	0.0013	0.0013
VOLTAGE(mV)	<.0001	<.0001	0.0032	0.0032	<.0001	<.0001
CURRENT(mA)	0.0025	0.0032	<.0001	<.0001	0.9309	0.9309
Current density(mA/m2)	0.0025	0.0032	<.0001	<.0001	0.9309	0.9309
power(mW)	0.0013	<.0001	0.9309	0.9309	<.0001	<.0001
power density (mW/m2)	0.0013	<.0001	0.9309	0.9309	<.0001	<.0001

Scatterplot Matrix

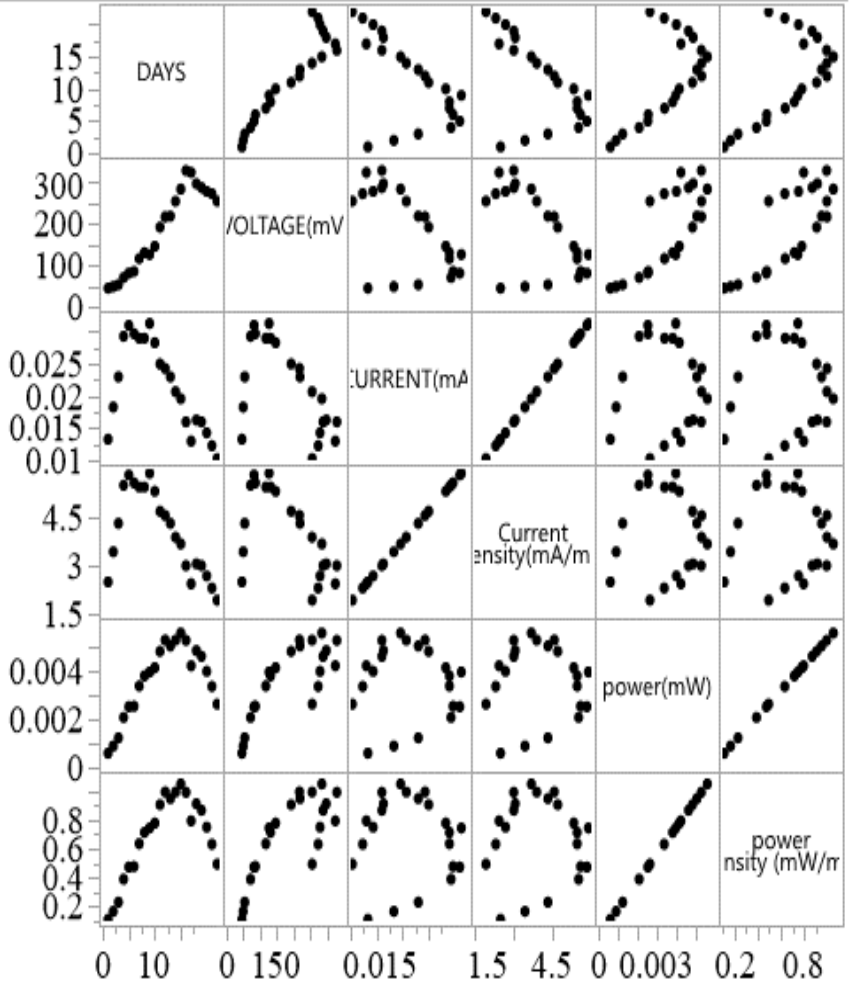

(d) Mixture

Correlation Probability

	DAYS	VOLTAGE(mV)	CURRENT(mA)	Current density(mA/m2)	power(mW)	power density (mW/m2)
DAYS	<.0001	<.0001	0.0199	0.0199	0.1914	0.1914
VOLTAGE(mV)	<.0001	<.0001	0.4096	0.4096	0.0005	0.0005
CURRENT(mA)	0.0199	0.4096	<.0001	<.0001	0.0056	0.0056
Current density(mA/m2)	0.0199	0.4096	<.0001	<.0001	0.0056	0.0056
power(mW)	0.1914	0.0005	0.0056	0.0056	<.0001	<.0001
power density (mW/m2)	0.1914	0.0005	0.0056	0.0056	<.0001	<.0001

Scatterplot Matrix

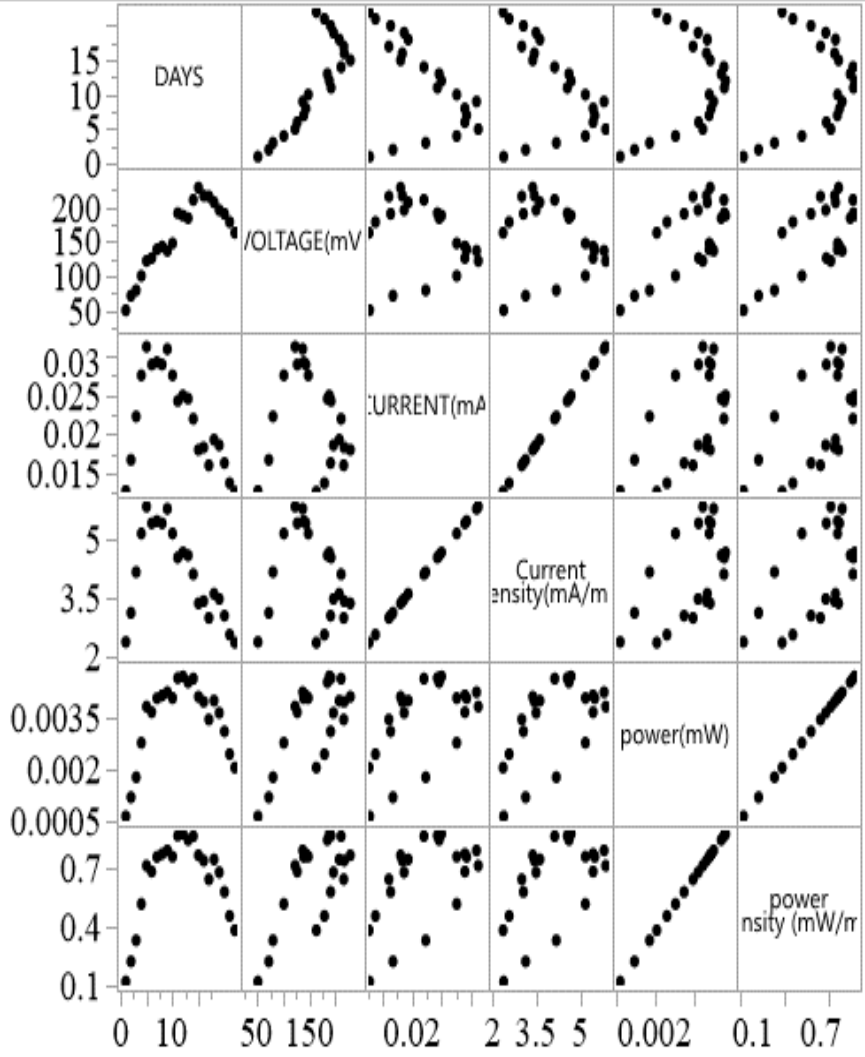

(e) Tomato

Correlation Probability

	DAYS	VOLTAGE(mV)	CURRENT(mA)	Current density(mA/m2)	power(mW)	power density (mW/m2)
DAYS	<.0001	<.0001	0.2530	0.2530	0.0242	0.0242
VOLTAGE(mV)	<.0001	<.0001	0.4091	0.4091	0.0024	0.0024
CURRENT(mA)	0.2530	0.4091	<.0001	<.0001	0.0020	0.0020
Current density(mA/m2)	0.2530	0.4091	<.0001	<.0001	0.0020	0.0020
power(mW)	0.0242	0.0024	0.0020	0.0020	<.0001	<.0001
power density (mW/m2)	0.0242	0.0024	0.0020	0.0020	<.0001	<.0001

Scatterplot Matrix

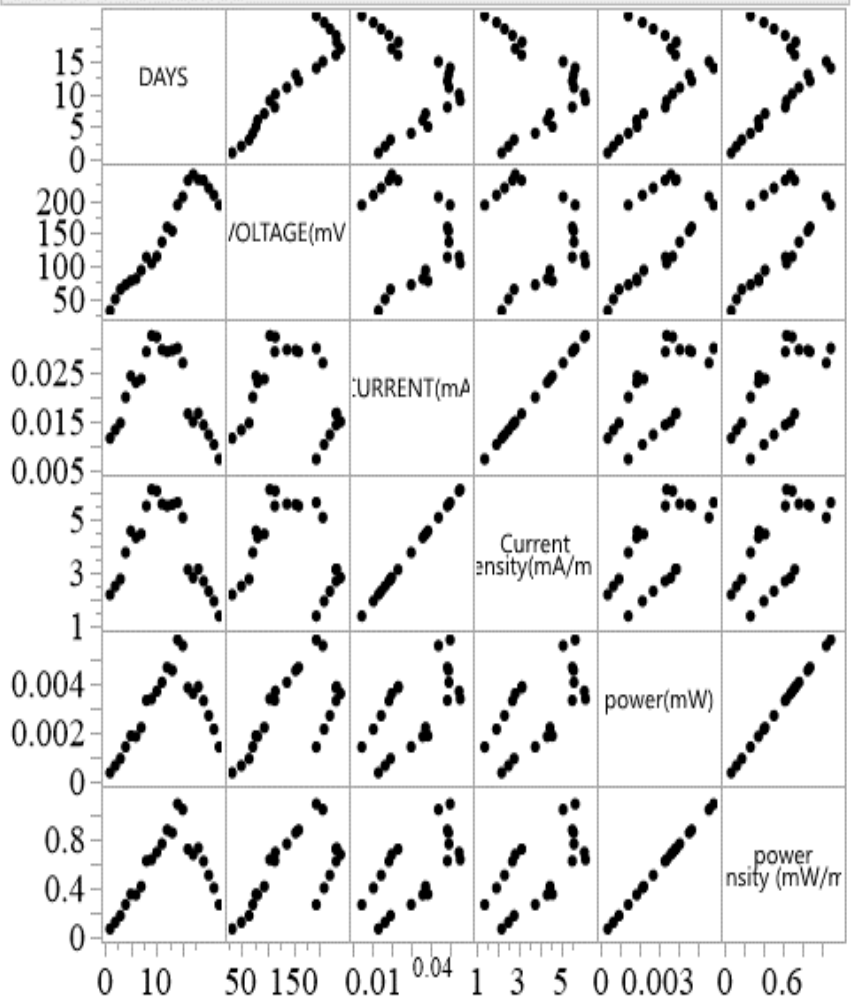

(f) Watermelon

Correlation Probability

	DAYS	VOLTAGE(mV)	CURRENT(mA)	Current density(mA/m2)	power(mW)	power density (mW/m2)
DAYS	<.0001	<.0001	0.0059	0.0059	0.2891	0.2891
VOLTAGE(mV)	<.0001	<.0001	0.0245	0.0245	0.0487	0.0487
CURRENT(mA)	0.0059	0.0245	<.0001	<.0001	0.0066	0.0066
Current density(mA/m2)	0.0059	0.0245	<.0001	<.0001	0.0066	0.0066
power(mW)	0.2891	0.0487	0.0066	0.0066	<.0001	<.0001
power density (mW/m2)	0.2891	0.0487	0.0066	0.0066	<.0001	<.0001

Scatterplot Matrix

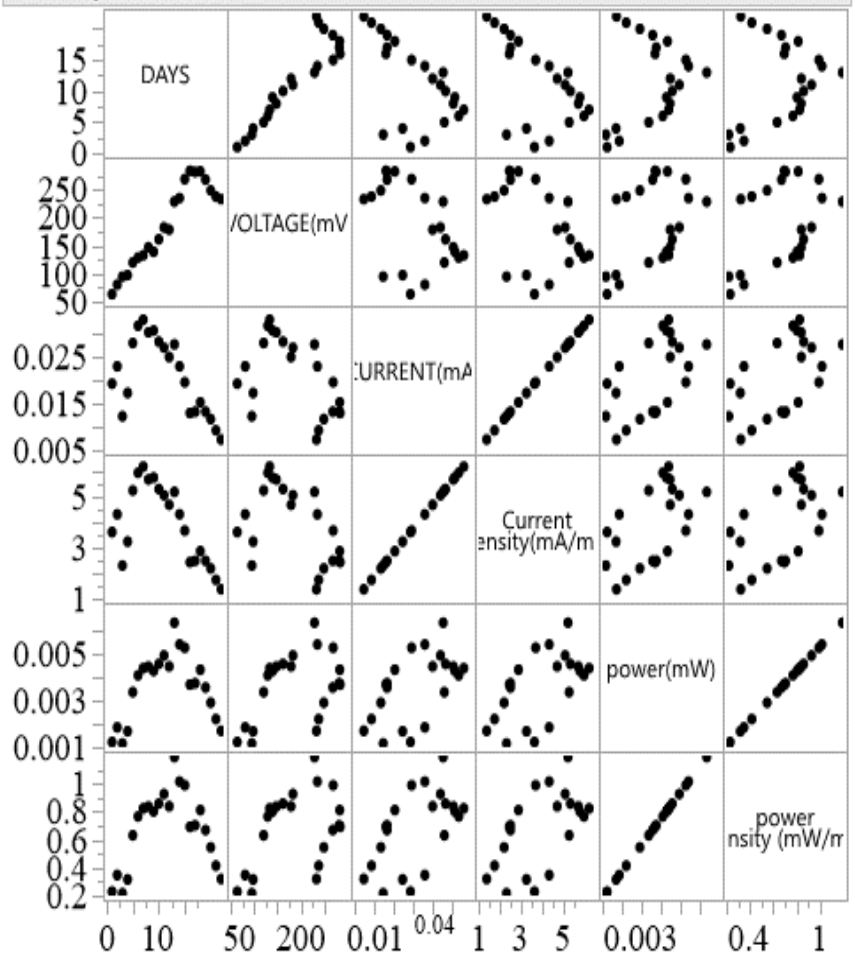

Appendix 12: Publications

1. **Imwene K.O.,** Mbui D.N., Mbugua J.K., Kinyua A.P., Kairigo P.K., Onyatta J.O. (2021). Kinetic Modelling of Microbial Fuel Cell Voltage Data From Market Fruit Wastes in Nairobi, Kenya; *International Journal of Scientific Research in Chemistry (IJSRCH), ISSN: 2456-8457,* **6**(5), 25-37. URL: https://ijsrch.com/IJSRCH21654.

2. Kinyua A.P., Mbugua J.K., **Imwene K.O**., Mbui D.N., Kithure J.G.N., Wandiga SO. (2021). Current and voltage data logging from microbial fuel cells using Arduino-based sensors. *Int Rob Auto J*.; **7**(3):90–93. DOI: 10.15406/iratj.2021.07.00232.

3. **Imwene K.O.,** Mbui D.N., Kinyua A.P., Mbugua J.K., Ahenda S and Onyatta J.O. (2021). Biotransformation of Biodegraded Organic Waste from a Batch Mode Microbial Fuel Cell to Organic Fertilizer. *Journal of Bioremediation and Biodegradation an open access journal ISSN: 2155-6199.* **12**(S8).